Imaging physiological ABC transporter expression and its relation to disease using Tc-99m-hexakis-methoxy-isobutyl isonitrile (Tc-99m-MIBI)

Sabina Dizdarevic

A Thesis Submitted in Partial Fulfilment of the Requirements of Brighton and Sussex Medical School for the Degree of Doctor of Philosophy

Division of Clinical and Laboratory Investigation

March 2015

Abstract

Aim: Tc-99m-MIBI is a substrate for ATP-binding cassette (ABC) transporter proteins, including P-glycoprotein (P-gp), and has been used to image their expression, mainly in cancer. Imaging P-gp expression may have a role in renal transplantation and investigating drug toxicity. The aim of the project was to develop a functional imaging assay for ABC-transporters using Tc-99m-MIBI.

Methods: Subjects comprised 30 healthy kidney transplant donors and 4 patients with psoriasis. Donors were imaged dynamically for 30 min following injection of Tc-99m-MIBI and Tc-99m-MAG3 on separate occasions. Tc-99m-MIBI images were acquired at 30 and 120 min and the rate constant of elimination (*k*) calculated. Psoriasis patients were imaged on 3 occasions with Tc-99m-MIBI i.e. baseline, 2 and 6-12 weeks after cyclosporine A (CsA) treatment. GFR was measured using Cr-51-EDTA. *ABCB1* polymorphisms were genotyped in 19 donors and 4 psoriasis patients and correlated with Tc-99m-MIBI kinetics.

Results: There were no significant differences in differential renal function and perfusion between Tc-99m-MIBI and Tc-99m-MAG3. Renal Tc-99m-MIBI activity peaked at 2-4 min then declined by 69 [5]% over 15 min. Bladder activity followed a similar, opposite time-course. Hepatic activity peaked at 6-8 min with variable elimination over 15 min (30 [14]%). Renal and hepatic *k* values were 0.36 (0.13) and 1.02 (0.23)% min^{-1}, respectively. Early hepatic elimination and renal *k* correlated with *ABCB1 3435C>T* genotype (p=0.083 and 0.087, respectively). Following CsA, early hepatic

and renal elimination rates fell in 2 patients with high blood CsA levels, whereas no change was noted in 2 with low levels. Patients homozygous for 1236CC genotype demonstrated different and opposite pharmacological effects of CsA on Tc-99m-MIBI kinetics when compared to those patients with at least one T allele, in both early and delayed phases of Tc-99m-MIBI elimination. There was no correlation between Tc-99m-MIBI kinetics and GFR.

Conclusions: Tc-99m-MIBI can replace Tc-99m-MAG3 for pre-transplant workup and provide an *in-vivo* assay of ABC-transporter expression. This is the first study to compare Tc-99m-MIBI with Tc99m-MAG3 confirming that Tc-99m-MIBI is a good renal agent. Pharmacological blockade with CsA alters Tc-99m-MIBI kinetics. Tc-99m-MIBI pharmacokinetics are influenced by CsA possibly through *ABCB1* SNPs 1236C>T and to a lesser extent 2677G>T rather than 3435C>T alone, while baseline Tc-99m-MIBI kinetics appeared more influenced by 3435C>T and not through other studied *ABCB1* SNPs. In the era of personalised medicine, further prospective trials are required to investigate the full impact of genotype and haplotype variation on ABC transporter-associated Tc-99m-MIBI elimination and imaging findings in routine clinical practice and research. This project provides the impetus for the development of imaging assay for predicting nephrotoxicity or dose selection of drugs that are ABC/P-gp substrates, including calcineurin inhibitors (CNI).

Author Declaration

I declare that the research contained in this thesis, unless otherwise formally indicated within the text, is the original work of the author. This thesis has not been previously submitted to this or any other university for a degree, and does not incorporate any material already submitted for a degree.

Signed:

Date: March 2015

Acknowledgments

Special note of thanks goes to my supervisor Professor Michael A Peters. I am extremely grateful for his guidance, patience and invaluable advices in the last six years.

I would like to express my sincere gratitude to Professor Kevin Davies, who chaired my non-supervisory thesis panel and guided me unwaveringly in my research. Without his encouragement and ingenious advices this work would not been finished yet.

I also wish to thank my other two thesis panel members, Dr Timothy Chavassut and my external assessor, Dr James Ballinger for their continuous support, directions and extremely helpful advices at six progress assessments during my part-time PhD programme. I shall miss my progress reviews and challenging scientific discussions with them.

Without one exceptional physicist, who was always available to help me, Mr Mark Aplin this project would not have been possible. Thank you Mark for your physics advices, help with data analysis and your support throughout.

I am also very grateful to Prof Kenneth Miles, who supervised me until he moved back to Australia and helped me with his invaluable advices.

I was fortunate to have Prof Melanie Newport to help me with genotyping and general advices. Thank you Mel.

I am also very grateful to Mr Scott Harfield, the best R&D manager I have ever met, who helped with research governance advices, guidelines for ethics applications and any possible administrative hurdle.

The work presented in this thesis required the help and assistance of a large number of people and I would like to acknowledge the contribution from my collaborators from renal and dermatology teams: Mrs Caroline Azmy, Prof Stephen Holt, Dr Lawrence Goldberg, Dr Lindsay Atkinson, Dr Elizabeth Derrick and Ms Carolyn Saunders. I would also like to acknowledge assistance from technical, nursing, physics, radiopharmacy and administrative team at the Department of Nuclear Medicine Brighton and Sussex University Hospitals NHS Trust, including Mr Lynn Jenkins, Miss Nicola Ryan, Mrs Angela Clarke, Mrs Helen Marie-Cripps, Mrs Katherine Day, Miss Helen Campbell, Ms Maryam Jessop, Mr Matthew Lee, Miss Emma Wroe and Mrs Nicola Goldsmith.

I am also grateful to my colleagues, consultants in nuclear medicine, for their frank support, Mr Charles Zammit for proofreading of the final draft of my thesis and Stephanie Goubet for statistical advice

I am immensely grateful to all the study participants, potential kidney transplant donors and patients with psoriasis, without whom none of the studies would have been possible.

Thanks to my friends for their encouragement. In particular, I would like to thank my friend Dr Deepa Gopalan who helped me keep smiling.

My deepest gratitude goes to my mum and my late dad, who inspired me to study medicine, for their unreserved parents' love and to my brother for his continuous encouragement to strive for excellence in medicine and research.

Last but not least, I would like to thank my caring husband Damir and son Benjamin for their love and unreserved support, for standing by me and helping me to balance between my routine clinical work requirements, my research and home commitments.

I would like to dedicate this thesis to my husband Damir, son Benjamin, and my parents.

Table of contents

List of tables

List of Figures

Abbreviations

ABC-transporter	ATP-binding cassette transporters
ATN	Acute tubular necrosis
ARSAC	Administration of Radioactive Substances Advisory Committee
BBB	Blood-brain barrier
BCRP	Breast cancer resistance protein (gene symbol *ABCG2*)
BNMS	British Nuclear Medicine Society
CIN	Contrast-induced nephropathy
CNI	Calcineurin inhibitors
Cr-51 EDTA	Chromium -51-ethylenediaminepentaacetic acid
CsA	Cyclosporine A
CYP3A	Cytochrome P450 3A
DMSA	Dimercaptosuccinic acid
DRF	Differential or divided renal function
DTPA	Diethytriaminepentaacetic acid
EANM	European Association of Nuclear Medicine
EVAR	Endovascular aneurysm repair
GFR	Glomerular filtration rate
HIDA	Hepatic Imino Diacetic Acid
MAG3	Mercaptoacetyltriglycine
MDR	Multidrug resistance
MPI	Myocardial perfusion imaging
MRP1	Multidrug resistance protein 1 (gene symbol *ABCC1*)
MRP2	Multidrug resistance protein 2 (gene symbol *ABCC2*)
mTOR	Mammalian target of rapamycin
NFAT	Nuclear factor of activated T-cells
NSAIDs	Non-steroidal anti-inflammatory drugs
PCR	Polymerase Chain Reaction

PET	Positron emission tomography
P-gp	P-glycoprotein (gene symbol *ABCB1*, formerly known as *MDR1*)
SPECT	Single photon emission tomography
Tc-99m	Technetium-99m
Tc-99m-MIBI	Tc-99m-hexakis-2-methoxy-isobutyl isonitrile
TDM	Therapeutic drug monitoring

Chapter 1 Introduction, including aims

1.1 Introduction

The ATP binding cassette (ABC) transporters belong to the largest transporter gene family and generally use energy derived from ATP hydrolysis for translocation of different substrates across biological membranes. ABC transporters are classified into 7 sub families based on phylogenetic analysis and designated as ABCA to ABCG (1). Among these, the *ABCB1* multidrug resistance gene 1 (*MDR1*) is the most studied drug transporter gene. The multidrug-resistant P-glycoprotein (Pgp), a 170-kDa plasma membrane protein encoded by the mammalian multidrug resistance gene (*ABCB1*, formerly known as *MDR1*), functions as an energy-dependent adenosine-5'-triphosphate (ATP) efflux pump (2).

1.1.1 Transporters responsible for multidrug resistance (MDR)

In tumour cell lines, multidrug resistance is often associated with an ATP-dependent decrease in cellular drug accumulation and attributed to the overexpression of certain ATP-binding cassette (ABC) transporter proteins. ABC proteins that confer drug resistance include (but are not limited to) P-gp (gene symbol *ABCB1*), the multidrug resistance protein 1 (MRP1, gene symbol *ABCC1*), MRP2 (gene symbol *ABCC2*), and the breast cancer resistance protein (BCRP, gene symbol *ABCG2*). In addition to their role in drug resistance, there is substantial evidence that these efflux pumps have overlapping functions in tissue defence. Collectively, these proteins are

capable of transporting a vast and chemically diverse array of toxicants including bulky lipophilic cationic, anionic, and neutrally charged molecules and many clinical drugs and toxins, as well as conjugated organic anions that encompass dietary and environmental carcinogens, pesticides, metals, metalloids, and lipid peroxidation products (3). Hydrophobic amphipathic compounds, including many clinically used drugs, interact with the substrate-binding pocket of these proteins via flexible hydrophobic and H-bonding interactions. Single nucleotide polymorphisms (SNP) in ABC drug-efflux pumps may play a role in responses to drug therapy and disease susceptibility. The effect of various genotypes and haplotypes on the expression and function of these proteins is not yet entirely clear, and their true impact remains controversial (4). Most prevalent of these ABC transporters is P-gp, which has been described as a molecular “hydrophobic vacuum cleaner”, pulling substrates from the membrane and expelling them to promote MDR (5).

1.1.2 Physiological role of P-gp

P-gp extrudes various hydrophobic drugs and peptides from the cell interior and has an important role in normal physiology by protecting tissues from toxic xenobiotics and endogenous metabolites. It also regulates the transport of various structurally unrelated substrates, like anticancer agents and toxins (6).

This protein has a role in the normal secretion of metabolites and certain P-gp-mediated drugs into bile, urine, and directly into the lumen of the gastrointestinal tract (7). The expression of P-gp in bronchial structures,

particularly at the epithelial apical surface, suggests an important role in human airways, although a physiological role of P-gp in the lungs is not clearly defined (8). At the blood-brain barrier, 3 factors, i.e. location, potency, and broad multi-specificity, make P-gp a key determinant of P-gp-mediated drug entry into the CNS. A high P-gp level may limit the uptake of sufficient amounts of drugs targeted to the brain, whilst a reduced level may lead to increased accumulation of toxic compounds in the brain and neurotoxicity (9). The molecular mechanisms regulating drug permeability across the choroid plexus (CP) epithelium are not well defined and contradictory data in the literature exist (10) (11).

Apart from its multidrug transporter role, normal physiological functions of P-gp have been reported. It seems that the transport function of P-gp is necessary to protect cells from death. P-gp could be responsible for translocation of platelet-activating factor (PAF) across the plasma membrane. It has been reported that high P-gp expression prevents stem-cell differentiation and over-expression of P-gp delays apoptotic cascade, so it seems that P-gp may play an important role in regulating programmed cell death (12).

1.1.3 Localisation of P-gp in normal human cells

Many tissues express P-gp, including the bronchopulmonary epithelium, hepato-biliary epithelium, renal tubular epithelium, GI tract, blood brain barrier and choroid plexus, which are all strategically located to protect against the passage of xenobiotics (Figure 1.1) (13) (14). Certain cell types in liver, pancreas, kidney, colon, and jejunum show specific localisation of

P-gp. In liver, P-gp is found exclusively on the biliary canalicular front of hepatocytes and on the apical surface of epithelial cells in small biliary ductules. In the pancreas, P-gp is found on the apical surface of the epithelial cells of small ductules but not larger pancreatic ducts. In the kidneys, P-gp is concentrated on the apical surface of epithelial cells of the proximal tubules (14). Colon and jejunum both show high levels of P-gp on the apical surfaces of superficial columnar epithelial cells. Adrenal glands show high levels of P-gp, diffusely distributed on the surface of cells in both the cortex and medulla (7). In the lungs, P-gp is detected at the apical surface of ciliated epithelial cells from the surface epithelium or ciliated collecting ducts, and on apical and lateral surfaces of serous cells from bronchial glands. P-gp is also present at the luminal surface of endothelial cells of bronchial capillaries, but not at the mucus-secreting cells (8). P-gp localization in the blood brain barrier at the luminal membrane of cerebral microvessels is consistent with P-gp being both a barrier to entry and a drug excretory pump in the brain (9).

P-gp is also expressed in human peripheral blood mononuclear cells (PBMCs) and subpopulations of lymphocytes. The differential expression of P-gp in many localised tissues and cells of the hematopoietic system, natural killer cells, antigen-presenting dendritic cells and T and B-lymphocytes, implies diverse physiological and pharmacological roles (12) (15). P-gp also displays restricted expression in the developing embryo. P-gp in the apical border of foetus-derived epithelial cells faces the maternal circulation and is therefore optimally placed to protect the foetus against toxins (12).

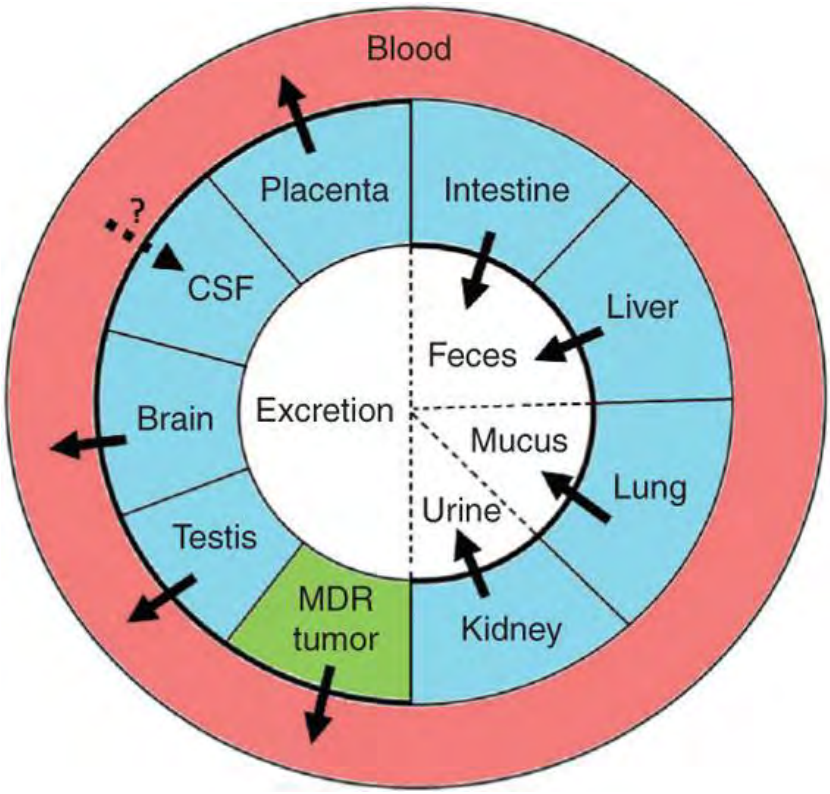

Figure 1.1 Direction of substrate transport by P-glycoprotein (P-gp) located in various organs of the human body.

P-gp is located in the lipid bilayer that forms a barrier between various organs (Figure 1.1: thick black line indicates lipid bilayer, red indicates vasculature, blue represents tissue and white indicates excreta, the bold solid arrows indicate the known direction of transport, whereas the dashed arrow indicates unclear direction of transport; reprinted with permission from Kannan P, John C, Zoghbi S, Halldin C, Gottesman M, Innis R, et al. Imaging the Function of P-Glycoprotein With Radiotracers: Pharmacokinetics and In Vivo Applications. Clin Pharmacol Ther. 2009; 86(4): p. 368–377 (Fig 2) (13) modified from Szakács G, Paterson JK, Ludwig JA et al. Targeting multidrug resistance in cancer. Nat Rev Drug Discov 2006; 5: 219–234 (14)).

1.1.4 A role of ABCB1 (MDR1) as a modulator of health and disease

In humans, the *ABCB1* (*MDR1*) gene is located on the long arm of 7th chromosome at q21.1 band position. It plays a significant role in ADME (absorption, distribution, metabolism and excretion) processes and drug-drug interaction. Variations in the *ABCB1* (*MDR1*) gene product can directly affect the therapeutic effectiveness, with over expression of P-gp resulting in increased efflux of anticancer drugs and development of drug resistance. The *ABCB1 (MDR1)* gene is highly polymorphic and 40 single nucleotide polymorphisms (SNPs) were identified of which some are known to influence *ABCB1* (*MDR1*) expression levels (6). *ABCB1 (MDR1)* C3435T polymorphism has recently attracted attention as a possible modulator of health and disease.

1.1.5 Genetically determined differences in P-glycoprotein expression

The variability of P-gp expression between individuals is linked to a C3435T polymorphism of the human *ABCB1* (*MDR1*) gene. *ABCB1* gene polymorphism in exon 26 at C3435T (silent polymorphism) is known to influence the expression of P-gp. The C/C genotype is associated with increased P-gp expression; individuals with T/C genotype show intermediate P-gp expression, while individuals who are homozygous carriers of T/T show functionally restrained P-gp (Figure 1.2).

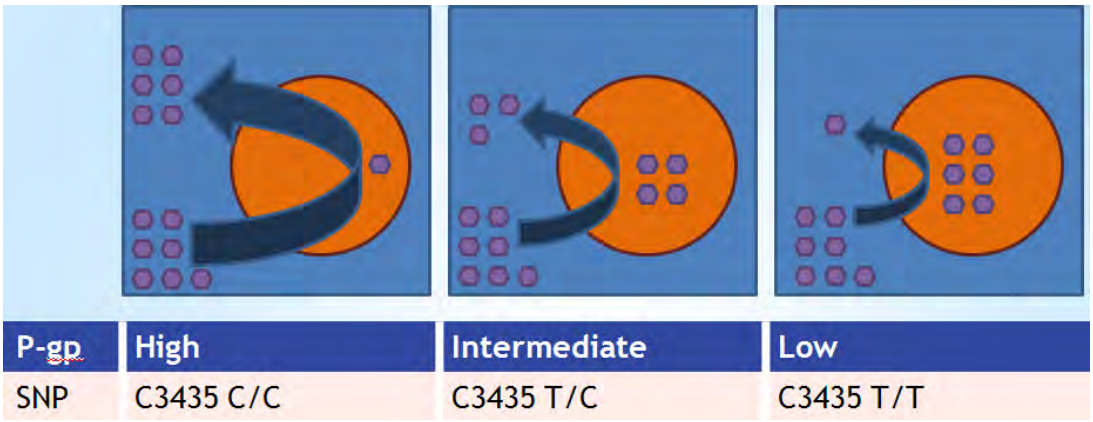

Figure 1.2 Genetically determined P-gp expression.
High P-gp expressers (C3435 C/C) are linked to MDR. Low P-gp expressers (C3435T/T) are prone to drug toxicity.

In the analysis of *ABCB1* (*MDR1*) variant genotype distribution in a large sample of white subjects, Cascorbi et al. first demonstrated that C3435T occurred in 53.9% of subjects heterozygously (T/C), while 28.6% of individuals were homozygous (T/T) carriers and 17.5% of the individuals were homozygous (C/C) carriers (16). Prevalence of the T/T genotype in Caucasian individuals has been shown to be between 24% and 29% (16) (17).

Racial variability within C3434T has also been demonstrated. Thus a significantly higher frequency of the C/C genotype in West Africans and African Americans (83% and 61%, respectively), compared with Caucasians (26% ($p<0.0001$), has been reported. These findings could affect use of drugs that are P-gp substrates, such as HIV-1 protease inhibitors and

cyclosporine (CsA) in African populations (18) due to a potentially higher rate of drug resistance.

When data were compared with respect to sex, T/T genotype frequency was increased in males. Exposure to carcinogens was found to be higher in males as compared to females indicating that males with TT genotype had greater risk to develop chronic myeloid leukaemia (CML) (6). An association with male glioblastoma and TT genotype has also been reported (6) (19).

Individuals carrying C/C genotype showed higher P-gp expression levels (2-fold) compared to TT individuals (6). Concentration of P-gp in intestinal epithelial cells and in a subset of lymphoid cells is substantially lower in people with the T/T genotype than those with the C/C genotype (17).

1.1.6 T/T genotype - link with drug toxicity and susceptibility to P-gp mediated disease

The T/T genotype is associated with low P-gp expression levels and with less efficiency to efflux toxins, resulting in higher intracellular concentrations of mutagens or toxins in the cell, leading to DNA damage and accumulation of mutations. C3435T/T polymorphism is associated with lower protection against specific P-gp-dependent xenobiotics and carcinogens. The TT genotype is associated with reduced drug transport, resulting in accumulation of intracellular toxins and therefore predisposition to drug toxicity (17).

Potential implications of this reduced mechanism of detoxification may also have implications for disease risk and therapeutic outcome due to development of drug toxicity.

Individuals with TT genotype were found to be at increased risk of CML (6), acute childhood lymphoblastic leukaemia (ALL) (20), renal epithelial tumours (21), colorectal cancer (22), glioblastoma (19) breast cancer (6) (23) and inflammatory bowel disease (17).

A silent mutation in exon 26 (C3435T) was also correlated with intestinal P-gp expression and oral bioavailability of digoxin. Subjects homozygous for the C3435T/T mutation (24% of Caucasians) have low intestinal P-gp levels, high plasma concentrations after oral digoxin and reduced P-gp function (17) in peripheral blood cells in comparison to the remainder of the population (17).

In the kidneys, genetically driven low constitutive *ABCB1* (*MDR1*) expression may limit local detoxification of carcinogens and hence increased risk for development of renal epithelial tumours (21). The T/T genotype at the *ABCB1* 3435 polymorphism of renal transplant donors (24), but not transplant recipients (25), has been shown to be associated with decreased expression of P-gp in the transplanted renal tissue and has also been shown to be a risk factor for developing subsequent CsA nephrotoxicity.

1.1.7 C/C genotype: link with multidrug resistance and poor risk prognosis

ABCB1 (*MDR1*) is also expressed on non-malignant cells in various organs and modulation of *ABCB1* (*MDR1*) expression in these normal cell types can also influence the activity and bioavailability of drugs. Increased C/C genotype is shown to be associated with multidrug resistance and potentially linked with poor disease prognosis (6).

In cancer therapy, high expression and activity of *ABCB1 (MDR1)* causes cancer cells to become refractory to treatment with many agents that are P-gp substrates. The functional significance of *ABCB1 (MDR1)* C3435T polymorphism with respect to Imatinib treatment was studied in terms of haematological and cytogenetic response. Haematological non-responders showed association with T/T genotype and cytogenetic non-responders with C/C genotype. When the data were analysed in relation to these two types of responses, the frequency of C/C genotype was increased significantly in cytogenetic non-responders and the increase was found to be inversely proportional to the degree of cytogenetic response.

The C/C genotype has also been demonstrated to be associated with poor prognosis in ALL and AML as a result of multidrug resistance (6) (20).

In renal transplant rejection, high P-gp expression in the renal epithelium of the graft and lymphocytes of the recipient (26), induced by CsA, is considered an analogue to MDR mechanism. Furthermore, C3C4CC genotype is recently shown to be associated with increased risk for kidney allograft failure (27) presumably due to development of 'immunosuppressive drug resistance' leading to chronic rejection. In addition, Naesens et al. showed that absent P-gp expression at the apical membrane of renal tubular

cells and combined donor-recipient homozygosity for C3435T are associated with increased risk of chronic allograft damage (28).

1.1.8 Other ABCB1 variants

As the C3435 site does not alter the protein sequence, it would appear likely that the effects on gene expression associated with this SNP may well be due to other SNPs that are physically linked to it. Therefore, C3435 may be associated with a polymorphism at a different site, which affects either *ABCB1 (MDR1)* expression or function.

There are other *ABCB1* variants that may also influence P-gp expression, such as those in exon 21 (G2677T/A) (29), exon 12 (C1236T) (29), exon 11 (G1199A) (13), but the published data are limited. There is less information about those SNPs, which although investigated in some diseases and drug pharmacokinetics, have a very limited number of published meta-analyses. Further studies should include analysis of the haplotype 1236T-2677T/A-3435T as well as other SNPs in MDR1, other transporters and drug metabolisers that may be related with the outcome (30).

1.1.9 In vivo Imaging of ABC Transporters

ABC transporters may be imaged *in vivo* with radiopharmaceuticals that are also MDR substrates or inhibitors.

Radiopharmaceuticals for the diagnosis of ABC-transporter-mediated multidrug resistance can be divided into single photon agents, generally labelled with technetium-99m (Tc-99m), and agents that emit positrons,

generally labelled with carbon-11 (C-11), gallium-68 (Ga-68) or fluorine-18 (F-18). They share the general functional property of being substrates or inhibitors for ABC transporters.

The term ‘radiopharmaceutical’ encompasses the association of a radionuclide with a pharmaceutical. The biological properties of the pharmaceutical determine the tissues in the body that are targeted by the radiopharmaceutical, while the radionuclide emits single photons or positrons that are externally detected and used to construct a functional image. Images are constructed from the detection of single photons using planar gamma camera imaging or single photon emission computed tomography (SPECT), and from the detection of positrons using positron emission tomography (PET).

1.1.9.1 Single Photon Emission Computed Tomography

A radioactive element has an unstable nucleus which when it emits a neutron and/or proton becomes a new element. The disintegration process is accompanied by the emission of electromagnetic radiation (photons) of a specific energy measured in KeV. Most radioactive elements in routine imaging use emit single gamma photons as discrete events in association with nuclear disintegration. Such photons can be detected using equipment that comprises firstly a transparent crystal, which absorbs the photon, and an array of photomultiplier tubes that detect the resulting flash of light (scintillation) and its location in the crystal that is imparted by the photon when its kinetic energy is converted into visible light within the crystal. Gamma cameras get their name by analogy with light cameras, where light is

replaced by gamma radiation. The focusing device of a gamma camera is its collimator, a lead disc perforated with hundreds of parallel holes of sufficient length-to-radius ratio to permit the passage only of photons travelling perpendicular to the collimator face. Like light cameras, gamma cameras generate 2-dimensional images. However by rotating the camera slowly around the subject and obtaining an image every 6^{o} of rotation, 3-dimensional images can be re-constructed.

1.1.9.2 Positron Emission Tomography

Some radionuclides emit positrons from the nucleus when it is unstable. A positron is positively charged and has the mass of an electron. Following emission from the nucleus, the positron is immediately attracted to a negatively charged electron with the result that the two particles collide and undergo mutual annihilation. Their energies are converted into two gamma photons of 511 KeV energy that leave the atom at exactly 180^{o} to each other. A ring of detectors that encircle the subject then simultaneously detects these co-incident photons. The direction of photon emission is random and their simultaneous detection allows the construction of a 3-dimensional tomographic image.

SPECT and PET provide images of function. Structural details of tissues are portrayed with relatively poor anatomical resolution. Modern SPECT and PET cameras therefore have ‘built-in’ CT machines so that the functional image generated by the gamma radiation can be precisely registered on to a high-resolution structural image (‘hybrid’ imaging such as SPECT-CT and

PET-CT). The latest technological development is a PET- MRI hybrid camera (31).

1.1.9.3 Radiopharmaceuticals that are ABC substrates or inhibitors

The most studied of these, and the first to be used, is Tc-99m-sestamibi (hexakis-methoxy-isobutyl isonitrile; MIBI), which is a substrate for P-gp, MRP1, MRP2 and BCRP and can therefore be used to image their expression *in vivo* (32). Tc-99m-tetrofosmin and several other Tc-99m-Q complexes that are closely related to Tc-99m-MIBI with respect to their clinical applications are also transport substrates for P-gp and MRP (33) (34) (35) (36). Although Tc-99m-tetrofosmin and Tc-99m-MIBI do not have identical physiological properties, the available data suggest that the clinical imaging and *in vivo* modulation of MDR function can be performed with either agent, but the two probably should not be used interchangeably (33) (37).

With respect to positron emitters, previous studies using the positron-emitter, Tc-94m-MIBI, and parallel previous studies with Tc-99m-MIBI showed essentially identical performance, thereby providing validation for microPET (38). In addition, several C-11-labelled P-gp-avid radioligands developed for PET, including C-11- colchicine, C-11-verapamil, C-11-daunorubicin, C-11-paclitaxel, and C-11-loperamide, have been evaluated in animals, but only C-11-verapamil and C-11-loperamide (39) have been extended to humans to investigate MDR and quantify P-gp expression in the blood brain barrier (13) (39). Other compounds that have been developed include (Ga-67/68-[3-

ethoxy-ENBDMPI])(+) tracers (40), 4- F-18-Fluoropaclitaxel (41) and the positron labelled P-gp inhibitor, C-11-Tariquidar (42).

Although many studies are currently focussing on functional imaging of P-gp, other ABC drug transporters have also attracted interest. Thus, Tc-99m-Hepatic Imino Diacetic Acid (HIDA) is transported only by MRP1, 2. Hepatic P-gp and MRP1, 2 could therefore be assessed by sequential use of both Tc-99m-MIBI and Tc-99m-HIDA (37) (43). Leukotrienes are substrates for MRP, so N-C-11- acetyl-leukotriene E4 could possibly be used to noninvasively image MRP function (37). Several lipophilic cationic copper(I) bis(diphosphine) complexes labelled with Cu-64 have been synthesised and evaluated *in vitro* as substrates for Pgp, offering a good basis for development of radiopharmaceuticals containing copper radionuclides, and this series of complexes should undergo further evaluation *in vivo* as positron emission tomography imaging agents for MDR (44).

The above imaging techniques, tracers and their relation to relevant ABC substrates and genotypes are summarised in Table 1.1 (31) (45) (46).

Imaging Modality	Radiopharmaceuticals	ABC Transporter	Gene symbol
SPECT	Tc-99m-MIBI (s)	P-gp MRP1,2 BCRP	*ABCB1 (mdr1)* *ABCC1,2* *ABCG2*
	Tc-99-m-tetrofosmin(s)	P-gp MRP1,2	*ABCB1(mdr1)* *ABCC1,2*
	Tc-99m-HIDA (s)	MRP1,2	*ABCC1,2*
	67Ga-[3-ethoxy-ENBDMPI] (s)	P-gp MRP1	*ABCB1(mdr1)* *ABCC1*
PET and micro PET(μ)	Tc-94m-MIBI (s, μ)	P-gp MRP1,2 BCRP	*ABCB1 (mdr1)* *ABCC1,2* *ABCG2*
	C-11- colchicines (i, μ)	P-gp	*ABCB1 (mdr1)*
	C-11-verapamil (i)	P-gp	*ABCB1 (mdr1)*
	C-11-loperamide (i)	P-gp	*ABCB1 (mdr1)*
	C-11-paclitaxel(i, μ)	P-gp	*ABCB1 (mdr1)*
	C-11-daunorubicin (i, μ)	P-gp	*ABCB1 (mdr1)*
	4-F-18-Fluoropaclitaxel (i, μ)	P-gp	*ABCB1 (mdr1)*
	C-11-Tariquidar (i, μ)	P-gp	*ABCB1 (mdr1)*
	68-Ga-[3-ethoxy-ENBDMPI] (s)	P-gp, MRP1	*ABCB1(mdr1);ABCC1*
	N-11-C-acetyl-leukotriene E4 (s)	MRP 2	*ABCC2*

Table 1.1 SPECT and PET ABC substrates (s) and Inhibitors (i) and their relationships to genes.

1.1.10 Properties of Tc-99m-sestamibi (MIBI)

Tc-99m-MIBI, a lipophilic cationic radiotracer, was originally introduced for imaging myocardial perfusion. Chemical analysis of ground state Tc-99m-MIBI reveals a stable monovalent cation with a central Tc(I) core surrounded by 6 identical MIBI ligands, coordinated through the isonitrile carbons in an octahedral geometry. In effect, the alkyl isonitrile ligands encase the metal in a sphere of lipophilicity, while enabling delocalisation of the cationic charge. The complex contains no ionisable functional groups and is extremely stable *in vivo*, without significant metabolism (2).

Tc-99m-MIBI accumulates by passive diffusion into cytoplasm and mitochondria. Its tissue uptake rate following intravenous injection is variable but broadly dependent on tissue blood flow and cellularity. Cellular transport of Tc-99m-MIBI is affected by apoptosis, i.e. Bcl-2 anti-apoptotic protein (cancer cells have high level of Bcl-2), proliferation and angiogenesis and it is therefore used as an imaging biomarker for cellular metabolism in tumours (47) (48).

Tissue retention of Tc-99m-MIBI is also variable and, because it is a substrate for P-gp, (2) (49) (50) is markedly influenced by tissue expression of P-gp. So the mechanism of Tc-99m-MIBI uptake clearly differs from its mechanism of washout. Elimination or washout of Tc-99m-MIBI from cells reflects activity of drug transporters, such as P-gp (Figure1.3).

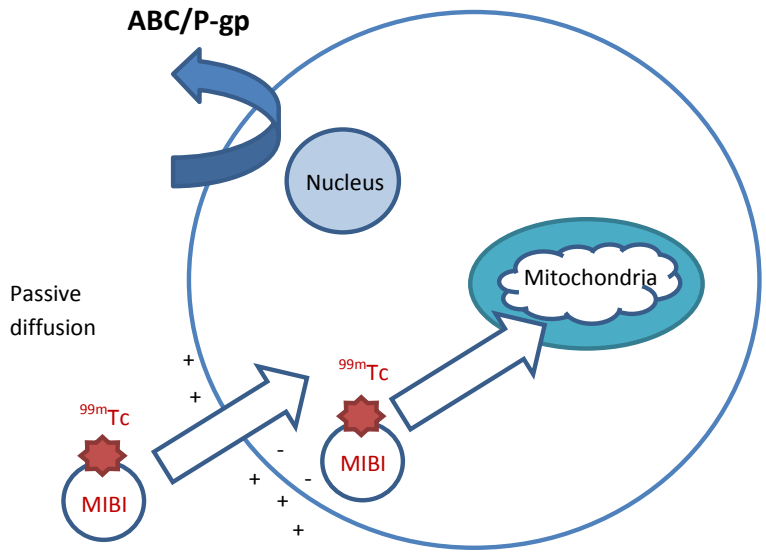

Figure1.3 Cellular transport of Tc-99m-MIBI.

Tc-99m-MIBI is a lipid soluble small organic cation enters cells by passive diffusion and accumulates in mitochondria. MIBI tracer clearance reflects activity of ABC proteins transporters such as P-gp

1.1.10.1 Imaging multidrug resistance by Tc-99m-MIBI in cancer

Tc-99m-MIBI has been validated as a transport substrate for P-gp in cultured multidrug-resistant rodent (34) (50) and human tumour cells (2) (51), as well as in cells over-expressing the recombinant human MDR1 gene (52). Piwnica-Worms et al. first demonstrated that Tc-99m-MIBI is a substrate for P-gp and that it can be used as a functional imaging agent for P-gp in tumour xenografts in nude mice (2). They and others have shown that tumour retention of Tc-99m-MIBI correlates inversely with the degree of P-gp expression and that this can be modified in human tissue *in vitro* in the presence of P-gp antagonists (53).

In rodent models, faster clearance of Tc-99m-MIBI has been observed in tumours that express P-gp compared with those that do not (51) (50).

The hepatic and renal excretion pathways of Tc-99m-MIBI are mediated by P-gp, and modulation of P-gp transport function can be detected in humans when this radiopharmaceutical is used in combination with cytotoxic drugs. Intravenous administration of a P-gp modulator increased retention of Tc-99m-MIBI in the liver and kidney in 3 patients investigated for multi-drug resistance (54).

It has been demonstrated that preoperative washout rates of Tc-99m-MIBI from primary breast tumours correlated with levels of P-gp found in the surgically resected specimens. Scintigraphic data in patients with breast cancer demonstrated that Tc-99m-MIBI washout rates from breast cancers over-expressing P-gp were threefold faster than those from cancers not expressing P-gp (55) (56).

In lung cancer, the sensitivity, specificity and accuracy of Tc-99m-MIBI for identifying responders to chemotherapy were 94%, 90% and 92%, respectively (57). There is also evolving evidence that Tc-99m-MIBI is cost-effective in predicting the response to chemotherapy in patients with lung cancer (57) and also for diagnosing breast cancer in patients with indeterminate mammography and dense breasts (58). Tc-99m-MIBI has also been used for imaging multidrug resistance in brain tumours, gastric cancer, head and neck cancer (59) and haematological malignancies.

In thyroid imaging, Tc99m-MIBI scintigraphy can be used to reliably exclude thyroid cancer when ultrasound-guided fine needle aspiration cytology (US-FNAC) is non-diagnostic, thus avoiding more invasive surgery and costs (60). It has, however, only recently been demonstrated that semi-quantitative Tc-99m-MIBI scintigraphy may preoperatively predict the malignant behaviour of non-oncocytic follicular thyroid nodules indeterminate at fine-needle aspiration biopsy. Moreover, a good correlation was found between immunohistochemical apical expression of MRP1 and Tc-99m-MIBI scintigraphy. A negative Tc-99m-MIBI retention index correlated strongly with those cases with high MRP1 expression. Tc-99m-MIBI scinitgraphy,

therefore, may provide information on the molecular expression of MRP1 in the thyroid (61).

A potential role for Tc-99m-MIBI scintigraphy has been investigated in the management of haematological malignancies, particularly multiple myeloma (MM), in which it has been shown that the rate of Tc-99m-MIBI elimination can predict response to chemotherapy. Patients showing disease progression at restaging had higher elimination rates (19.3 ± 9.8%) than patients in remission (12.8 ± 6.9%, $p<0.05$). Disease-free survival was significantly longer in patients with lower elimination rates. When patients treated with melphalan were excluded from the analysis, 87.5% of patients in remission had slow elimination (62).

In general and in relation to a range of malignancies, patients whose tumours showed Tc-99m-MIBI uptake responded well to chemotherapy, whereas those whose tumours showed little or no uptake, or a rapid rate of Tc-99m-MIBI washout, did not respond well (13).

Genetically determined responses to some anticancer drugs may also influence anti-cancer treatment. It has been shown that imaging the liver with Tc-99m-MIBI may provide pre-treatment indicators of *ABCB1*–mediated hepatic drug clearance in cancer patients. Tc-99m-MIBI hepatic elimination rate (kH) was significantly reduced in patients with SNPs in exons 21 and 26. The mean Tc-99m-MIBI kH was respectively 1.90 times and 2.21 times higher in subjects homozygous for the wild-type alleles compared with those homozygous for these SNPs (29).

1.1.10.2 Tc-99m-MIBI Scintigraphy in "non-cancer" P-gp mediated disease

The use of Tc-99m-MIBI scintigraphy in imaging the physiological expression of P-pg and "non-cancer" P-gp-mediated disease has been limited and minimally explored up to now.

P-gp inhibition induced by a single dose of CsA has previously been demonstrated *in vivo* by others using radionuclide imaging in a limited number of subjects and usually in multidrug resistance studies. A two-week oral course of CsA caused retention of Tc-99m-MIBI and delayed washout from the liver in non-cancer patients of whom 2 were renal transplant recipients (49). Single i.v administration of CsA induced down-regulation of P-gp at the blood brain barrier as assessed by C-11-verapamil (39).

Limited data also exist on Tc-99m-MIBI pharmacokinetics in the brain and liver in relation to multidrug resistance in patients with drug-resistant epilepsy. Vazquez et al. suggested that liver clearance of Tc-99m-MIBI might be accelerated in refractory epileptic patients (63). Preliminary data also suggested that low Tc-99m-MIBI uptake in the choroid plexus may identify patients with a clinically unfavourable prognosis and implied that integration of clinical data, *ABCB1* genotype and Tc-99m-MIBI scintigraphy may be promising for identifying drug-resistant epileptic patients (64). It has also been suggested that the influence of *ABCB1* polymorphism on antiepileptic drugs may vary among races, i.e. influencing drug response in Asian, but not European epileptic patients (65).

There is an unexplored potential for use of Tc-99m-MIBI imaging in a variety of diseases where P-gp has a probable important pathophysiological role. Tc-99m-MIBI imaging has not been used in renal transplant assessment and autoimmune disease up to now. It would be also interesting to investigate a role of Tc-99m-MIBI imaging in other P-gp mediated and linked diseases (see Chapter 7) such as neurodegenerative disease, including Alzheimer's disease (AD), and Parkinson's disease (PD), rheumatoid arthritis and inflammatory bowel disease.

In addition, Tc-99m-MIBI imaging modality may further be utilised for the development of novel imaging biomarkers in monitoring effects of important drugs that are transported by P-gp and known P-gp substrates or inhibitors, such as immunosuppressive drugs (CsA and Tacrolimus), Ca^{2+} channel blockers (Verapamil, Diltiazem), cardiac drugs (digoxin), dipyridamole, HIV protease inhibitors, antirheumatics (Methotrexate), some antibiotics (Rifampicin, Erythromicin), and many antineoplastic drugs (9).

1.2 Aims of project

The aim of the project is to develop a novel *in vivo* functional assay for ABC-transporters, including P-gp expression in humans using Tc-99m-MIBI, primarily in the kidneys, but also in the liver and its relation to expression in normal subjects and disease. It is hoped that this will extend our understanding of this membrane transport protein in human physiology and of the implications for P-gp-mediated drug resistance and toxicity and disease risk, particularly a response to immunosuppressive drugs such as calineurin inhibitors (CsA and Tacrolimus) in the context of development of nephrotoxicity and renal transplant rejection.

The aim of this work therefore was to investigate the renal and hepatic kinetics of Tc-99m-MIBI in relation to subject genotype, gender and other organs as a platform to develop an imaging assay for constitutional ABC/P-gp expression. In order to establish Tc-99m-MIBI for routine use in this context, I also set out to demonstrate that differential renal function (DRF), measured with Tc-99m-MIBI, is comparable to, and could therefore replace, DRF measured from Tc-99m mercaptoacetyltriglycine (MAG3).

A further aim was to demonstrate and quantify pharmacological ABC-transporter/P-gp suppression *in vivo* by Tc-99m-MIBI imaging illustrated by effect of CsA on Tc-99m-MIBI pharmacokinetics in relation to *ABCB1* genotype in a proof of principle study. This can be used as a platform for a development of an *in vivo* imaging assay to predict drug toxicity, dose selection and adjustment of treatment regimens of important drugs that are

also P-gp-substrates such as other calineurin inhibitors (Tacrolimus), some HIV drugs and antibiotics, Digoxin and Verapamil.

Chapter 2 General Methods

2.1 Study population

The local research ethics committee and the Administration of Radioactive Substances Advisory Committee of the United Kingdom approved the studies covered by these methods (Chapters 3, 4, 5 and 6). All participants gave written informed consent.

Two groups of subjects were recruited. Firstly, normal healthy subjects (potential kidney transplant donors) were recruited to validate Tc-99m-MIBI for measuring divided renal function (Chapter 3) and for establishing the normal kinetics of Tc-99m-MIBI in the kidney and liver (Chapter 4). The healthy potential kidney transplant donors who were referred to MAG3 renogram, as per standard pre-transplant assessment, were selected and recruited through the renal transplant assessment clinic with the help of transplant nurse in the period between May 2009 and November 2011.

Secondly, patients with skin disease but who were otherwise healthy were selected and recruited by a dermatology consultant in dermatology outpatients clinics, in the period between June 2012 and November 2013 to investigate the effect of pharmacological P-gp blockade, using CsA, on renal and hepatic Tc-99m-MIBI kinetics (Chapter 6).

Both groups of patients had dynamic and delayed static Tc-99m-MIBI imaging, 'formal' measurement of glomerular filtration rate (GFR) with Cr-51-EDTA and were genotyped for ABC transporter proteins.

The first group comprised 30 healthy prospective kidney transplant donors (age range 25 -72, mean 49 [SD 12.6] y; 13 male). On separate days (between 2 and 7), they had renography with Tc-99m-MAG3 and Tc-99m-MIBI.

The second group comprised 4 patients with skin disease, mostly psoriasis. They were recruited in the dermatology clinic and given an information sheet when the decision was made by the dermatologist to start treatment with CsA. They were given adequate time to decide if they wanted to take part.

The written consent was taken in Department of Nuclear Medicine, Royal Sussex County Hospital, Brighton and Sussex University Hospitals NHS Trust.

Nineteen normal volunteers and all 4 patients with skin disease were genotyped from a saliva sample for polymorphism in C3435 (exon 26; rs1045642), G2677T/A (exon 21; rs2032582), C1236T (exon 12; rs1128503) and G1199A (exon 11; rs2229109) using established Polymerase Chain Reaction (PCR) based techniques and restriction fragment length polymorphism techniques that are also already established.

2.2 Procedure/imaging for healthy potential kidney donors

2.2.1 Tc-99m-MAG3

Conventional renography was performed over 20 min following iv injection of 100 MBq Tc-99m-MAG3. Participants were well hydrated and asked to empty their bladders prior to injection.

2.2.2 Tc-99m-MIBI

A renogram acquisition protocol identical to Tc-99m-MAG3 was used following iv injection of 400 MBq Tc-99m-MIBI. In addition, posterior static images of the kidneys, abdomen and lower chest were acquired at 30 min and 2 h after injection.

2.2.3 Glomerular Filtration Rate

Glomerular filtration rate (GFR) was measured from routine Cr-51-EDTA plasma clearance on the same day as MAG3.

2.3 Procedure/ Imaging for patients

2.3.1 Tc-99m-MIBI scanning

Three Tc-99m-MIBI scintigraphies were performed. Tc-99m-MIBI scanning was performed prior to starting CsA and again at 1-2 weeks and 6-12 weeks post-treatment. This included continuous scanning for 30 min after injection of 400 MBq Tc-99m-MIBI, followed by a 5-min static view and tomographic imaging of kidneys. Further scanning was performed for about 25 min, starting 2 h after Tc-99m-MIBI injection, once again to include a 5-min static view followed by tomographic imaging.

2.3.2 Glomerular Filtration Rate

Glomerular filtration rate (GFR) was measured from routine Cr-51-ethylenediaminepentaacetic acid (Cr-51-EDTA) plasma clearance at

baseline and 6-12 weeks post-treatment, or earlier if the patient came off treatment.

2.3.3 Clinical assessment

Psoriasis severity was assessed with standard psoriasis severity scoring systems, i.e. Psoriasis Area and Severity Index (PASI) and Dermatology Quality of Life Index (DLQI).

2.3.4 Data acquisition for MIBI scintigraphy

Each subject was scanned supine with a large field of view gamma camera to include the posterior view of the kidneys, heart and bladder in the field of view (Table 2.1).

MAIN PLANAR IMAGING PARAMETERS	
Collimator	General purpose, Parallel Hole
Energy window	20%, centred at 140 keV, 3% offset
Matrix size	128x128W Dynamic and static images
Pixel size	4.51 mm
Time per frame	Dynamic: perfusion phase 60 x1s, the rest 60x20 s (total time 1260s i.e. 21 min) Static Image: 5 min

Table 2.1 The main acquisition parameters.

2.3.5 Effective dose

Effective dose per administration of 400 MBq of Tc-99m-MIBI is 4 mSv (66). The quantity of radiation delivered to the subject is equivalent to about 6

months of natural background radiation in Cornwall, or rather longer in other parts of the UK, where background radiation levels are lower (67). The risk is similar to that exposed to anyone driving 12,000 miles in a car.

2.4 Region of interest (ROI) placement and generation of time activity curves

2.4.1 Differential renal function (DRF)

Regions of interest (ROIs) were placed over the kidneys and bladder as per routine practice, with background correction based on ROIs over the tissue immediately below the poles of the kidney and aorta, as for Tc-99m-MAG3 renography. Differential renal function based on the initial 3 min of data, as for Tc-99m-MAG3 renography, was measured from the posterior view.

2.4.2 ROI for organ Tc-99m-MIBI kinetics

2.4.2.1 Kidney

For images acquired at 30 and 120 min, only the upper pole of the left kidney was analysed because of superimposed or overlying gastrointestinal activity frequently seen adjacent to the right kidney. ROIs were restricted to the parenchyma of the kidney, avoiding collecting system activity.

2.4.2.2 Liver, spleen and myocardium

Small ROIs were placed over the liver parenchyma (avoiding bile duct activity), over the spleen (avoiding the hilum), and over the left ventricular myocardium.

2.5 Data analysis

2.5.1 Data analysis for renography

To visually compare perfusion phase images, Tc-99m-MAG3 dynamic images were summed as 4 x 1-sec frames per image for comparison with the dynamic Tc-99m-MIBI series, which were displayed as 1-sec frames at 4-sec intervals due to 4 times higher administered Tc-99m-MIBI activity than Tc-99m-MAG3.

DRF was calculated for both Tc-99m-MAG3 and Tc-99m-MIBI using the initial 1-3 min of data from relative area under uptake phase of the renogram curves, as per routine clinical practice.

2.5.2 Data analysis for organ Tc-99m-MIBI kinetics

From renal Tc-99m-MIBI data, a) the 30 min/peak ratio and b) the exponential rate constant (*k*) based on the images at 30 min and 120 min were calculated. Peak count rate, which was usually at 2 or 3 min, was based on the same ROI as for 30 min. Similar ratios and *k* values were

calculated for the liver. For spleen and myocardium, only *k* values were calculated.

2.6 Genotyping

For genotyping, DNA was extracted from saliva using the Oragene kits – a non-invasive method that yields high quality genome DNA (www.dnagenotek.com). Nineteen of the 30 patients consented to genotyping from saliva samples for C3435 polymorphism (exon 26) using established PCR based techniques. I also investigated *ABCB1 (MDR1)* variants in exon 21 (G2677T/A), exon 12 (C1236T) and exon 11 (G1199A). Specific primers were used to amplify DNA across the polymorphisms and the PCR products subjected to restriction enzyme digestion followed by agarose gel electrophoresis to determine the individual genotype.

2.7 Statistics

Bland-Altman analysis was used to assess agreement between DRF respectively measured with Tc-99m-MIBI and Tc-99m-MAG3. Mean difference (bias) between the two tracers with respect to the contribution of the left kidney to total function and the standard deviation (SD) of this difference (precision) were measured.

The plotted data (histogram) confirmed that the distribution was normal (symmetric), therefore the use of mean and SD as measures of location and spread respectively was justified. Moreover, the sample size was large enough for the central limit theorem to hold, allowing for the use of parametric tests.

Renal indices were expressed as means ± SD. Homozygous negative (TT), heterozygous (CT) and homozygous positive (CC) genotypes were correlated with renal and hepatic indices and *k* values using ANOVA. Two-tailed *t*-testing was used to assess differences in renal and hepatic Tc-99m-MIBI elimination between male and female subjects.

Student's paired *t*-test and Pearson's correlation coefficient were used to compare and correlate *k* and GFR. ANOVA test for significance was used to compare the allele and genotype frequencies for the *ABCB1* SNPs in high and low expressers.

Chapter 3 Replacing Tc-99m-MAG3 with Tc-99m-MIBI for renography

3.1 Introduction

Functional investigations with radionuclides play a prominent role in the diagnostics and follow up of various kidney diseases (68). Renography is a non-invasive, widely available test that can evaluate renal function and urine transit in a single procedure (69) (70). The use of tracers that are taken up and excreted by the kidney allows the estimation of renal perfusion, divided function, collecting system drainage and the assessment of the lower urinary tract. The radiopharmaceutical is administered intravenously to the patient whilst they are in front of the gamma camera. A dynamic study is performed for between 20 and 40 min showing uptake of tracer into the kidneys and elimination into the bladder. The activity-time curves generated from this dynamic study are known as the renogram, which can be used to assess renal function and drainage. Renography can be supplemented by additional static images of kidneys and bladder after the end of the dynamic study (71).

Three tracers rely on tubular extraction and secretion: I-123-hippuran, Tc-99m-mercaptoacetyltriglycine (MAG3) and Tc-99m-ethylenedicysteine (EC). Tc-99m- MAG3 (tiatide) is the most widely used agent for renography. It gives good renal uptake and it is cleared almost exclusively by tubular secretion. It is the agent of choice in children and in patients with impaired renal function (71). The Administration of Radioactive Substances Advisory Committee (ARSAC) diagnostic reference level for adults is 100 MBq (66).

Tc-99m-diethytriaminepentaacetic acid (DTPA) is also widely used for renography. It is cleared only by glomerular filtration, and so can also be used for measurement of GFR. However the renal uptake is less than Tc-99m-MAG3 and so non-renal background is more significant in patients with poor renal function. Tc-99m-MAG3 has a greater renal extraction than Tc-99m-DTPA resulting in a lower background activity and a higher kidney to background ratio. For these reasons Tc-99m-MAG3 is preferred to Tc-99m-DTPA for estimation of DRF particularly in infants, for diuretic renography and indirect radionuclide cystography. Tc-99m-DTPA may be useful following renal transplantation when both blood flow as well as formal glomerular filtration rate (GRF) estimation is required (72) (73).

The relative function of each kidney, i.e. differential or divided renal function (DRF), is expressed as a percentage of the sum of the right and left kidneys. It is computed from the same time interval of the renogram, that is initial 1-3 min data of renogram and 60-120 s from the peak of the cardiac (vascular) curve. The European Association of Nuclear Medicine (EANM) guidelines (73) recommend either the integral method or the Patlak-Rutland plot method (74) (75) (76) (77) (78).

The information obtained during this initial three min interval, however, still contains non-renal activity (background), which should be subtracted. The tissue component and part of the vascular component can be removed by subtracting some activity around the kidney; the remaining part of the vascular component may be eliminated by using the Patlak /Rutland method of analysis (75) (79).

Tc-99m-MAG3 scintigraphy has been used for the purpose of estimation of renal function for approximately twenty years (80) (81) (82).

In the pre-transplant setting, functional renal imaging with Tc-99m-MAG3 or Tc-99m-dimercaptosuccinic acid (DMSA) is used in clinical practice to assess differential function of healthy potential kidney donors (83) (84).

Tc-99m-DMSA scintigraphy is also generally accepted procedure for estimation of differential kidney function, which is calculated from the posterior view by drawing regions of interest (ROI) around each kidney. A background ROI should also be drawn in any nearby non-renal area. The position of the background ROI makes very little difference except with very poorly functioning kidneys. Counts in the background region are used to subtract background counts from each kidney ROI (scaled for the relative size of the ROIs). DRF of each kidney should then be calculated from the percentage of background-subtracted counts in each kidney from the posterior view. This DRF may not be accurate if the two kidneys lie at significantly different depths (68) (85). An anterior view should then be obtained and background subtracted kidney counts calculated from this image. The geometric mean of the posterior and anterior background-subtracted counts in each kidney should then be calculated. This approach is regarded as the gold standard for measurement of DRF (72) (73) (86).

The second function, which can be assessed by renography, but not by DMSA scintigraphy, is the elimination or disappearance of the tracer from the kidney. The disappearance rate can simply be estimated by assessing the renogram curve: an early peak followed by a rapidly descending phase is

typical for normal excretion. An important delay in excretion is characterised by a continuously ascending curve (72) (73). Collecting system dilatation without obstruction can be diagnosed by observing a drainage response to an intravenously administered diuretic (69) (87).

Tc-99m-MIBI is a potentially interesting renal agent. As the only known mechanism of Tc-99m-MIBI elimination from renal tubular cells involves ABC transporter proteins, Tc-99m-MIBI kinetics may allow inference of renal P-gp/MRP1/2 status (88).

Although Tc-99m-MIBI has been used to study physiological MDR function in gut (89), liver (32) (89), blood-brain barrier (90) and lungs (91) (92), the kidney has received little attention despite an important potential role for P-gp in renal transplantation (26) (28). The kidney is relatively functionally complex in the setting of MDR because xenobiotics could access renal tissue either via glomerular filtration and tubular reabsorption or peritubular capillary blood. Likewise, elimination could occur either through tubular secretion, blockade of tubular reabsorption of filtered tracer or into peri-tubular capillary blood.

This is potentially clinically useful as calcineurin inhibitors (CNI) are also substrates for ATP-binding cassette (ABC) multi-drug resistance (MDR) transporter proteins, such as P-gp, so monitoring Tc-99m-MIBI pharmacokinetics may be useful for adjusting CNI treatment dose.

The main purpose of this study therefore was to demonstrate that DRF, as measured in the potential kidney donor with Tc-99m-MIBI, is comparable to that measured with Tc-99m-MAG3, so that Tc-99m-MIBI could replace Tc-

99m-MAG3 on a routine basis in the transplant setting. Secondly, the aim was also to develop a method for quantifying elimination of the Tc-99m-MIBI from the cells, which can potentially be used as an indirect assay for ABC-transporters/P-gp expression in the kidneys using Tc-99m-MIBI renography.

Methods and data analysis are described in the general methodology chapter (procedures /imaging for healthy kidney donors 2.1.1, 2.1.2 and 2.1.3).

3.2 Results

Tc-99m-MIBI and Tc-99m-MAG3 gave similar perfusion images (Figure 3.1). Although their patterns of renal elimination were different (Figure 3.4), differential renal function was not significantly different (Figure 3.3).

3.2.1 Tc-99m-MIBI renogram 0-20 min

3.2.1.1 Perfusion phase

Tc-99m-MIBI is an excellent perfusion agent and routinely used for the imaging of myocardial perfusion (93). It is also a known excellent vascular agent used to image angiogenesis in tumours (94).

Tc-99m-MIBI gave excellent high quality perfusion phase images with clear outlines of both kidneys. The tracer activity was seen in the kidneys as soon as activity was noted in aorta and at same time as the spleen.

Renal perfusion is as well portrayed using Tc-99m-MIBI as it is with Tc-99m-MAG3 allowing for different administered activities (Figure 3.1).

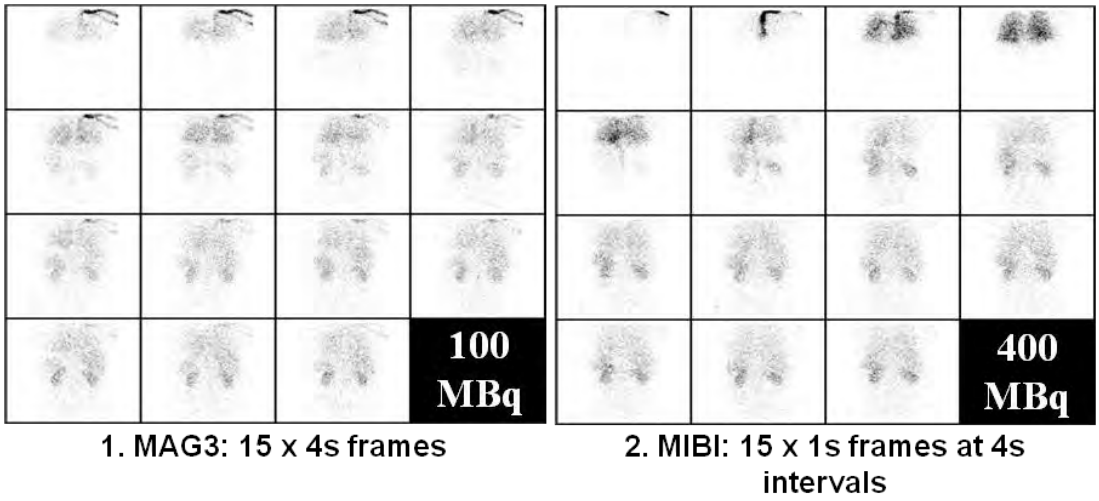

Figure 3.1 Dynamic imaging immediately following injection (perfusion phase) of 1) Tc-99m-MAG3 and 2) Tc-99m-MIBI. Please also see **Figure 3.6** Tc-99m-MAG3 renogram and **Figure 3.5** Tc-99m-MIBI Renogram.

To compensate for differing administered activities, frames for Tc-99m-MAG3 (100 MBq) are of 4 sec duration and continuous, while for Tc-99m-MIBI (400 MBq) 1-sec frames at 4-second intervals are shown in perfusion phase (Figure 3.1).

A typical Tc-99m-MIBI renogram is compared with a typical Tc-99m-MAG3 renogram. After an early peak and a relatively steep decline, the Tc-99m-MIBI renogram became relatively constant between 15 and 20 min. The time course of the steep decline corresponded with that of urinary accumulation of activity in the bladder.

Visual analysis showed high quality MIBI images, comparable to MAG3 with similar cortical outline.

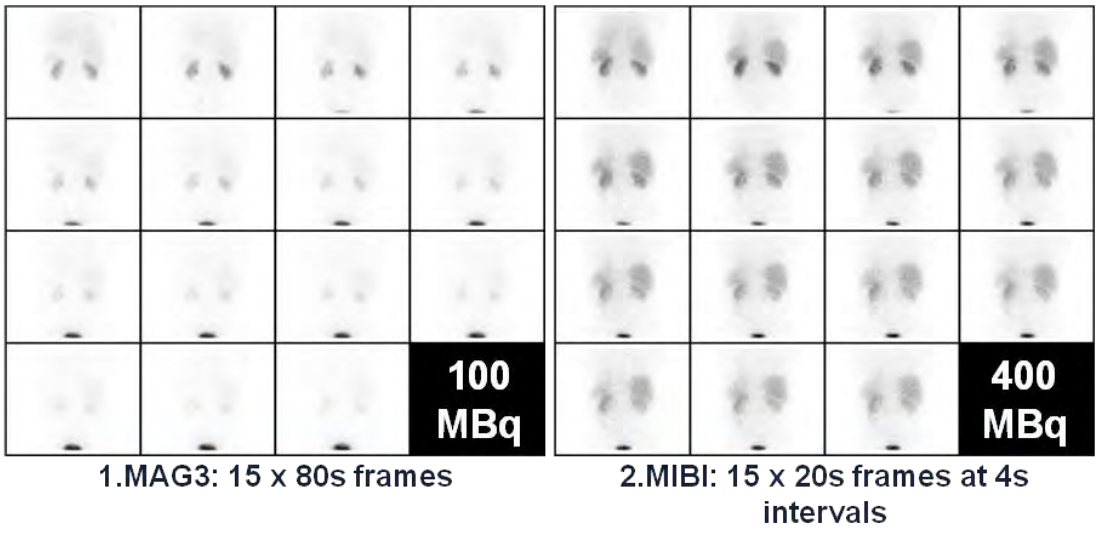

Figure 3.2 Dynamic imaging between 2 and 20 min following injection of 1) Tc-99m-MAG3 and 2) Tc-99m-MIBI. Please also see **Figure 3.6** Tc-99m-MAG3 renogram and **Figure 3.5** Tc-99m-MIBI Renogram.

To compensate for differing administered activities, frames for Tc-99m-MAG3 (100 MBq) are of 15 x 80s frames, while for Tc-99m-MIBI (400 MBq) 15 x 20s frames at 4s intervals are shown after 2 min post intravenous injection of tracers (Figure 3.2).

3.2.2 DRF based on Tc-99m-MIBI

The mean difference between Tc-99m-MIBI and Tc-99m-MAG3 with respect to the contribution of the left kidney to total function (bias) was -0.014% (not significantly different from zero) with a precision (SD) of 2.8% (Figure 3.3).

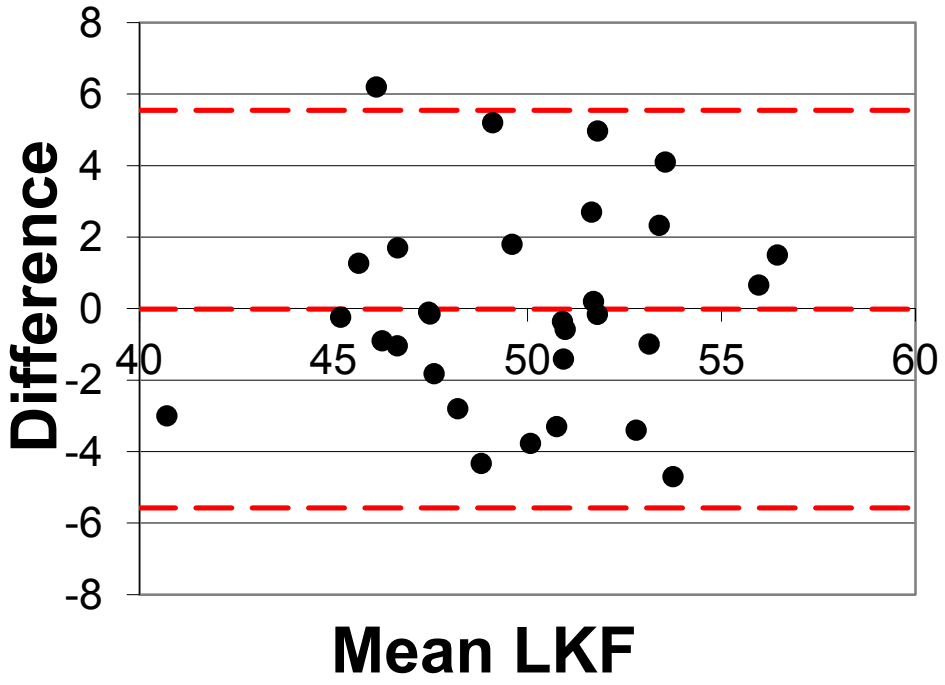

Figure 3.3 Bland-Altman plot of left kidney function (LKF): Tc-99m- MIBI vs. Tc-99m-MAG3 DRF.

The middle dashed line is the mean difference betweenTc-99m-MIBI ad Tc-99m-MAG3 DRF. The outlying dashed lines represent mean difference +/- standard deviations.

No correlation between difference and average DRF (mean difference: -0.014%, SD: 2.8%).

3.2.3 Renal elimination of Tc-99m-MIBI

3.2.3.1 Renal Tc-99m-MIBI handling: biphasic kidney curves and bladder curve

The Tc-99m-MIBI renogram was biphasic (Figure 3.4). The T1/2 of blood Tc-99m-MIBI clearance is 2.2 min (95), so that glomerular filtration will be largely be completed by 10-12 min. Elimination of activity by tubular secretion and/or excretion into the blood is then visualised from 12 min onwards.

The time course of bladder activity was also visualised.

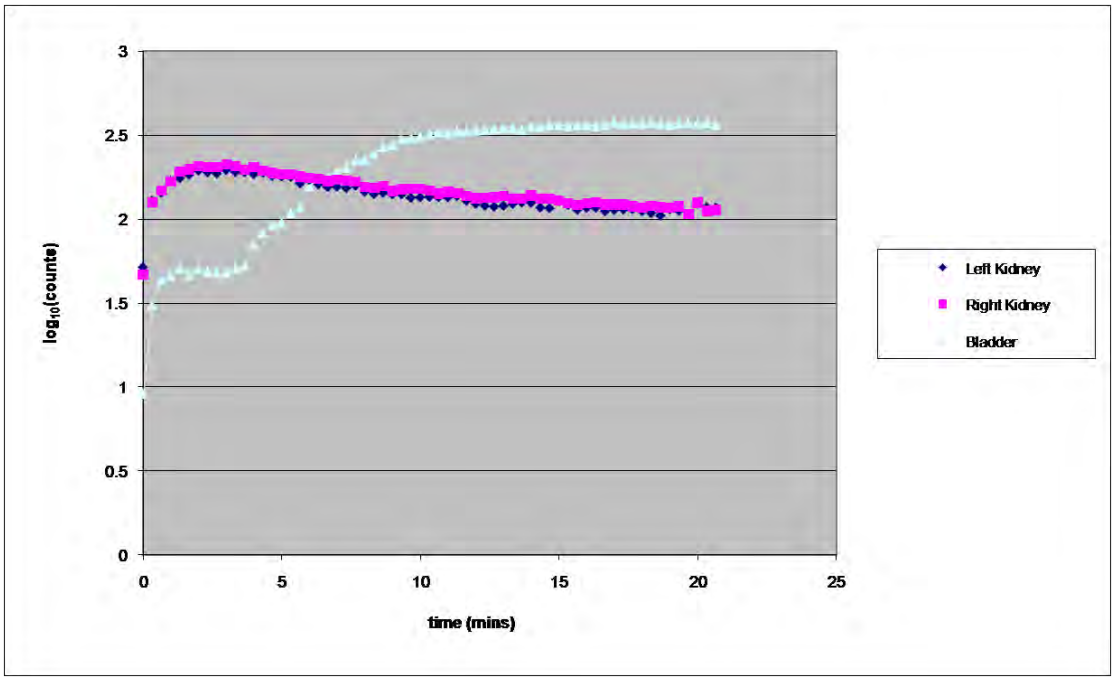

Figure 3.4 Biphasic Tc-99m-MIBI renogram curves and bladder curve.

3.2.4 3.2.4. Tc-99m-MAG3 vs. Tc-99m-MIBI Time-Activity curves

Both Tc-99m-MAG3 and Tc-99m-MIBI renogram curves showed similar and comparable uptake phases and times to peak and hence no significant difference in DRF, as described above. However, a different pattern of elimination or washout of the two tracers was seen (Figure 3.5 and Figure 3.6). P-gp is physiologically expressed in renal tubular cells, and pumps in the direction of tubular cell to lumen. Tc-99m-MIBI is filtered at the glomerulus and is also extracted directly from blood by the tubular cell and then presumably secreted into the tubular lumen. The time course of Tc-99m-MIBI renal activity was biphasic and therefore consistent with this handling (Figure 3.4 and Figure 3.5).

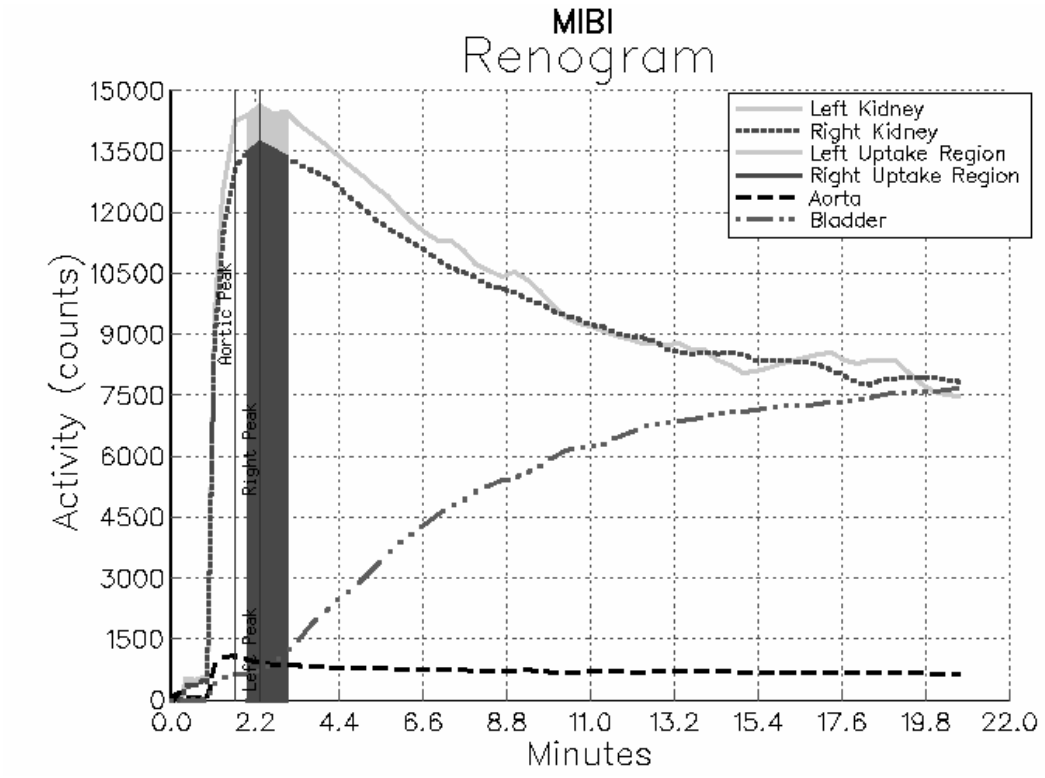

Figure 3.5 Tc-99m-MIBI Renogram

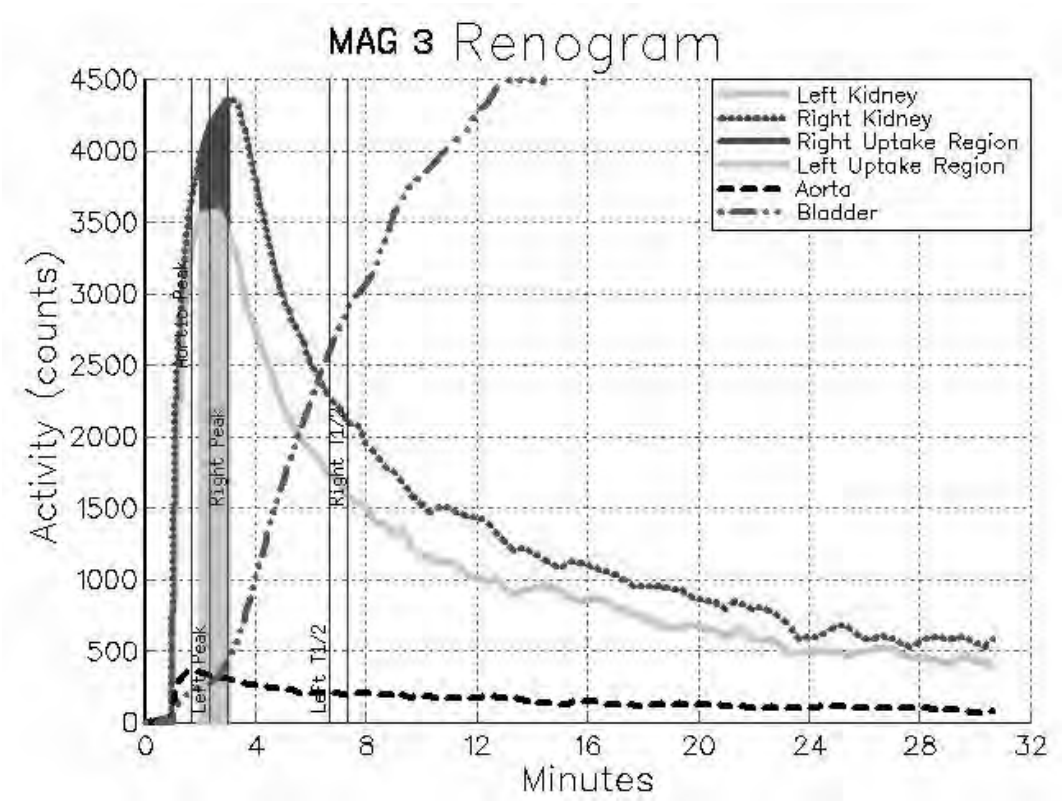

Figure 3.6 Tc-99m-MAG3 renogram

A typical Tc-99m-MIBI renogram (Figure 3.5) is compared with a typical Tc-99m-MAG3 renogram (Figure 3.6). After an early peak and a relatively steep decline, the Tc-99m-MIBI renogram became relatively constant, reaching a plateau around 15 min. Tc-99m-MIBI washout was shown to be slower than Tc-99m-MAG3 and after 15 min, elimination of Tc-99m-MIBI was very slow. The time course of the steep decline corresponded with that of urinary accumulation of activity in the bladder.

3.2.5 Delayed renal elimination (k)

Typical gamma camera appearances 30 and 120 min following Tc-99m-MIBI injection are shown in Figure 3.7 and Figure 3.8. Mean rate constant of elimination *(k)* from kidney was 0.0036 [0.0013] min^{-1} (Figure 3.9 and see Chapter 5, Table 5.1). Mean activity in the left kidney at 30 min, as a percentage of peak activity, was 49 [SD 5.6] %.

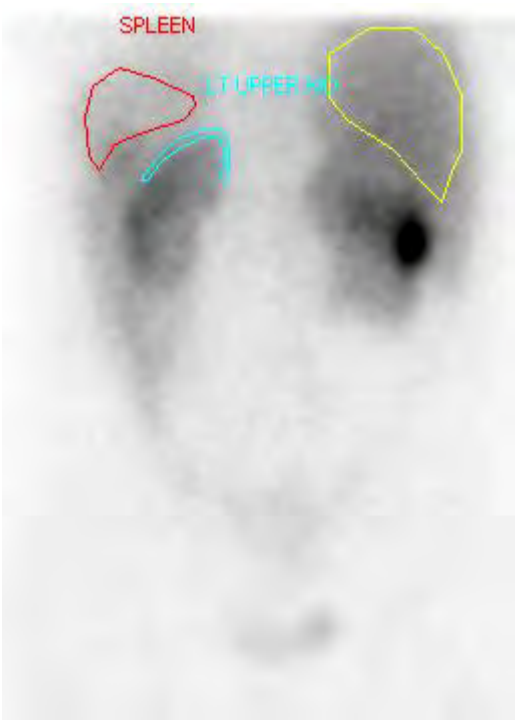

Figure 3.7 Tc-99m-MIBI Posterior images of abdomen 30 min post injection

Figure 3.8 Tc-99m-MIBI Posterior images of abdomen 2 h post injection

Figure 3.7 and Figure 3.8 demonstrated posterior gamma camera images obtained 30 min and 120 min following injection of Tc-99m-MIBI. Regions of interest are also shown for kidney, spleen and liver and Tc-99m-MIBI handling by those organs and myocardium is described in Chapter 5.

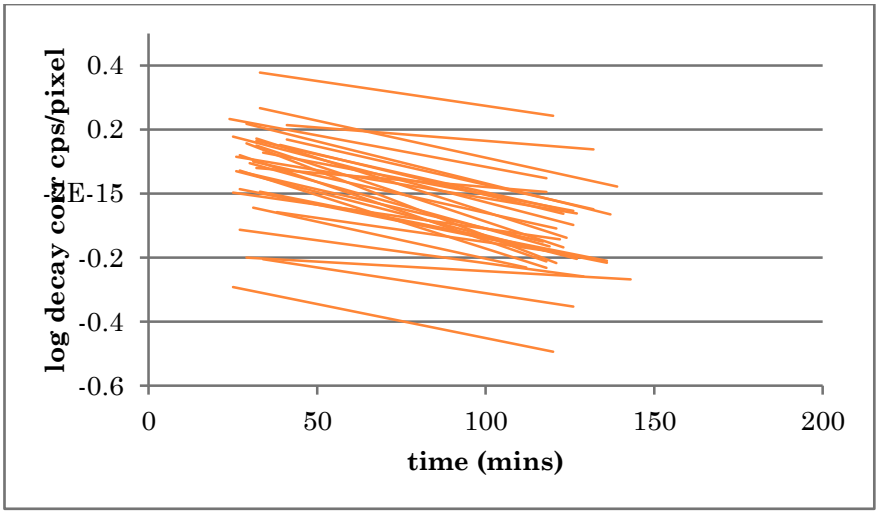

Figure 3.9 Composite graph of log decay-corrected renal Tc-99m-MIBI "washout" in 30 healthy prospective kidney transplant donors

3.3 Discussion

3.3.1 Comparison of Tc-99m-MIBI with Tc-99m-MAG3: differential function and perfusion

Tc-99m-MIBI gave DRF values very close to those of Tc-99m-MAG3 and can therefore be used routinely to derive DRF in clinical practice. Moreover, Tc-99m-MIBI gave excellent high quality perfusion phase images with clear outlines of both kidneys. The tracer activity was seen in the kidneys as soon as activity was noted in aorta and at same time as the spleen. From visual analysis, Tc-99m-MIBI perfusion images were similar, if not superior to those of Tc-99m-MAG3 after allowance was made for different administered activities. Although the effective dose from Tc-99m-MIBI is higher than that from Tc-99m-MAG3 using the administered activities described (400 MBq of Tc-99m-MIBI was used as for routine clinical scanning of other organs e.g. parathyroid or myocardium vs. 100 MBq of Tc-99m-MAG3 (66)), it is still

reasonable, well within diagnostic limit and justified in view of the additional potential diagnostic information given by Tc-99m-MIBI, but also more appropriate for use in single photon tomographic imaging. Both, ARSAC (66) and Ethics committee have approved this dose for this research project.

3.3.2 Tc-99m-MIBI elimination: potential use in renal transplant work up

Tc-99m-MIBI renography could be useful in renal transplant work up. In the pre-transplant setting, Tc-99m-MIBI can replace Tc-99m-MAG3 in the assessment of differential renal function in healthy kidney donors.

Tc-99m-MIBI appears to behave as both a filtration (like Tc-99m-DTPA) and tubular (like Tc-99m-DMSA) agent (96), although the exact kinetics of early elimination require further study. Hurwitz et al. described that Tc-99m-MIBI showed similar scan appearances to Tc-99m-DTPA (97). It should therefore be a useful radiopharmaceutical for renal pre-transplant workup. In addition, as Tc-99m-MIBI is a known Pg-p substrate, it could potentially provide additional information predicting renal graft outcome in recipients in post-transplant assessment. However, its general diagnostic value in post-transplant applications awaits further experience.

Radionuclide tests are generally valuable in renal transplantation since they provide a non-invasive means to evaluate transplant function qualitatively and quantitatively, and also screen for surgical complications. Scintigraphic studies are able to separate function of the graft from residual function of the native kidneys or any remaining prior failed graft (84). There are a wide

variety of techniques advocated for renal transplant imaging. In many centres, baseline scintigraphic studies are obtained shortly after transplantation; in others they are only done when complications occur. An advantage of renography is that it provides functional information at the time of the study, while creatinine assessment lags behind. Because of this, it can be helpful in evaluating the recovering of function after acute tubular necrosis (ATN) or rejection. However, the use in differential diagnosis of ATN and rejection is controversial. Heaf et al. in their study found that renography performed early after transplantation could predict primary graft non-function, long time graft function, low discharge Cr-51-EDTA clearance, and low 1- and 5-year graft survivals, while renography performed at discharge could predict late (>6 months) graft loss (98). However, the renogram changes do not contribute to the differential diagnosis between acute rejection, acute tubulo-interstitial nephropathy and CsA toxicity. In obstruction, it can be used with Furosemide. Urinary leaks may be identified by the presence of radioactivity in an abnormal location. If hypertension develops, captopril renography can identify transplant and renal artery stenosis as the cause (83) (84) (99).

Renal transplant dysfunction is a devastating event and appropriate management of immunosuppression and complications that arise in these patients is necessary to avoid graft failure.

Currently, ultrasound (US) is the primary modality for evaluating renal transplant dysfunction (100). Radionuclide tests using Tc-99m-MAG3 or Tc-99m-DTPA can evaluate renal transplant function qualitatively and quantitatively, and screen for surgical complications (101). MRI and CT can

also be used for evaluating renal transplants; however, there are concerns of using MRI due to gadolinium toxicity in a population at risk of renal dysfunction (102) (103) (104).

Comprehensive evaluation of renal transplants has been important in differential diagnosis of medical and surgical complications in the early post-transplantation period and long-term follow-up, including selection of patients for biopsy and for various drug regimens. This is true especially in patients with ATN and in patients with developing chronic rejection. Improving indices of renal function (effective renal plasma flow, uptake of tubular tracers) can indicate resolution of tubular injury, such as in ATN, while there is still no improvement in plasma creatinine. In patients with chronic rejection, plasma creatinine increases only after approximately 30% of renal function is lost due to graft fibrosis. Early recognition of this condition could permit treatment and delay re-transplantation (83) (84).

Of relevance in this context is the finding of Pedersen at al. that Tc-99m-MIBI parenchymal uptake is reduced more than perfusion in acute ischaemia-reperfusion injury, which they interpreted as mitochondrial injury (105).

Tc-99m-MIBI retained in tissues following early elimination is bound to mitochondria. The rate of elimination from 30 min therefore reflects mitochondrial release, but the predominant routes of excretion from the kidney, i.e. tubular secretion or elimination into blood, require further elucidation.

Additionally, evidence is growing that individual P-gp response to CNI may be linked to nephrotoxicity or rejection. Koziolek et al. showed histologically

that high renal P-gp levels are associated with rejection and low levels with nephrotoxicity (26).

A simple, widely available non-invasive diagnostic imaging test that would inform clinicians of the relative risks of nephrotoxicity and rejection and help tailor individual drug regimens could transform the outcome of renal transplantation in many patients. The only currently available technique is renal biopsy, which is invasive and potentially harmful (but with low reported fatality rate of 0.07%) to the graft (106).

Moreover, histological interpretation of biopsy specimens is not straightforward and histopathologists disagree concerning the diagnosis of calcineurin inhibitor nephrotoxicity.

P-gp is involved in the cellular efflux of immunosuppressants that are also nephrotoxic. The only known mechanism of Tc-99m-MIBI elimination from cells involves ABC transporter proteins, so Tc-99m-MIBI kinetics may allow inference of renal P-gp status (88) and Tc-99m-MIBI renography may represent a novel imaging assay for the assessment of functionality of ABC – transporters, including P-gp in kidneys, which is of clinical relevance in renal transplantation.

3.3.3 Other potential applications for Tc-99m-MIBI renography in clinical practice

3.3.3.1 Simultaneous assessment of differential renal function and myocardial perfusion imaging

Tc-99m-MIBI is an established agent for assessment of myocardial perfusion (93) and hence Tc-99m-MIBI scintigraphy offers the potential to combine myocardial and renal imaging in clinical practice in patients with suspected or known coronary artery disease. This idea is not new. Hurwitch et al. demonstrated that ancillary renography during rest injection of Tc-99m-MIBI could be useful tool for assessment of selected patients with suspected ischaemic heart disease and hypertension (107). Hypertensive patients referred for myocardial perfusion scintigraphy have an increased incidence of renovascular disorders. Subsequent quantitative analysis confirmed that Tc-99m-MIBI has higher renal uptake, but less excretion than Tc-99m-DTPA (97). Hurwitz et al. correlated Tc-99m-MIBI and Tc-99m-DTPA studies in hypertensive patients with a spectrum of findings, including aortic aneurysms, asymmetry due to renovascular disease, cysts, bilateral renal dysfunction, and horseshoe kidney, concluding that Tc-99m-MIBI images had persisting background activity in the liver and spleen, but showed renal structure and function in adequate detail (97). However, this is the first study to compare Tc-99m-MAG3 with Tc-99m-MIBI, confirming that Tc-99m-MIBI can be a good renal agent.

3.3.3.2 Ancillary Tc-99m-MIBI renography in pre-operative risk assessment of patients with vascular disease

Non-invasive assessment of myocardial perfusion is used pre-operatively in patients with peripheral vascular disease, including prior to abdominal aortic aneurysm repair (108) (109) (110). Myocardial perfusion imaging (MPI), allows detection of coronary artery disease and evaluation of myocardial viability and function. MPI is therefore a useful test for prediction of peri-operative cardiac risk and pre-operative risk stratification (111) (112) (113).

In some of these patients, renal assessment by imaging is also required to plan surgery and stent placement. In a substantial proportion of these patients, estimation of differential renal functional and renal perfusion, which is concurrent with myocardial imaging, could extend the clinical usefulness of the test and help to plan vascular surgery.

In addition, recent studies have shown that progressive renal dysfunction may develop in patients after endovascular aneurysm repair (EVAR). Data are conflicting about the effect of EVAR on renal function compared with open repair (OR).

After EVAR, there may be a continuous decline in renal function and some patients develop contrast-induced nephropathy (CIN). This seems independent of pre-existing renal insufficiency. Furthermore, the risk of renal function impairment after EVAR should be taken into consideration in selecting patients with preoperative renal insufficiency (114) (115) (116). The role of Tc-99m-MIBI scinitgraphy in the assessment of renal function and prediction of deterioration of renal function in these patients, while

concurrently performed during the assessment of myocardial perfusion, should be investigated.

3.4 Limitations

I have correlated Tc-99m-MIBI with Tc-99m-MA3 handling in healthy kidney donors with normal renal function. The only occasion when a dynamic renogram may provide inadequate differential function is in the presence of very poor renal function (117) or when there is an ectopic kidney present (85). In these circumstances Tc-99m-DMSA is the agent of choice (86) (118). In patients with unilateral hydronephrosis, dynamic renal scintigraphy in 25% has shown 'supranormal' renal function. The explanation for this finding is unclear, but in most cases it is caused by technical problem, likely the inadequate background subtraction of Tc-99m-MAG3 taken up in the liver (119) (120). Further studies are required for estimation of DRF with Tc-99m-MIBI in patients with impaired renal function and unilateral hydronephrosis. More importantly, further studies are planned to investigate Tc-99m-MIBI kinetics in renal transplant patients.

In delayed views, while assessing Tc-99m-MIBI elimination, activity in the background, particularly within the overlying bowel has caused occasional difficulties with positioning region of interests and analysing scans. This can become even more apparent in imaging the graft because anterior images are required in this clinical indication. Usually, the left upper pole in native kidneys has been rather clear of this superimposed activity and was used for analysis. To overcome this issue, SPECT images were obtained in

subsequent pharmacokinetic Tc-99m-MIBI studies in patients before and after CsA treatment (see Chapter 6).

3.5 Conclusion

In conclusion, Tc-99m-MIBI and Tc-99m-MAG3 show different patterns of renal elimination, but good agreement with respect to perfusion phase imaging and differential renal function estimation. DRF can be accurately measured with Tc-99m-MIBI and hence Tc-99m-MIBI can replace Tc-99m-MAG3 for pre-transplant work-up (121). Tc-99m-MIBI may also be useful in other clinical situations, such as simultaneous assessment of renal function and myocardial perfusion in patients undergoing myocardial perfusion imaging with Tc-99m-MIBI. Tc-99m-MIBI renography may be used as ancillary tool for assessment of renal function in hypertensive patients referred for MPI or for pre-operative risk assessment in surgical planning for major vascular surgery, such as abdominal aortic aneurysm repair. Its role in the potential assessment of renal function and prediction of outcome in patients undergoing EVAR is yet to be investigated.

The rate of renal Tc-99m-MIBI elimination may represent an *in vivo* assay of renal ABC-transporters/P-gp expression and Tc-99m-MIBI renography may therefore be a useful, novel imaging modality in renal transplantation, and a novel assay for monitoring and/ or predicting P-gp-mediated drug-induced nephrotoxicity or allograft failure in the setting of renal transplantation, thereby providing useful information regarding dose selection not only of immunosuppressants, but also other nephrotoxic drugs that are ABC/P-gp substrates.

Chapter 4 Physiological renal and hepatic Tc-99m-MIBI kinetics

4.1 Introduction

MDR proteins are widely expressed physiologically, generally at critical biological membranes, including the blood-brain barrier (BBB) (122), hepato-biliary (123), gastro-intestinal (89) and renal tubular epithelia (26), and the pulmonary blood-gas barrier (8). The location of MDR proteins within the cell is such as to prevent xenobiotics from entering the body or to promote their elimination from the body. Thus, they are located in the bronchopulmonary epithelium on the airway side of the cell, in the renal tubular epithelium on the luminal side of the cell, in hepatocytes on the bile canalicular side of the cell and in the BBB on the luminal side of the endothelial cell. There are a growing number of publications on the physiology of ABC (MDR) proteins, focussing mainly on the gut, lungs and blood-brain barrier (BBB), but to a lesser extent, the liver and kidneys.

As previously described (Chapters 1 and 3), Tc-99m-MIBI is a substrate of ABC/P-gp used to image ABC/P-gp expression in several settings, especially cancer in which it has been shown that tracer accumulation correlates inversely with immunohistochemical P-gp expression and predicts response to drug treatment (124) (125).

Physiological studies of P-gp expression with Tc-99m-MIBI are also important, especially in the liver because of the impact of the tracer on myocardial perfusion imaging (126), and in the kidney in relation to the

potential imaging of transplant rejection and nephrotoxicity of anti-rejection drugs (26).

The aim of this work was to study, compare and contrast the normal renal and hepatic kinetics of Tc-99m-MIBI elimination in order to gain insight concerning physiological ABC/P-gp function in these organs (96).

4.2 Methods

Thirty healthy kidney transplant donors received intravenous Tc-99m-MIBI followed by dynamic scintigraphy for 20 min and static imaging at 30 and 120 min. Time-activity curves were generated from parenchymal ROIs. An assumed mono-exponential Tc-99m-MIBI blood clearance with rate constant of 0.3 min^{-1} was used to predict the Tc-99m-MIBI that would have accumulated in the organs had none left. The activities leaving were then calculated by subtraction and expressed as percentages of the predicted total accumulated activities.

4.2.1 Imaging

Each participant received approximately 400 MBq of Tc-99m-MIBI by bolus intravenous injection followed by continuous dynamic imaging over the abdomen using a double-headed gamma camera at a frame rate of one per minute up to 20 min. Accurately timed static images were obtained at about 30 and 120 min post-injection.

Within 7 days of the Tc-99m-MIBI study, glomerular filtration rate (GFR) was measured using Cr-51-ethylenediaminepentaacetic acid (EDTA) from 4 blood samples taken at 120, 160, 200 and 240 min post-injection.

4.2.2 Data analysis

Regions of interest (ROI) were placed over the parenchyma of the left kidney and right lobe of the liver, avoiding collecting system and bile duct activity, respectively. Time-activity curves were generated up to 20 min (1 frame per min; phase 1). The decrease in count rate between the 30 and 120 min images was assumed to be exponential for both organs and expressed as $\%min^{-1}$.

The activities leaving the kidney and liver over the duration of the lifetime of Tc-99m-MIBI in the blood stream were measured as percentages of the total activities that would have accumulated within the organs if none had left. The total accumulated activity was estimated by fitting an exponential function, with rate constant *k,* to the first two frame counts of the dynamic (phase 1) time-activity curve. This assumes that no activity had left the organ by 120 sec.

Then

$$y(t) = A(1 - e^{-kt}) + B$$

The predicted total count rate is (A+B). B is introduced because of timing variations in relation to the injection time.

This approach is analogous to that used in the measurement of renal output efficiency in isotope renography in which activity leaving the kidney is expressed as a percentage of the total taken up from the blood (127). *k* is equal to the rate constant with which Tc-99m-MIBI leaves blood and was assumed to be 0.3 min^{-1} (corresponding to a Tc-99m-MIBI halftime in blood of 2.2 min) (95).

4.2.3 Liver

The frame-by-frame activity in the liver was subtracted from the predicted total accumulated activity (A+B) and expressed as a percentage of A+B to give the elimination curve (Figure 4.1). The differential of the elimination curve was then obtained by subtracting the counts in each one-minute frame of the curve from the counts in the preceding frame to give the liver outflow concentration-time curve (Figure 4.1). The average of the activity in the 11^{th} and 12^{th} frames of the elimination curve was recorded as the percentage elimination of tracer over the lifetime of Tc-99m-MIBI in the blood. The 11^{th} and 12^{th} frames were chosen because this is the earliest time at which an exponential function with a halftime of 2.2 min (the assumed blood Tc-99m-MIBI disappearance curve) has decreased to <5%, so their average time corresponds to the time at which Tc-99m-MIBI blood clearance was almost completed.

4.2.4 Kidney

The same analysis was applied to the kidney to give the percentage elimination curve from the kidney. The average of the activity in the 15^{th} and

16th frames of the elimination curve was recorded as the percentage renal elimination of tracer over the lifetime of Tc-99m-MIBI in the blood. The 15th and 16th frames (i.e. later than those used for the liver) were chosen to allow for the transit time of Tc-99m-MIBI through the renal parenchyma.

GFR was calculated using the slope-intercept approach and scaled to body surface area (BSA) of 1.73 m^2. One-compartment correction was performed using the equation of Brochner-Mortensen (128).

4.2.5 Statistics

Values were expressed as mean (SD). The plotted data (histogram) confirmed that the distribution was normal (symmetric), therefore the use of mean and SD as measures of location and spread respectively was justified. Moreover, the sample size was large enough for the central limit theorem to hold, allowing for the use of parametric tests.

Two-tailed Student *t*-testing was used to assess differences between liver and kidney in both Tc-99m-MIBI elimination phases. Pearson correlation analysis was used to test associations between GFR and renal elimination and between liver and kidney elimination rates in both phases.

4.3 Results

4.3.1 Liver

4.3.1.1 Phase 1

The liver time-activity curve generally increased to a peak at about 10 min before declining (Figure 4.1), reminiscent of Tc-99m-HIDA hepatic time-activity curves. The elimination curve (difference between recorded and predicted curves) generally increased rapidly over 10-15 min and then rose more slowly. The derived outflow curves corresponded to the biphasic nature of the elimination curve (Figure 4.1) consistent with early rapid elimination, over 11-12 min of a substantial percentage of the total hepatic activity accumulated (A+B). This percentage was highly variable, ranging from 5 – 56% (mean 30 [14%]) of A+B. The remaining activity was eliminated more slowly, contributing a small 'tail' to the outflow curve (Figure 4.1).

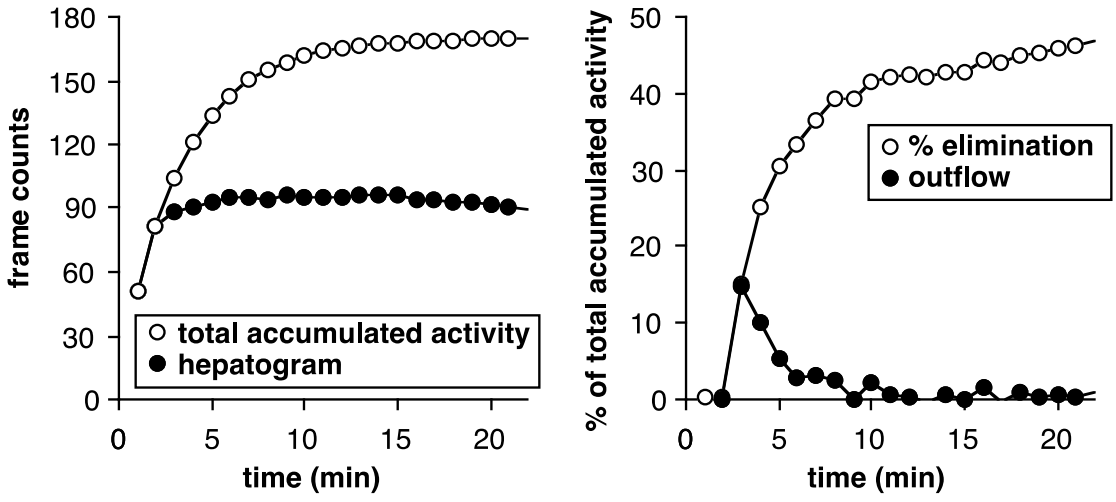

Figure 4.1 Intrahepatic Tc-99m-MIBI handling.

Left panel: the total activity accumulated by the liver (open circles) was estimated from a monoexponential function with rate constant 0.3 min^{-1} that was forced to go through the first and second frame counts. The recorded hepatogram is shown as closed circles.

Right panel: the percentage activity eliminated from the liver (open circles) is the difference between the total predicted activity and the recorded hepatogram, expressed as a percentage of the total accumulated activity at 20 min. The estimated hepatic venous outflow concentration curve is the differential of the % elimination curve (closed circles). In this patient, 42% of the total accumulated activity had been eliminated by 11-12 min, the time at which the blood Tc-99m-MIBI concentration falls below 5%. Note the shape of the % elimination curve, the later part heralding the start of the second phase, assumed to be activity slowly released from hepatocyte mitochondria.

4.3.1.2 Phase 2

Between 30 and 120 min, activity left the liver at a mean rate of

1.02 (0.23) $\%min^{-1}$.

4.3.2 Kidney

4.3.2.1 Phase 1

After an early peak and a relatively steep decline, the kidney activity-time curve became essentially constant between 15 and 20 min (Figure 4.2) reaching a level of 31 (5)% of the predicted total accumulated activity and

corresponding to 69 (5)% rapidly eliminated. The time course of this steep decline corresponded with that of urinary accumulation in the bladder.

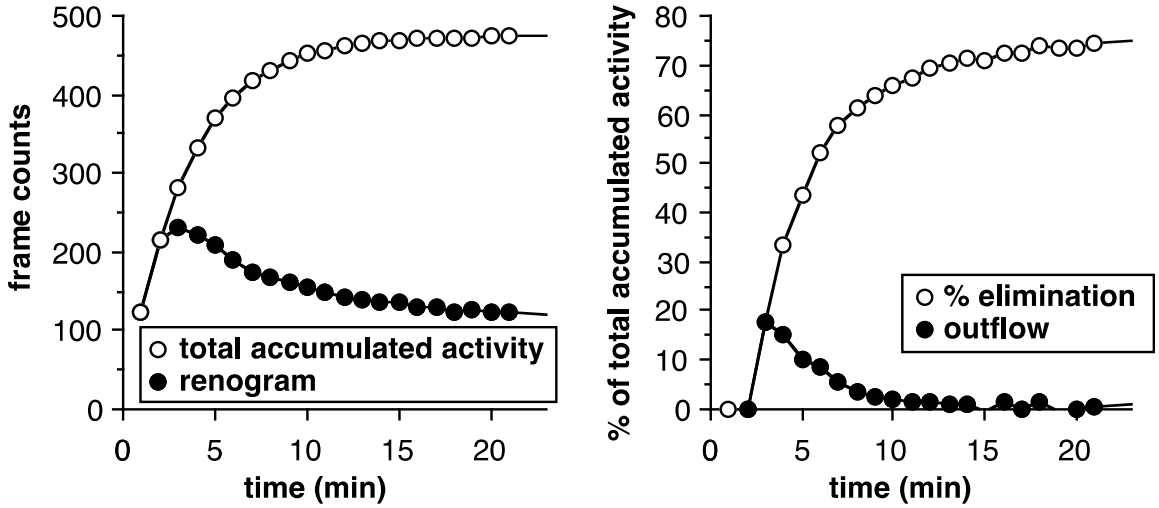

Figure 4.2 Intra-renal Tc-99m-MIBI handling.

Left panel: the total activity accumulated by the kidney (open circles) was estimated as for the liver. The recorded renogram is shown as closed circles.

Right panel: the percentage activity eliminated from the kidney (open circles) is the difference between the total predicted activity and the recorded renogram, expressed as a percentage of the total accumulated activity at 20 min. The estimated renal venous outflow concentration curve is the differential of the % elimination curve. In this patient, 72% of the total accumulated activity had been eliminated by 15-16 min, the time at which the blood Tc-99m-MIBI concentration falls below 5%, plus 3-4 min for intra-renal transit. Note the biphasic nature of the % elimination curve. The second phase, as for the liver, is assumed to be predominantly activity slowly released from the tubular cell, probably from mitochondria, by ABC transporter proteins including P-gp.

4.3.2.2 Phase 2

Between 30 and 120 min (phase 2), activity left the kidney at a rate of 0.36 (0.13) %.min^{-1} ($p < 0.001$ versus phase 2 in the liver).

4.3.2.3 Correlation with GFR

GFR/BSA ranged from 72 to 125 [mean 94 (13) ml.min^{-1}.1.73 m^{-2}]. There were no correlations between GFR/BSA and renal elimination rates in either phase.

4.3.3 Correlation between liver and kidney MIBI elimination

There were no correlations between the activities respectively eliminated by the liver and kidney either in phase 1 (Figure 4.3) or phase 2. There were no correlations between phase 1 and phase 2 elimination rates in either organ.

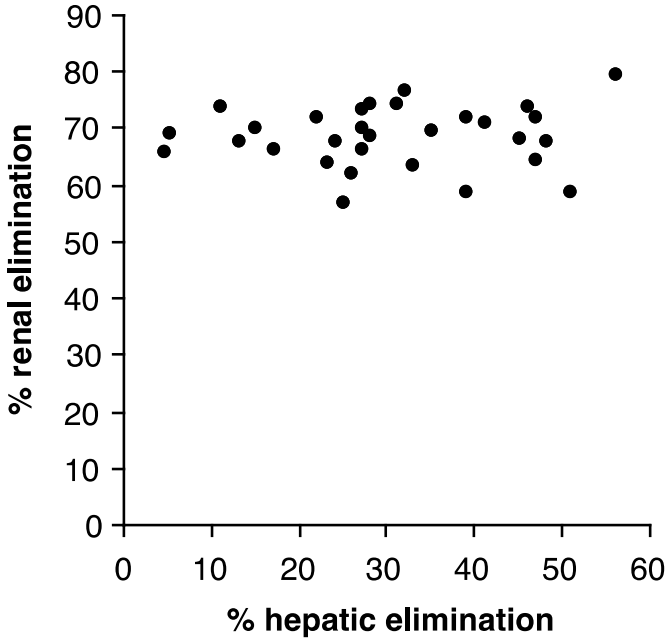

Figure 4.3 Relation between percentages of activities respectively eliminated from the liver at 11-12 min post-injection and from the kidney at 15-16 min post-injection.

Note the much wider variation in values for the liver. No correlation is evident.

4.4 Discussion

4.4.1 Hepatic handling of Tc-99m-MIBI

A variable proportion of total accumulated hepatic activity was rapidly eliminated from the liver over the period post-injection of the Tc-99m-MIBI lifetime in blood. Tc-99m-MIBI was previously shown to leave blood with a halftime of 2.2 min, so that by 11 min, the blood Tc-99m-MIBI concentration would have decreased to <5% of its starting value. As Tc-99m-MIBI is a P-gp substrate, the amount of activity re-entering hepatic parenchyma from bile is presumably dependent on the expression of P-gp at the bile/hepatocyte barrier. The proportion of activity rapidly eliminated was highly variable (5-56% of total predicted accumulated activity), perhaps as a result of variable P-gp expression at the bile/hepatocyte barrier, but this remains to be determined with experiments in which P-gp is inhibited.

The activity that is not rapidly eliminated is likely to enter mitochondria. This would therefore range from 42-95% of total activity cleared from blood by the liver. Elimination of Tc-99m-MIBI from 30 min post-injection, which occurs at a rate of ~1% per min, presumably depends on the rate of escape from mitochondria (47) and subsequent prevention of re-entry into the hepatocyte from bile. Also, some transport of Tc-99m-MIBI from hepatocyte back into blood, as occurs with the organic anions such as hepatobiliary iminodiacetic acid (HIDA), bromosulphthalein and bilirubin, cannot be excluded, although it must be small as negligible Tc-99m-MIBI remains in blood beyond 20 min post-injection. A model representing Tc-99m-MIBI kinetics in the liver is therefore complex and illustrated in Figure 4.4.

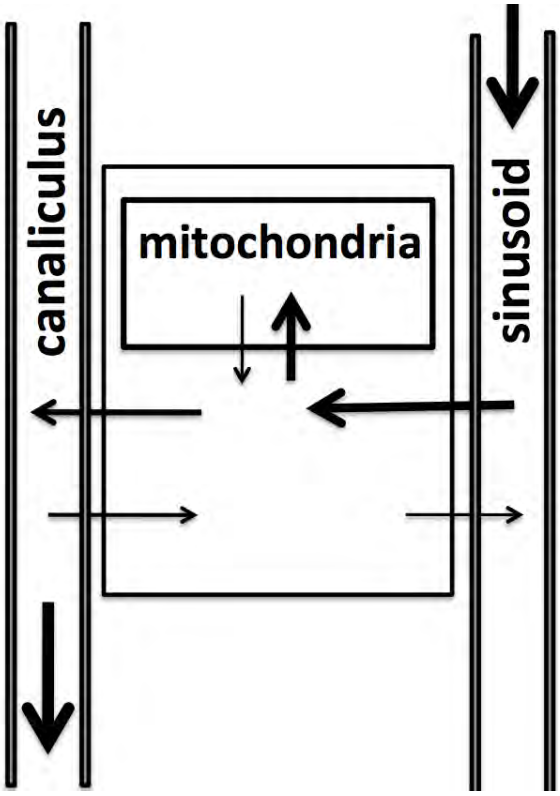

Figure 4.4 Proposed model for intrahepatic Tc-99m-MIBI kinetics.

4.4.2 Renal handling of Tc-99m-MIBI

The renal handling of Tc-99m-MIBI contrasts with hepatic handling. Firstly, the proportion of activity eliminated over the lifetime of Tc-99m-MIBI in blood is much greater, amounting to about 70%. Secondly, this proportion is much less variable (coefficient of variation of 7% compared with 45%; Figure 4.3). Nevertheless, the finding of significant rapid tracer elimination from the liver over the Tc-99m-MIBI lifetime in blood is important because it implies that the same process may occur in the kidney via tubular secretion. It would, however, be obscured by filtered tracer. The greater early elimination of tracer from the kidney compared with the liver is therefore almost certainly the result of superimposed filtration of tracer, especially as it coincided in

time with the appearance of urinary activity in the bladder. A lower coefficient of variation combined with a greater proportion of rapidly eliminated activity would suggest that most of the latter is via filtration rather than tubular secretion, though this remains to be proved. As in the liver, the retained activity is released slowly and is presumably governed firstly by the rate of mitochondrial release [12] and secondly by the P-gp activity at the tubular-luminal interface maintaining secreted activity within the renal tubular lumen. The model for renal handling is the same as the model for the liver with, in addition, a pathway for glomerular filtration (Figure 4.5).

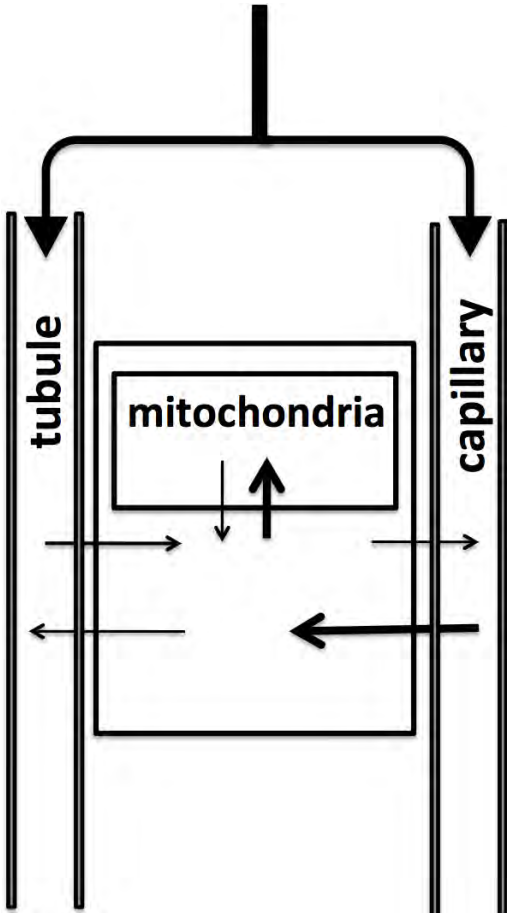

Figure 4.5 Proposed model for intra-renal Tc-99m-MIBI kinetics.

4.4.3 Study limitations

There are several limitations to this study. Firstly, a simplified approach to predict total activity cleared by the kidney and liver was applied, using only the first 2 points in the time-activity curves and a simple analytical approach. Whilst it is unlikely that any activity leaves the kidney before 2 min post-injection, this assumption may be less secure for the liver. Activity leaving the liver before 2 min would lead to underestimation of the total amount accumulated and overestimation of the proportion of activity rapidly eliminated over the first 10 min.

Secondly, large quantities of Tc-99m-MIBI enter the gastro-intestinal tract. The left kidney is less vulnerable to this artefact, explaining why analysis was restricted to this kidney. Gastro-intestinal activity has less influence on liver counts as it is in general moving away from the parenchymal ROI over the liver. These ROIs, nevertheless, like those over the kidney, are necessarily small in order to be restricted to the parenchyma and be free of 'contamination' by biliary activity.

Thirdly, in order to predict the total accumulated activities in kidney and liver, we assumed that Tc-99m-MIBI is cleared from blood exponentially with a rate constant of 0.3 min^{-1}. This approach is supported by the similarity between the time courses with which the renal time-activity curve approached the 15 min plateau and the predicted total accumulated activity approached its maximum (Figure 4.2). Using a rate constant of 0.25 min^{-1} (corresponding to a Tc-99m-MIBI half-life in blood of 2.8 min) instead of 0.3 min^{-1} increased the value of A + B by about 12% (data not shown). This

would have the effect in, for example, a kidney with 30% retention in phase 1 of increasing the % rapidly eliminated activity from 70 to 73%.

4.5 Conclusions

With respect to the liver, a variable amount of Tc-99m-MIBI is rapidly transported from blood to bile, possibly by passive diffusion, and then prevented from returning to the hepatocytes by ABC transporter proteins. This is followed by slow excretion into bile of mitochondrial-bound tracer. Passive diffusion of some tracer back into blood is likely, as happens with bilirubin and HIDA analogues. Early renal Tc-99m-MIBI elimination in contrast is probably predominantly by glomerular filtration and urinary excretion. In this first phase, P-gp located at the urine/tubule barrier prevents reabsorption of Tc-99m-MIBI and therefore indirectly influences Tc-99m-MIBI elimination from, and retention within, the kidney. Later elimination (second phase), as from the liver, is presumably governed by mitochondrial tracer release and subsequent elimination of Tc-99m-MIBI from cells by ABC transporters (96).

Chapter 5 Tc-99m-MIBI renal and hepatic biokinetics and correlation with genotype, gender, other organs and glomerular filtration rate

5.1 Background

Inter-individual expression of P-glycoprotein (P-gp) is known to be associated with C3435T polymorphism in exon 26 of *ABCB1* (formerly known as *MDR1 gene)*.

Evidence is growing that individual P-gp response to CNI may be linked to nephrotoxicity or rejection. P-gp, an ATP-binding cassette (ABC) transporter protein, is involved in the cellular efflux of immunosuppressants that are also nephrotoxic. The only known mechanism of Tc-99m-MIBI elimination from cells involves ABC transporter proteins, so Tc-99m-MIBI kinetics may allow inference of renal P-gp status (88). Previous studies have indicated a role for decreased P-gp expression and genetic polymorphism in *ABCB1* of donors in the development of CNI nephrotoxicity (24). Koziolek et al. showed histologically that high renal P-gp levels are associated with rejection and low levels with nephrotoxicity. Likewise, P-gp upregulation in lymphocytes increases resistance to anti-rejection therapy (26). Naesens et al. showed that absent P-gp expression at the apical membrane of renal tubular cells and combined donor-recipient homozygosity for C3435T are associated with increased risk of chronic allograft damage. In this prospective cohort of 252 adult renal allograft recipients (744 renal allograft biopsies) treated with a combination of tacrolimus, mycophenolate mofetil and corticosteroids, the

effects of *ABCB1* genotype were only evident when both donor and recipient were homozygous for the TT variant. They hypothesised that this unexpected finding could be explained by the high prevalence of epithelial chimerism after kidney transplantation. However, further studies should also investigate whether this relates to the type of CNI used (28), particularly there was no association between *ABCB1* genotype of transplant recipients receiving CsA and the graft outcome previously demonstrated (25), but an interplay between donor and recipient *ABCB1* genotypes was not assessed in this study (25). Prospective larger studies would assess the relation of Tc-99m-MIBI handling with *ABCB1* polymorphism, including combined donor-recipient genotypes. Increased renal P-gp expression determined by CC genotype at C3435T (16) (17) was shown to be associated with increased renal injury in an animal model of ischaemic injury (129) (130), likely leading to chronic rejection and increased risk of long-term graft failure (27). Tc-99m-MIBI renal and lymphocytes kinetics may therefore provide relevant information regarding CNI treatment response and dose selection to identify patients who are likely to benefit most from a CNI minimisation regimen. So, in line with the above, there is a need to develop novel non-invasive methods for assessing functional P-gp activity particularly in the setting of renal transplantation to achieve a balance between efficacy and toxicity through optimal individualised therapy.

A possible role for P-gp in gender-dependent differences in drug availability also remains unresolved. It has been reported, for example, that hepatic P-gp expression in men is 2.4-fold higher than in women (131). In contrast, others have demonstrated that P-gp is not differentially expressed between

genders (132). The current evidence also suggests that the expression of ABC transporters, including P-gp, is not co-ordinately regulated, ruling out the use of one tissue as a surrogate for another (133) in the same individual.

In clinical practice, glomerular filtration rate (GFR) is taken as a standard measure of renal function and also used to monitor drug toxicity. Estimating GFR is essential for clinical practice, research, and public health. Appropriate interpretation of estimated GFR (eGFR) requires understanding the principles of physiology, laboratory medicine, epidemiology, and biostatistics used in the development and validation of GFR estimating equations (134). GFR is routinely measured using radiotracers that are cleared exclusively by glomerular filtration, the most common being Cr-51-ethylenediaminetetraacetic acid (Cr-51-EDTA) (135), and Tc-99m-DTPA (136) (137). Cr-51-EDTA gives a more accurate assessment of renal function and can identify renal function impairment even before eGFR, but unfortunately in many cases already too late to prevent renal damage by potentially nephrotoxic drugs, although in some case it may be recovered. An imaging tool, which could predict drug toxicity before deterioration of renal function would therefore be useful in clinical practice.

Hence, the aim of this study was to investigate baseline organ elimination rates of Tc-99m-MIBI in relation to genetic variation in *ABCB1*, gender, inter-organ correlation and GFR measured with Cr -51-GFR.

5.2 Methods

Thirty healthy prospective kidney transplant donors (17 female, 13 male) were imaged for 30 min following injection of 400 MBq Tc-99m-MIBI. Posterior static 5-minute images of the abdomen, including myocardium, were acquired at 30 and 120 min (see Chapter 3, Figure 3.7 and Figure 3.8). The 30-min/peak ratios and the exponential 2-point (30 and 120 min) rate constant (*k*) were calculated.

Nineteen donors were genotyped for the C3435T (exon 26), G2677T (exon 21), C1236T (exon 12) and G1199A (exon 11) *ABCB1* (*MDR1)* polymorphisms using a polymerase chain reaction (PCR) - based technique.

Further to successful scanning of the first 15 potential kidney donors, an amendment for protocol to scan additional 15 potential kidney donors and prospectively include genotyping has been approved by the Ethics Committee. Fifteen prospectively genotyped donors have all consented to give their saliva sample just before their first Tc-99m-MIBI scanning in the Department of Nuclear Medicine, Brighton and Sussex University Hospitals NHS Trust. They were all successfully genotyped.

The amendment was also approved to approach the first 15 potential donors to obtain a retrospective informed consent for their saliva sample to be sent by the post.

Clinical notes of the first 15 recruited and scanned donors were re-assessed with the transplant nurse regarding their accessibility. Five kidney donors sent their saliva specimens back by post. Deoxyribonucleic acid (DNA) failed to extract from one specimen due to a low yield of the saliva sample containing very little DNA. This donor was not willing to re-send the sample, so in total 19 donors were successfully genotyped. DNA was extracted from saliva using the Oragene kits – a non-invasive method that yields high quality genome DNA using established PCR based techniques. The Oragene DNA OG-500 kit was used, which contained 2ml of the oragene buffer solution. All donors were asked to add 2ml of saliva in the tube, making to total volume of 4ml. Most donors required around 2-5 minutes to deliver a saliva sample. They were asked to relax and rub their cheeks gently for 30 sec to create saliva. If they found hard to give enough saliva sample ¼ tsp of white table sugar was placed on their tongue. They were also asked not to eat, drink, smoke or chew gum for 30 min before giving their saliva sample.

Genotyping was performed by the Laboratory of the Government Chemist (LGC) from a sample of saliva using standard PCR and restriction fragment length polymorphism techniques that are already established.

GFR was measured from routine Cr-51-EDTA plasma clearance on the same day as renography with Tc-99m-MAG3 in all 30 donors. Glomerular filtration (unlike tubular secretion) is not influenced by normal variations in the degree of hydration, because of autoregulation mechanisms. Although specific hydration is not usually required, a steady intake of fluids over the duration of the study is recommended (approximately 200 ml/h). Participants

were asked to avoid excessive intake of drinks containing caffeine, including tea, coffee and coke, after 10 pm the night before the test because of their diuretic effect (136) and avoid high protein intake, which could increase GFR, before the study in line with the guidelines for the measurement of GFR using plasma sampling adopted by British Nuclear Medicine Society (136).

Some drugs that can reduce renal function, e.g. diuretics (frusemide), aminoglycoside antibiotics, penicillins, sulphonamides and aluminium were recorded prior to the study being performed.

Restriction of exercise before the study was also suggested for good reproducibility.

As per protocol, all donor details were checked together with an assessment of the possibilities of pregnancy for women of childbearing age (12-55) and of breast-feeding (66).

Donors' height and weight for determination of body surface area (BSA) (138) were recorded.

Three MBq of Cr-51- EDTA was administered in line with the adult diagnostic reference level given by ARSAC (Administration of Radioactive Substances Advisory Committee) (66).

The slope-intercept method was used for analysis, with the mean Brochner-Mortensen equation (128) being applied to correct for the one-pool approximation. GFR values have been expressed as both absolute GFR in ml/min and also normalised to body size using BSA.

5.2.1 Statistics

The plotted data (histogram) confirmed that the distribution was normal (symmetric), therefore the use of mean and SD as measures of location and spread respectively was justified. Moreover, the sample size was large enough for the central limit theorem to hold, allowing for the use of parametric tests.

Homozygous negative (TT), heterozygous (TC) and homozygous positive (CC) genotypes were correlated with renal and hepatic 30 min/peak ratios and *k* values using ANOVA. Two-tailed *t*-testing was used to assess differences in renal and hepatic Tc-99m-MIBI elimination rates between males and females. *k* values were correlated between different organs and GFR results.

5.3 Results

5.3.1 Relations to genotype

There was a negative trend between the hepatic 30 min/peak ratio and C3435T (*ABCB1*) genotype (mean CC: 0.8374 ± 0.0502; TC: 0.6806 ± 0.1300; TT: 0.6919 ± 0.1506; p = 0.083; Figure 5.1).

Splenic, myocardial and renal 30min/peak ratios did not correlate with any genotype.

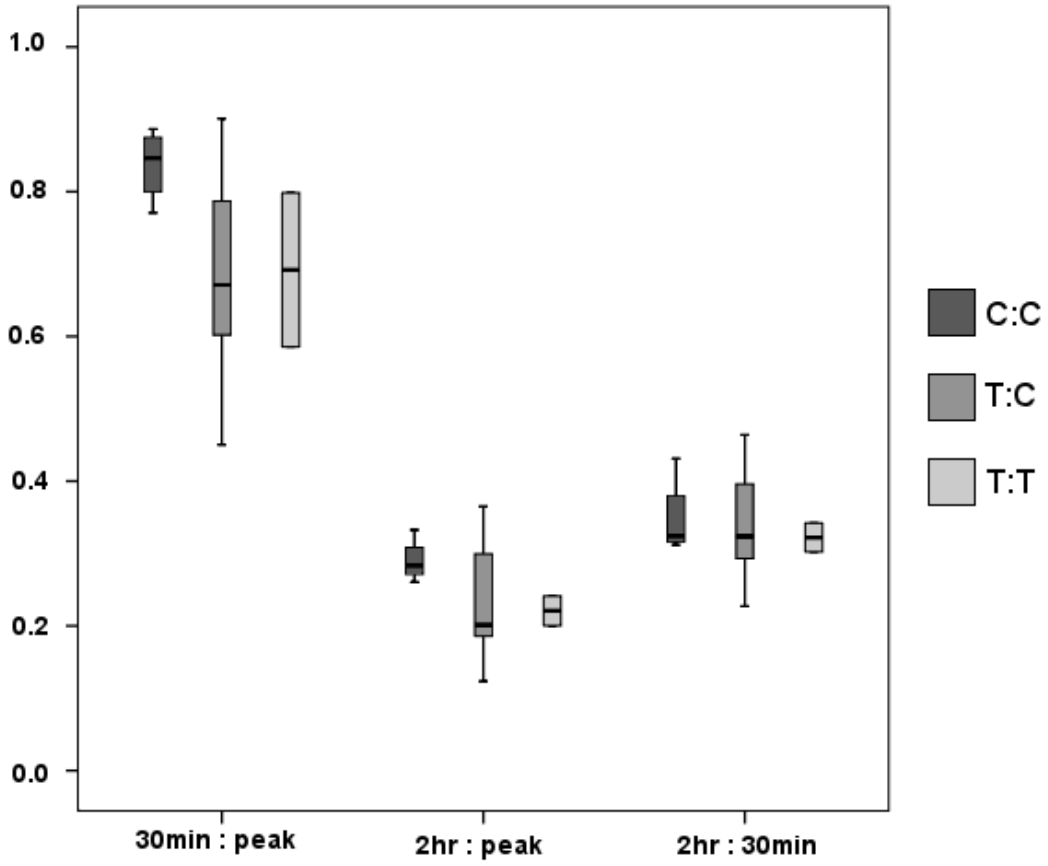

Figure 5.1 Relations between 30 min/peak ratio and C3435T (*ABCB1*) genotype shown for liver (p = 0.083).

Renal *k* showed a negative trend with C3435T (*ABCB1*) genotype (CC: -0.0021 ± 0.0020 min^{-1}; TC: -0.0037 ± 0.0013 min^{-1}; TT: -0.0040 ± 0.0012 min^{-1}; p = 0.087; Figure 5.2), but with no other genotypes. Hepatic, splenic and myocardial *k* values did not correlate with any genotype.

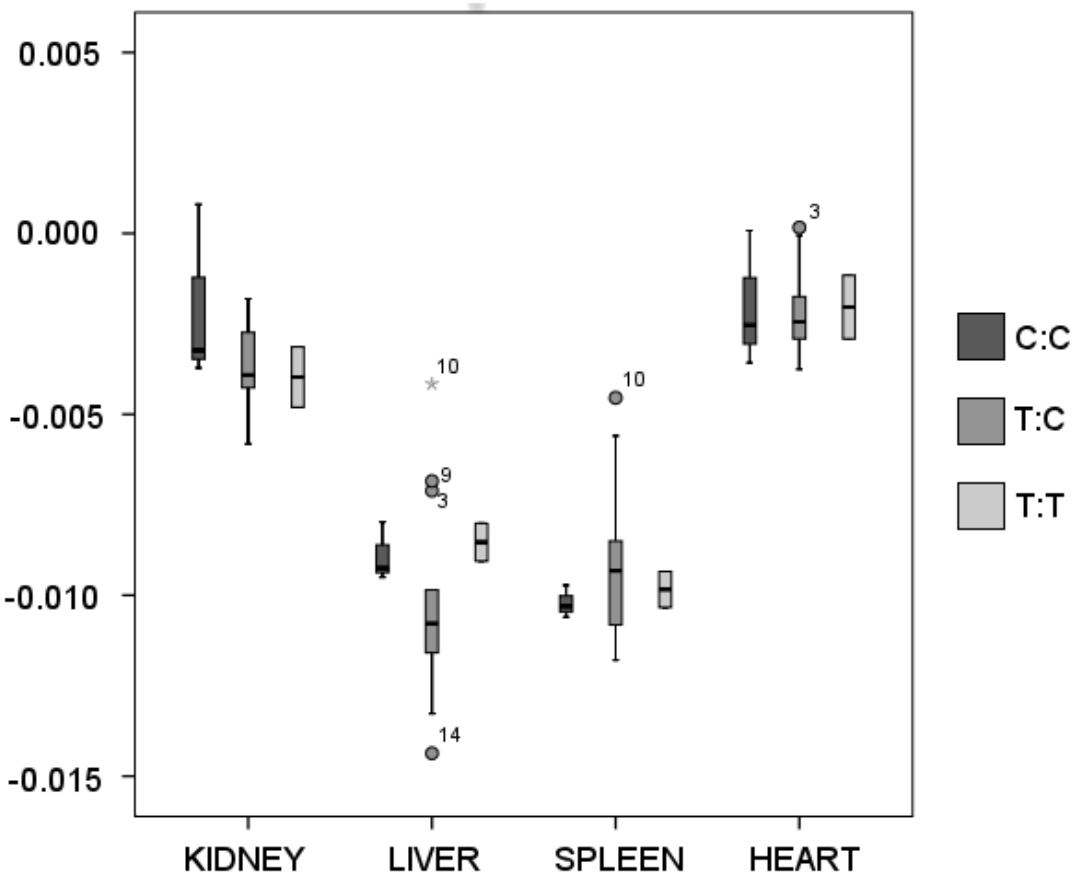

Figure 5.2 Relations between *k* values and C3435 (*ABCB1*) genotype shown for kidney (p = 0.087), liver (NS), spleen (NS) and myocardium (NS).

5.3.2 Relations to gender

There were no significant differences between females and males with respect to either renal or hepatic 30 min: peak indices (NS) and *k* values (NS).

5.3.3 Comparison with other organs

With respect to the liver, Tc-99m-MIBI behaved like a hepatobiliary agent, generating a hepatogram with a peak generally at about 10 min. Mean activity in the liver at 30 min, as a percentage of peak activity, was 71 [SD 12]% and subsequent *k* between 30 and 120 was 0.0102 [SD 0.0023] min^{-1}.

Mean *k* was not significantly different between liver (0.0102 [SD 0.0023] min^{-1}) and spleen (0.0097 [0.00185] min^{-1}; p=0.096), but was significantly lower in kidney (0.0036 [0.0013] min^{-1}; p<0.001) and myocardium (0.0022 [0.00125] min^{-1}; p<0.001), which displayed the lowest *k* values (Table 5.1 and Figure 5.3).

Organ	**Rate Constant (*k*) Mean [SD] min^{-1}**
Myocardium	0.00219 [0.00125]
Kidney	0.0036 [0.00134]
Liver	0.0102 [0.00230]
Spleen	0.00973 [0.00185]

Table 5.1 Mean exponential rate constants (*k*) based on the images at 30 min and 120 min for kidney, liver, spleen and myocardium.

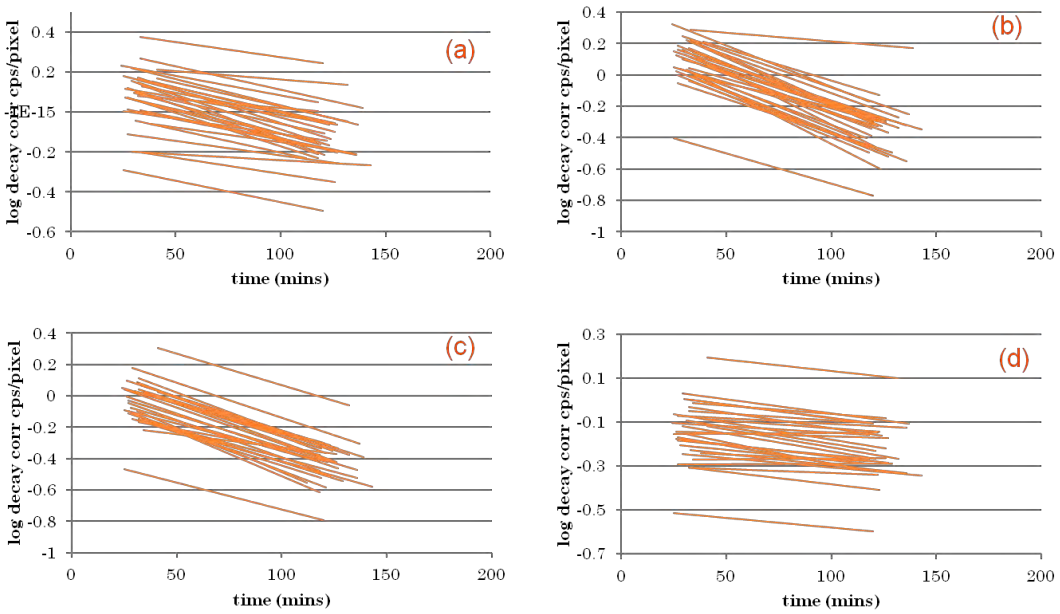

Figure 5.3 Composite graphs of log decay-corrected renal (a), liver (b), spleen (c) and myocardium (d) Tc-99m-MIBI "washout" in 30 donors.

5.3.4 Correlation between different organs

Hepatic (h), splenic (s) and myocardial (m) *k* values correlated with each other (R^2 h:m = 0.17, $p < 0.05$; h:s = 0.25, $p < 0.01$; s:m = 0.41, $p < 0.001$;Figure 5.4, Figure 5.5, Figure 5.6), but not with renal (r) *k* values (R^2 r:h = 0.001; r:s = 0.005; r:m = 0.01;Figure 5.7,Figure 5.8, Figure 5.9). No correlation with respect to *k* between kidney and other organs i.e. 1) renal and hepatic, 2) renal and spleen and 3) renal and myocardium.

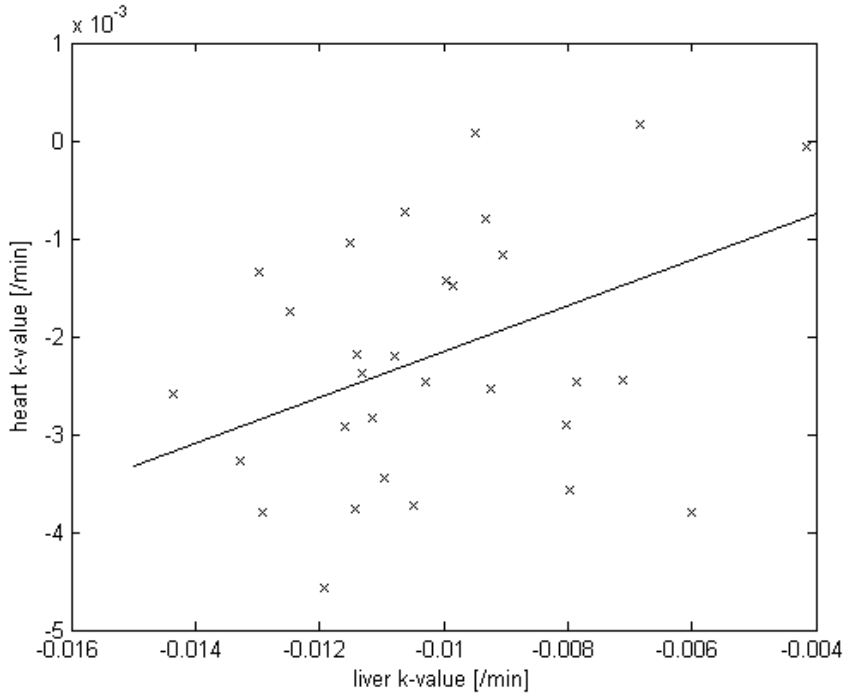

Figure 5.4 Correlation between liver and myocardial *k* values.

There is a significant but weak correlation between liver and myocardial *k* values ($R^2 = 0.17$; $p < 0.05$).

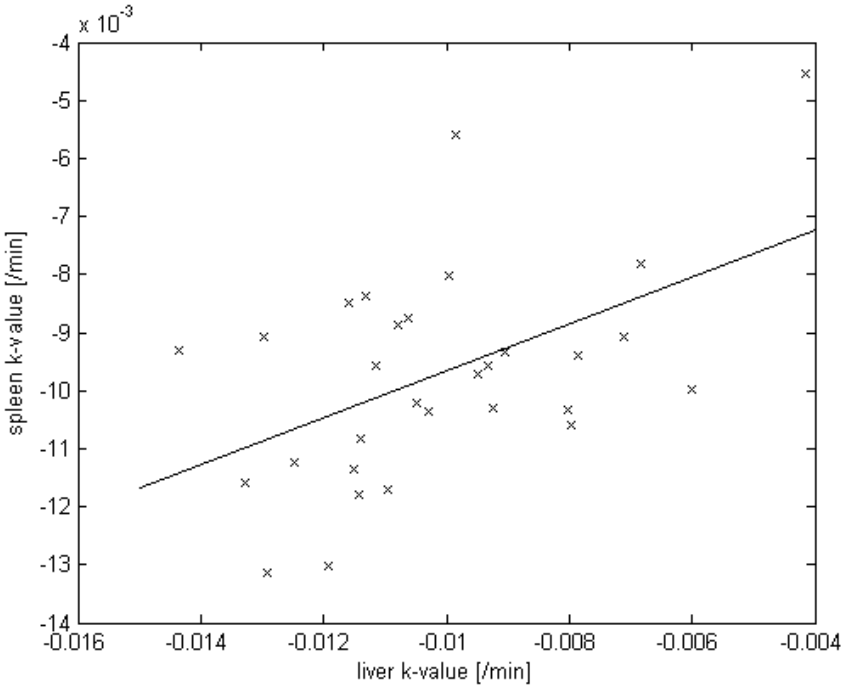

Figure 5.5 Correlation between liver and splenic *k* values.

There is a significant but weak correlation between liver and splenic *k* values (R^2 = 0.25; p < 0.01).

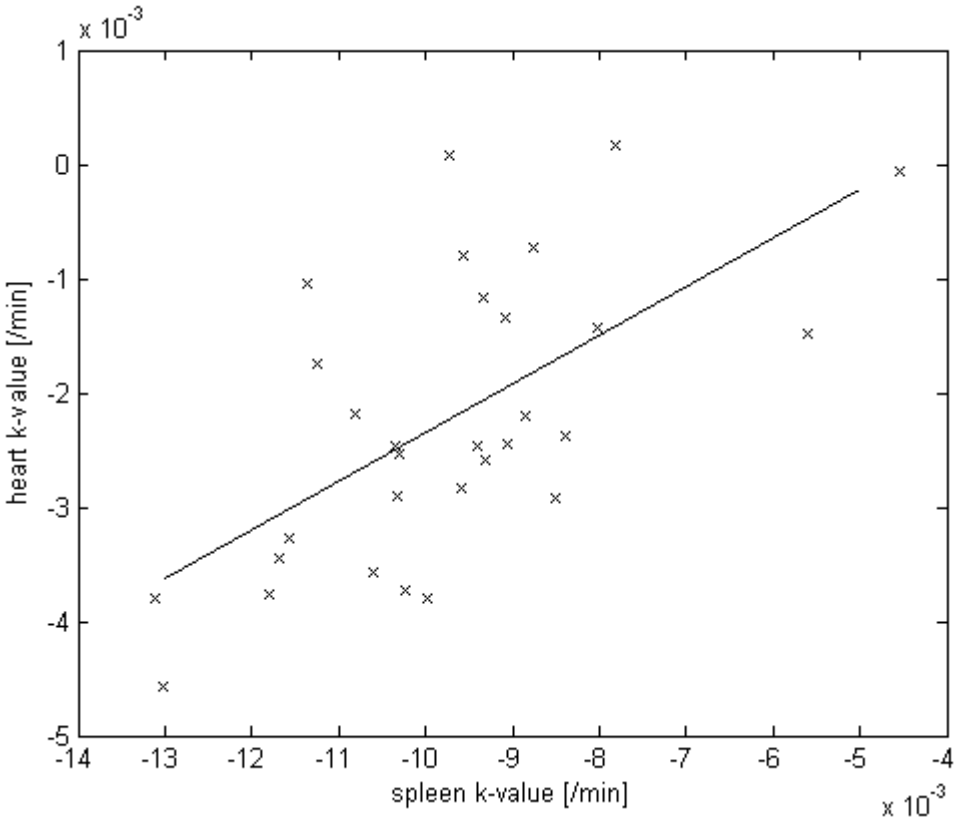

Figure 5.6 Correlation between splenic and myocardial *k* values

There is a significant but weak correlation between splenic and myocardial *k* values (R^2 = 0.41; p < 0.001).

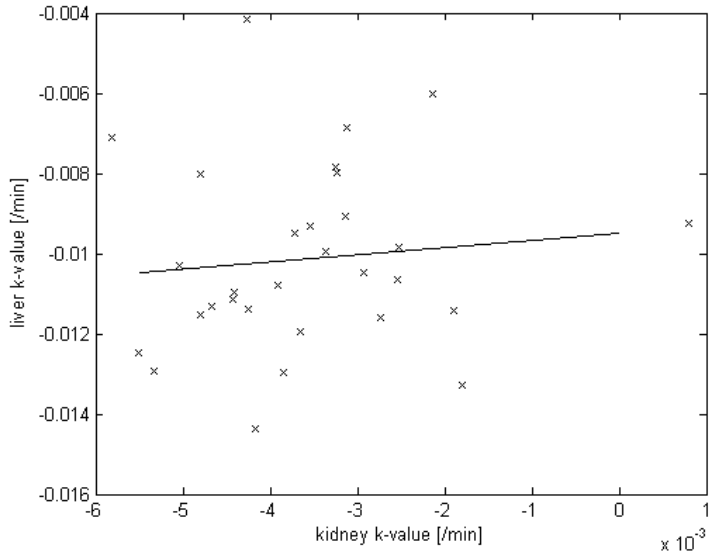

Figure 5.7 Correlation between renal and hepatic *k* values.

Figure 5.7 demonstrates no correlation between renal and hepatic *k* values (R^2 = 0.001).

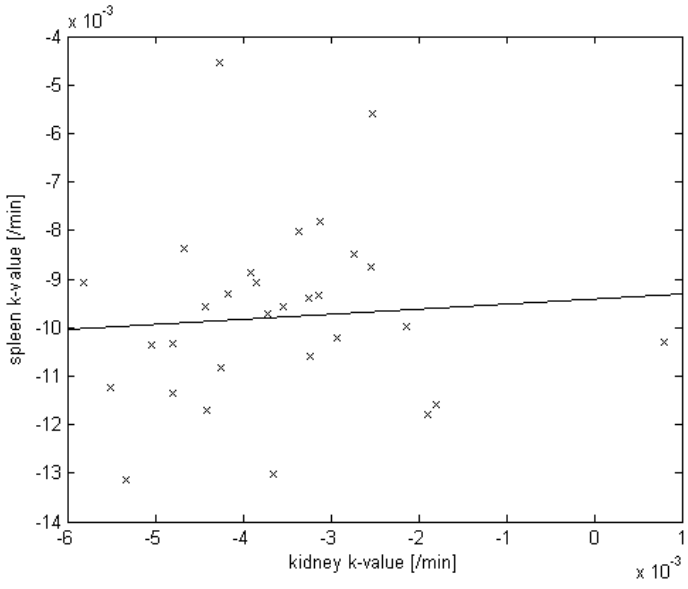

Figure 5.8 Correlation between renal and splenic *k* values

Figure 5.8 demonstrates no correlation between renal and splenic *k* values (R^2 = 0.005)

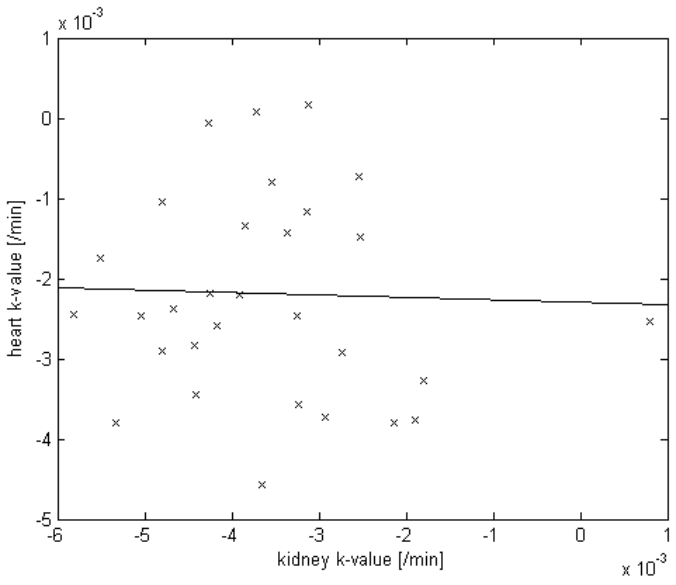

Figure 5.9 Correlation between renal and myocardial *k* values.

Figure 5.9 demonstrates no correlation between renal and myocardial *k* values ($R^2 = 0.01$).

5.3.5 Correlation between GFR and Tc-99m-MIBI elimination

Thirty healthy kidney potential donors were studied. Average normalised GFR was 93.4 [13.4] ml/min/1/73m^2 with range from 72 to 125 ml/min/1.73m^2 (Table 5.2).

There was no correlation between GFR and early and delayed renal elimination (NS) nor hepatic elimination (NS).

Parameter		All patients	Male only	Female only
Normalised GFR	Average	93.4	95.5	91.8
	St Dev	13.4	14.7	12.5
	Max	125.0	123.0	125.0
	Min	72.0	72.0	76.0
Absolute GFR	Average	100.3	107.2	95.1
	St Dev	19.0	20.1	16.7
	Max	146.0	146.0	137.0
	Min	67.0	84.0	67.0
Half-time	Average	108.9	112.4	106.2
	St Dev	17.8	14.3	20.1
	Max	142.0	140.0	142.0
	Min	77.0	94.0	77.0
Slope only GFR	Average	91.9	87.2	95.4
	St Dev	17.4	11.2	20.5
	Max	132.0	106.0	132.0
	Min	67.0	69.0	67.0
Dist Vol	Average	17.7	19.8	16.2
	St Dev	3.2	2.9	2.5
	Max	26.0	26.0	20.0
	Min	12.0	17.0	12.0

Table 5.2 Cr-51-GFR results for 30 healthy kidney donors confirming normal renal function.

5.4 Discussion

5.4.1 Tc-99m-MIBI kinetics and genotyping

In humans, the *ABCB1* (formerly known as *MDR1*) gene is located on the long arm of 7th chromosome at q21.1 band position. It plays a significant role in ADME processes (absorption, distribution, metabolism, and excretion) and drug-drug interaction. Variations in the *MDR1* gene product can directly affect therapeutic effectiveness, with over-expression of P-gp resulting in increased efflux of drugs that are P-gp substrates and development of drug resistance, and under expression resulting in drug toxicity. The *ABCB1* gene is highly polymorphic and 40 single nucleotide polymorphisms (SNPs) have been identified, of which some are known to influence *ABCB1* expression levels (6). *ABCB1* (*MDR1)* C3435T polymorphism has recently attracted attention as a possible modulator of health and disease.

ABCB1 (MDR1) gene polymorphism in exon 26 at C3435T (silent polymorphism) is known to influence the expression of P-gp. The CC genotype is associated with increased P-gp expression; individuals with CT genotype show intermediate P-gp expression, while individuals that are homozygous carriers of TT show functionally restrained P-gp (17). Racial variability within C3434T has also been demonstrated. Thus there is a significantly higher frequency of the CC genotype in West Africans and African Americans (83% and 61%, respectively), compared with Caucasians (26% ($p<0.0001$) (16). These findings could affect use of drugs that are P-gp substrates (such as immune-suppressants and HIV-1 protease inhibitors) in African populations (18) due to a potentially higher rate of drug resistance.

Our patient group was a rather homogenous racial Caucasian population, but further research is needed to assess whether racial variability may influence Tc-99m-MIBI elimination.

The relation between *ABCB1* (*MDR-1)* genotypes and previous imaging results is not clear; thus a relation with Tc-99m-MIBI clearance from liver to bile, which can be markedly reduced with a P-gp inhibitor (88), has been demonstrated (29), whereas, in contrast, there was no relation between BBB P-gp function, investigated with C-11-verapamil, and *ABCB1* polymorphisms in normal Japanese men (139). There have been no data reported previously on the relation between renal Tc-99m-MIBI handling and genotypes.

Since the C3435 site does not alter the protein sequence, it would appear likely that the effects on gene expression associated with this single nucleotide polymorphism (SNP) may well be due to other SNPs that are physically linked to it. Therefore C3435 may be associated with a polymorphism at a different site, which either affects *MDR1* expression or function. Hence I have also examined other *MDR1* variants that may have influenced P-gp expression, such as those in exons 21 (G2677T/A), 11 (G1199A) and 12 (C1236T). My preliminary results, however, have demonstrated a trend only between *ABCB1* C3435 and baseline renal Tc-99m-MIBI elimination (*k*) and 30min: peak hepatic indices, and no correlation with the other genotypes studied (121).

Further prospective larger studies are required to assess the relation of Tc-99m-MIBI handling with *ABCB1* polymorphism TT genotype at C3435T (24) and haplotype variant 1236T/2677T/3435T (140), which seems to strongly

influence renal function and graft loss due to nephrotoxicity. On the other hand, the relation with CC genotype at C3435T, which was shown to be associated with death-censored allograft failure (27), presumably due to increased renal P-gp expression, also requires further assessment. It has been demonstrated that increased renal P-gp expression is associated with increased propensity to renal injury in an animal model of ischaemic injury (129) (130), leading to chronic kidney damage and chronic rejection (27).

5.4.2 Tc-99m-MIBI elimination and gender

Many studies have reported gender differences in both toxicity and therapeutic outcomes for various agents. However, there is controversial literature (131) (132) (141) on the gender differences in P-gp expression in the liver and no literature on gender-related differences in kidneys. Gender differences in pharmacokinetics and pharmacodynamics of drugs have been appreciated as a contributor to variability in drug response. The realisation of a possible dynamic interplay between drug metabolism and drug efflux has positioned drug transporters, including P-gp, as important mediators of genders differences in drug deposition and therapeutic response. However, a role of P-gp in drug availability due to sex differences still remains unresolved (141).

It has been reported that hepatic P-gp expression is gender-dependant with men displaying a 2.4 fold higher level of expression than women (131). Contrary to these results, Wolbold et al. demonstrated that P-gp was not differentially expressed between sexes in human liver, but CYP3A4, which is a major human drug-metabolising cytochrome P450 (CYP), was gender-

dependant (132). In contrast, higher basal hepatic levels of P-gp in female rats relative to male rats have been reported, but it should be noted that human CYP3A4 does not have a direct orthologue in the rat (142).

There are no significant differences between females and males with respect to either renal or hepatic 30 min: peak indices and *k* values, implying that ABC (P-gp) expression is not gender-dependant.

5.4.3 Organ elimination of Tc-99m-MIBI from the kidney, liver, spleen and myocardium and correlation between different organs

The route of excretion of Tc-99m-MIBI from the kidney from 30 min, i.e. tubular secretion or elimination into blood, is not entirely clear from this study, but is nevertheless likely to be influenced by ABC protein transporters. The myocardium has not previously been regarded as expressing P-gp and instead has been used as a negative control (49), but its Tc-99m-MIBI clearance rate, albeit slow, was measurable in this study, consistent with subsequently described expression of P-gp in human myocardium and its localisation in the endothelial wall (143).

I have demonstrated no correlation between kidney and other organs. The current evidence therefore suggests that the expression of ABC transporters, including P-gp, is not co-ordinately regulated, ruling out the use of one tissue as a surrogate for another (133) in the same individual. Involvement of different ABC transporters (not only P-gp) in the handling MIBI in different organs could also explain this finding.

5.4.4 5.4.4. Glomerular filtration rate versus renal and hepatic Tc-99m-MIBI elimination

The generally accepted gold standard technique for GFR assessment uses inulin infusion. This technique is difficult and time-consuming to perform and therefore considered inappropriate for routine clinical use. Measurement of Cr-51-EDTA clearance from a single injection emerged as an adequate simpler technique (128). It is recommended that the plasma clearance of Cr-51-EDTA from venous samples is taken as the standard measure of GFR. Cr-51-EDTA is the most widely used radiopharmaceutical for GFR measurement in the UK and venous plasma sampling is a precise and convenient technique. It is considered that, among the various methods for measuring Cr-51-EDTA plasma clearance, the slope-intercept method provides the best compromise between accuracy and reliability on the one hand and simplicity on the other hand (136).

On the basis of amount of urinary activity and the fact that it follows the time course of renal handling, early Tc-99m-MIBI elimination is predominantly consistent with either filtration or rapid tubular secretion; however there was no significant correlation between GFR and either renal or hepatic 30 min: peak indices and *k* values. This was an expected finding particularly for renal *k* values and hepatic Tc-99m-MIBI elimination, but also indicative that a proportion of early Tc-99m-MIBI elimination is dependent on glomerular filtration, allowing for a narrow range of normal GFR results in potential healthy kidney donors.

5.4.5 Limitations

Further prospective larger studies are required to assess the relation of Tc-99m-MIBI handling with the ABCB1 due to the limited number of kidney donors genotyped. The group of patients studied was a rather homogeneous white population, but further research is needed to assess whether racial variability may influence Tc-99m-MIBI elimination as P-gp expression is found to be variable and influenced by race (16).

Although this study represents a platform for further research, the potential impact of genotype variation on Tc-99m-MIBI imaging findings in routine clinical practice and research requires further prospective trials. I have conducted a preliminary pharmacological proof-of-principle study (see Chapter 6), but further pharmacological as well as correlative prospective studies with immunohistochemistry (e.g. in the post-renal transplant setting) and Tc-99m-MIBI elimination from different organs may also help an understanding of a full role of ABC transporters in Tc-99m-MIBI handling. However, immunohistochemistry studies may also have some limitations, as P-gp/ABC protein transporters histological status may not fully match their functional expression *in vivo* and hence molecular imaging studies may have an important role in the assessment of functionality of ABC transporters and their implications in clinical practice.

5.5 Conclusions

Although limited, my preliminary data suggest that baseline renal and hepatic Tc-99m-MIBI bio-kinetics may be influenced by *ABCB1* C3435T polymorphism.

In the era of personalised medicine, further prospective trials are required to investigate the full impact of genotype and haplotype variation on ABC transporter-associated Tc-99m-MIBI elimination and imaging findings in routine clinical practice and research (121).

In clinical practice for example, further *ABCB1* genetics studies are suggested to investigate the clinical implications of constitutional ABC/P-gp expression in liver. In particular, a possibility of the hepatic washout rates being *ABCB1* influenced and hence resulting in individual artefactual gut activity obscuring the inferior wall on myocardial perfusion imaging should be further investigated (144).

A role for P-gp in renal Tc-99m-MIBI handling needs to be confirmed with further experiments, including studies based on immunohistochemical staining and challenge studies with P-gp inhibitors such as CsA (see Chapter 6).

Neither renal nor hepatic Tc-99m-MIBI kinetics appear to be gender-dependant, which may be a relevant finding while studying pharmacokinetics of different drugs that are P-gp substrates in different sexes. The 4 organs studied showed variable tissue elimination rates from 30 min, with the myocardium the lowest. The tissue elimination rate of Tc-99m-MIBI may

represent an *in vivo* assay of constitutional ABC, effectively P-gp, transporter expression, but one organ cannot be a surrogate for another. Although correlation with GFR is non-significant, on the basis of the amount of urinary activity, early MIBI elimination is governed by combination of either filtration or rapid tubular secretion and ABC/P-gp/MRP1,2 related transports. Delayed MIBI elimination as expected is not related to glomerular filtration, but most likely linked to the ABC-transport mechanism, which provides an additional dimension in overall renal function assessment.

The way may be open to investigate Tc-99m-MIBI scintigraphy as a mean of predicting nephrotoxicity of anti-rejection therapy or allograft failure in the setting of renal transplantation, thereby providing useful information regarding dose selection of immunosuppressants, but also other nephrotoxic drugs that are P-gp substrates (121)

Chapter 6 Effects of CsA on Tc-99m-MIBI kinetics

6.1 Background

Calcineurin inhibitors (CNI), including CsA , are substrates for ATP-binding cassette (ABC) multi-drug resistance (MDR) transporter proteins such as P-gp and MRP1, 2. P-gp/MRP1, 2 are involved in the cellular efflux of many drugs (“detoxification“) (3) (5), including both Tc-99m-MIBI and CsA.

The introduction of the CNI (CsA) in human kidney transplantation in the late 1970s revolutionised transplantation medicine, and made transplantation a preferable therapeutic intervention for end-stage renal disease (145) (146) (147). CsA binds to cyclophilin with the synergistic action of calcium and suppresses activation of calcium-dependent phosphatase calcineurin, thus leading to the block of T cell activation and cytokine release, such as IL-2 (148).

In 1984, the potent immunosuppressive properties of another CNI, tacrolimus, were discovered, and tacrolimus was used successfully in human liver, kidney, and heart allograft recipients (147) (149) (150).

Calcineurin (151) and nuclear factor of activated T-cells (NFAT) isoforms (five different isoforms; only NFAT5 is not calcineurin-dependent) (152)) are, however, not T cell-specific, and inhibition of this pathway by CsA and tacrolimus may produce toxicity beyond immunosuppression (147) (153). This is the case not only for kidney transplantation, in which the direct nephrotoxicity of these agents represents a huge challenge in clinical practice, but also a major concern in non-renal solid organ transplantation

and many other diseases, including skin disease requiring therapy with CNIs (147).

Chronic CNI nephrotoxicity is associated with mostly irreversible histologic damage to all compartments of the kidneys, including glomeruli, arterioles, and tubulo-interstitium. The pathophysiologic mechanisms underlying CNI nephrotoxicity are partly elucidated, although the main question whether nephrotoxicity is secondary to the actions on the calcineurin-NFAT pathway remains largely unanswered.

Local renal factors seem more important for susceptibility to CNI nephrotoxicity than systemic exposure to CsA and tacrolimus. These factors include variability in P-gp and CYP3A4/5 expression or activity, older kidney age, salt depletion, the use of NSAIDs, and genetic polymorphisms in genes. Prevention and eventually therapy for CNI nephrotoxicity is aimed at lowering total systemic blood levels and decreasing local renal exposure to the CNIs or their metabolites.

It has been demonstrated that CNI levels in renal tissue are much higher than in blood (147) (154) (155) for both CsA and tacrolimus, but the degree of inter-individual variability and the determinants of local CsA or tacrolimus levels are currently not known. There is, however, accumulating evidence indicating that the inter-individual variability in local renal CsA or tacrolimus exposure in kidney tissue contributes significantly to chronic CNI nephrotoxicity. It has been demonstrated that mTOR inhibitors sirolimus and everolimus interact with CsA excretion in tubular epithelial cells through competition for P-gp (147) (156), and hence lead to accumulation of CsA in

these cells increasing chronic nephrotoxicity of CNIs, both in rats and in humans (147). Local renal accumulation of CsA was demonstrated *in vitro* by Anglicheau et al. (156) and *in vivo* by Napoli et al. (157) and Podder et al. (147) (158).

Further evidence for the importance of local renal CNI concentrations is found in studies associating P-gp expression or function with CNI nephrotoxicity. P-gp is expressed at the apical side of tubular epithelial cells and is the main protein responsible for the excretion of the CNIs, tacrolimus and CsA (159) (160), although the renal excretion of these CNIs is only limited.

Using immunohistochemistry and Western blotting in a rat model of chronic CNI nephrotoxicity, Del Moral et al. suggested that variability in local P-gp expression is important for chronic CNI nephrotoxicity, but also demonstrated that the up-regulation of P-gp was inversely related to the incidence of arteriolar hyalinosis, interstitial fibrosis, and periglomerular fibrosis (161). Another study in rats showed that exposure of cultured renal tubular cells to CsA induces P-gp overexpression (162). Human studies confirmed the animal data and suggest that inter-individual variability in local renal P-gp expression contributed to the local susceptibility to CNI nephrotoxicity. In human studies, lower expression of P-gp in renal allograft biopsies correlated with CNI nephrotoxicity (26) (163). However, these case-control studies need to be validated in larger prospective studies, as any association does not prove a causal role of local P-gp expression variability. Previous studies have also demonstrated that variability in P-gp function could be important in the development of CNI nephrotoxicity and that a single nucleotide

polymorphism in *ABCB1*, the 3435TT genotype of the donor, was associated with chronic CNI nephrotoxicity (24). This frequent polymorphism has been associated with altered function of P-gp (164) (165) (166). However, another case-control study in liver transplant recipients found an association of the TT genotype at position 2677 with lower risk for kidney dysfunction (167), indicating that this SNP may be in linkage disequilibrium with the TT genotype at position 3435.

It has been demonstrated that when P-gp is down-regulated, CsA accumulates in kidney cells, producing nephrotoxicity (26). Tc-99m-MIBI is a proven ABC/P-gp substrate, so Tc-99m-MIBI imaging may allow assessment of functional P-gp status (2). If P-gp is functionally down-regulated, Tc-99m-MIBI should be slowly eliminated from the cells at a rate measureable from scanning (49) and *vice versa* if P-gp is up-regulated. Used before and after the patient starts CsA, Tc-99-m-MIBI may be used for dose selection or predict nephrotoxicity. As the only known mechanism of Tc-99m-MIBI elimination from renal tubular cells involves transport proteins, including P-gp (88) (Figure 6.1), the continuous reduced Tc-99m-MIBI elimination rate from the kidney following CsA administration may potentially predict nephrotoxicity.

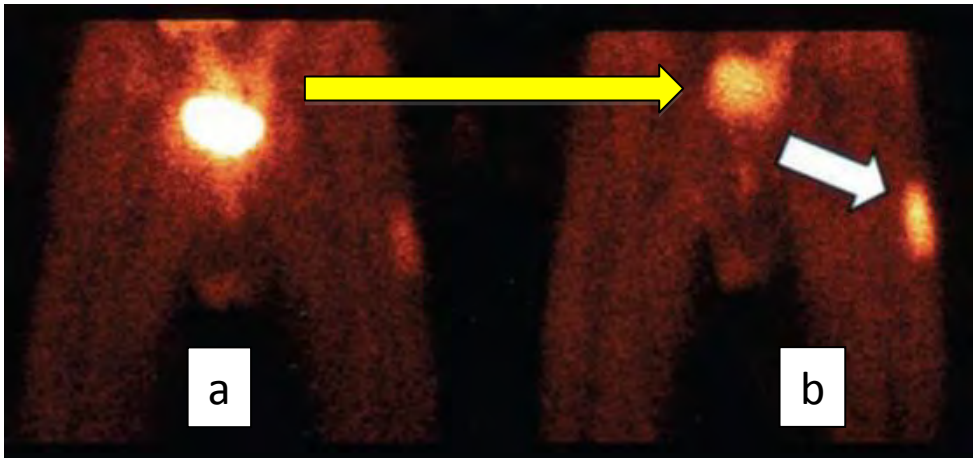

Figure 6.1 Tc-99m-MIBI images before (a) and after administration (b) of Tariquidar, which is a known P-gp inhibitor.

Compared with (a), the image (b) demonstrates increased accumulation of Tc-99m-MIBI in a metastasis of a known P-gp expressing tumour, but reduced urinary activity in the bladder likely due to blockade of renal P-gp and reduced Tc-99m-MIBI elimination from kidney, supporting the hypothesis that P-gp promotes excretion of Tc-99m-MIBI into the urine. Reprinted from Agrawal M, et al. Clin Cancer Res 2003;9:650–656. with permission of the American Association for Cancer Research (88).

P-gp is encoded by a gene (*ABCB1*) that exists in several functional states (16) (17) (24) (29), so phenotypic association with *ABCB1* genotypes may also be relevant. Initially, as a result of CsA administration, the rate of Tc-99m-MIBI elimination is expected to reduce in patients receiving CsA who have not previously been treated with this drug. This early effect of administration of a competing Pgp/MRp1,2 inhibitor (CsA) would be due to functional inhibition of P-gp; i.e. down-regulation. Subsequently, in response to sustained exposure to CsA, this initial effect of P-gp down-regulation should be followed by physiological up-regulation, which represents a mechanism of defence against the drug. Failure to up-regulate P-gp, or the

prior existence of constitutionally low P-gp expression, have been shown to be linked to CsA-induced nephrotoxicity (26).

A slow Tc-99m-MIBI elimination rate, or failure to subsequently increase the elimination rate in response to the drug, were therefore expected to be predictors for the development of nephrotoxicity. On the other hand, Tc-99m-MIBI kinetics could provide valuable information leading to dose selection of the relevant drug, e.g. a slow Tc-99m-MIBI elimination rate following drug administration may indicate a need for dose reduction or minimisation regimen; and vice versa, i.e. fast elimination of Tc-99m-MIBI, would allow a high dose regimen to be continued.

6.2 Aims

The primary aim of this project was to investigate the pharmacological effect of a drug which is also a P-gp/MRP1,2 substrate, namely CsA, on renal and hepatic Tc-99m-MIBI elimination and to test the hypothesis that renal and hepatic Tc-99m-MIBI kinetics are influenced by ABC/MDR transporter protein expression using pharmacological inhibition by CsA**.**

My second aim was to quantify the functional activity of ABC/P-gp in the kidney and liver by measuring the rate of Tc-99m-MIBI elimination before and after starting CsA treatment.

I also aimed to correlate imaging results with the *ABCB1* genotype that determines P-gp expression to assess if there is any potential relevant link between genotypes and Tc-99m-MIBI pharmacokinetics in response to CsA and to address the hypothesis that renal and hepatic Tc-99m-MIBI kinetics,

and changes in early and delayed Tc-99m-MIBI elimination rates, are influenced by ABC/MDR transporter protein expression and *ABCB1* genotype.

A further aim was to investigate the longer-term effects of CsA on T-99m-MIBI pharmacokinetics, as very little is known about the time course of up-regulation of P-gp expression and function following chronic dosing. My final aim was to test the hypothesis that patients with sustained functional under-expression of renal P-gp are at increased risk of developing CsA nephrotoxicity, whilst conversely those up-regulating or not under-expressing P-gp do not develop nephrotoxicity.

6.3 Methods

6.3.1 Subjects (patient with skin conditions)

Four patients with psoriasis were recruited in the dermatology clinic and given an information sheet when the decision was made by the dermatologist to start them on CsA. They were given adequate time to decide if they wanted to take part. Written consent was taken in Department of Nuclear Medicine, Royal Sussex County Hospital, Brighton and Sussex University Hospitals NHS Trust.

6.3.1.1 Inclusion criteria

1. Patients with skin disease (psoriasis) about to start CsA treatment.

2. Aged 18 years or over.

3. Willing and able to give informed consent.

4. Normal renal function (GFR >60 ml/min/1.73 m^2).

6.3.1.2 Exclusion criteria

1. Pregnancy and lactation.

2. Not willing or unable to provide informed consent.

3. Pre-existing renal disease (eGFR < 60 ml/min).

6.3.2 Protocol

Three Tc-99m-MIBI renograms were performed for each patient. Tc-99m-MIBI scanning was performed prior to starting CsA and again at 1-2 weeks and 6-12 weeks post-treatment.

It has previously been demonstrated that CsA reduced hepatic Tc-99m-MIBI elimination 1-2 weeks after oral administration of CsA (49). The follow up scanning was therefore done 1-2 weeks after the start of oral CsA treatment to demonstrate a 'sub-acute ' pharmacological effects of CsA on MIBI renal kinetics and to re-investigate effects on the Tc-99m-MIBI bio-distribution in the liver. Further to discussion with dermatology consultants, 6-12 weeks period was considered appropriate in the context of 3-6 months CsA treatment course to investigate the longer-term effects of CsA on T-99m-MIBI pharmacokinetics, as very little is known about the time course of up-regulation of ABC/P-gp expression and function following chronic dosing.

The imaging protocol included continuous scanning for 30 min after intravenous injection of Tc-99m-MIBI, followed by a 5-min static view and single photon tomographic imaging (SPECT) of the kidneys and liver (phase 1). Further scanning was performed for about 25 min, starting 2 h after Tc-99m-MIBI administration, once again to include a 5-min static view followed by tomographic imaging (phase 2). Glomerular filtration rate (GFR) was measured from routine Cr-51-EDTA plasma clearance at baseline and 6-12 weeks post-treatment, or earlier if the patient came off treatment. GFR was measured using the conventional clinical technique in which Cr-51-EDTA plasma clearance is measured from blood samples taken at 120, 160, 200 and 240 min after intravenous Cr-51-EDTA injection prior to the baseline and 3rd Tc-99m-MIBI studies. Cr-51-EDTA is metabolically inert and not a substrate for P-gp.

Genotyping was performed from a sample of saliva before the first Tc-99m-MIBI study using standard polymerase chain reaction and restriction fragment length polymorphism techniques that are already established.

Since the C3435 site does not alter the protein sequence, it would appear most likely that the effects on gene expression associated with this single nucleotide polymorphism (SNP) may well be due to other SNPs that are physically linked to it. Therefore the 3435 may have been associated with a polymorphism at a different site, which either affects MDR expression or function. Therefore I have also documented other ABCB1 variants that may have influenced P-gp expression, such as those in exon 21 i.e. (G2677GT/A) (29), 11 (G1199A) (13) and 12 (C1236T) (29) that have been previously

studied in the context of the *ABCB1 (MDR1)* gene and Tc-99m-MIBI elimination (29).

Early and delayed elimination rates were also measured using SPECT in all 4 patients before, 1-2 and 6-12 weeks after starting first-time treatment with CsA (CsA; 3 mg/kg, target: 100-300 µg/ml). Neoral (novartis) brand CsA was used in all patients to standardise bioavailability of CsA.

Four functional *ABCB1* single nucleotide polymorphisms (SNPs) were genotyped: 3435C>T (exon 26), 2677G>T (exon 21) and 1236C>T (exon12) and G1199A (exon11).

Psoriasis severity was assessed with standard psoriasis severity scoring systems, i.e. Psoriasis Area and Severity Index (PASI) and Dermatology Quality of Life Index (DLQI).

Routine blood tests and follow up by the patient's dermatologist occurred as per standard clinical practice.

Blood CsA levels were measured at the time of study 2 (first follow-up Tc-99m-MIBI study); i.e.2 weeks after starting CsA treatment (3mg/kg/day, divided in two doses). They were measured 30 min after the morning dose and immediately before Tc-99m-MIBI administration

6.3.3 Analysis

The Tc-99m-MIBI early (*ir* = peak:20 min renal index ratio and *ih* = peak:30 min hepatic index ratio) and delayed exponential elimination rates from the kidney and liver (k min^{-1}) were considered to be the primary measures of

functional ABC/P-gp expression. Baseline and changes in *i* and *k* were correlated with changes in GFR, as a marker of nephrotoxicity, and genotypes.

The SPECT data were processed using iterative reconstruction with resolution recovery. The coronal slices containing the kidney were summed to create a composite volume slice, including all kidney and liver slices, whilst excluding the overlying and underlying activity in adjacent organs, such as bowel and spleen.

6.3.4 Outcome measures

a) Early ratio (*i*) and delayed Tc-99m-MIBI elimination rates from the kidneys and liver (*k*) for baseline (study 1) and two subsequent follow up Tc-99-MIBI studies (studies 2 and 3);

b) baseline and changes in *i* and *k* between 1st and 2nd studies, 2st and 3rd studies and 1st and 3rd studies with respect to early (phase 1) and delayed (phase 2) data acquisition intervals were correlated with *ABCB1* genotype, blood CsA level and changes in GFR.

6.4 Results

6.4.1 Blood CsA levels

Blood CsA level was determined 2 weeks following 3mg/kg/day oral treatment, divided into two doses, and 30 min following oral administration of the morning dose. All 4 patients had markedly different blood CsA levels in spite of the same treatment regimen. The target range was 100-300 μg/ml.

Two patients had high blood CsA levels, above the target range (810 and 473 µg/ml), one patient had a blood CsA level within the target range (175 µg/m), and one had a low, below target, blood CsA level (58 µl/ml) (Table 6.1).

6.4.2 Genotypes

ABCB1 SNPs that may have influenced P-gp expression, such as those in exon 26 (C3435>T), exon 21 (2677G>T/A), 12 (1236C>T), 11 (1199G>A), were determined for all patients. 1199G>A genotype was the same for all patients. With respect to 3435C>T (exon 26), one patient was homozygous for CC and other 3 patients were heterozygous for TC. At exon 12, with respect to 1236C>T, two patients were homozygous for CC, one patient was homozygous for TT and one patient was heterozygote for TC. At exon 21, with respect to 2677G>T, two patients, who were also homozygous for 1236CC, were homozygous for GG. The other two patients were heterozygous for 2677TG. Two patients who were homozygous for 1236CC/2677GG had lower blood CsA levels than the patients with at least one T allele. The patient who was homozygous for 1236TT had the highest blood CsA level (Table 6.1).

Patient	1199G>A	3435C>T	2677G>T/A	1236C>T	Blood CsA 100-300 µg/l
1	G:G	T:C	T:G	T:T	810
2	G:G	T:C	T:G	T:C	473
3	G:G	C:C	G:G	C:C	175
4	G:G	T:C	G:G	C:C	58

Table 6.1 *ABCB1* SNPs (1199G>A, 3435C>T, 2677G>T/A and 1236C>T) in 4 patients (determined before CsA treatment) and their blood CsA levels 2 weeks after the same CsA treatment regimen.

6.4.3 Effect of CsA on early Tc-99m-MIBI elimination versus genotypes

CsA effects occurred predominantly before 20 min post-Tc-99m-MIBI in the kidney and after 20 min in the liver.

In the 2nd studies, Tc-99m-MIBI elimination was slower from both the liver and kidneys in 2 patients with high blood CsA levels, both of whom had at least one T allele at 1236 site. The 20 min renal retention, expressed as a percentage of the estimated total Tc-99m-MIBI delivered to the organ (index renal ratio=*ir*) over the Tc-99m-MIBI lifetime in blood (~15 min), increased in 2 patients with high blood CsA levels (target range: 100-300 µg/l) of 810 and 1236TT genotype (Figure 6.2; patient 1) and 473 µg/l and 1236CT genotype (Figure 6.4; patient 2) between the first and second studies.

However, there was no apparent inhibition in the early Tc-99m-MIBI elimination rate noted in the other 2 patients with CsA within the target range (175 μg/l) (Figure 6.6; patient 3) or low CsA (58 μg/l) (Figure 6.8; patient 4) between 1st and 2nd studies. Actually, Tc-99m-MIBI elimination became slightly faster and retention indices lower between the 1st and 2nd studies, likely due to compensatory up-regulation of P-gp/Mrp1,2. Both of them had the same 1236CC and 2677GG genotypes at exon 12 and 21, respectively.

In the early phase (phase 1), the third studies gave similar but slightly variable results compared to the second study in all patients (Figure 6.2 to Figure 6.9).

With respect to 1236 site, 2 patients who had CC homozygote demonstrated a different and opposite pharmacological effect of CsA on Tc-99m-MIBI kinetics when compared to other 2 patients with at least one T allele.

No correlation with 1199G>A at exon 11 was observed. All patients had the same 1199GG genotype.

There was little correlation with 3435C>T at exon 26, namely one patient had 3435CC genotype (CsA within the target), while other 3 patients had CT genotypes.

No apparent changes were seen in GFR. Only one patient who was homozygous for CC at three sites, namely 3435CC/1236CC/2677GG, showed an increase in GFR between baseline (92 ml/min/1.73m^2) and the 3rd study (104 ml/min/1.73 m^2) following 12 weeks treatment with CsA. All other patients showed a slight but not clinically relevant reduction in GFR between the 1st and 3rd studies (Figure 6.2 to Figure 6.9,Table 6.2, Table 6.3, Table 6.4).

Patient (study_no)	**Kidney *ir***	**Liver *ih***	**CsA (ug/l)**	**Genotype 1236C>T**	**GFR ml/min/ 1.73m2**
1-1	0.43	0.81	810	T:T	108
1-2	0.56	1.00			
1-3	0.55	1.11			104
2-1	0.43	0.89	473	T:C	91
2-2	0.61	1.02			
2-3	0.58	0.93			81
3-1	0.62	0.95	175	C:C	92
3-2	0.54	0.90			
3-3	0.51	0.83			104
4-1	0.61	0.97	58	C:C	88
4-2	0.53	0.92			
4-3	0.65	0.90			78

Table 6.2 Renal (*ir*) and hepatic (*ih*) phase 1 indices ratios in relation to blood CsA levels, 1236C>T genotype and GFR.

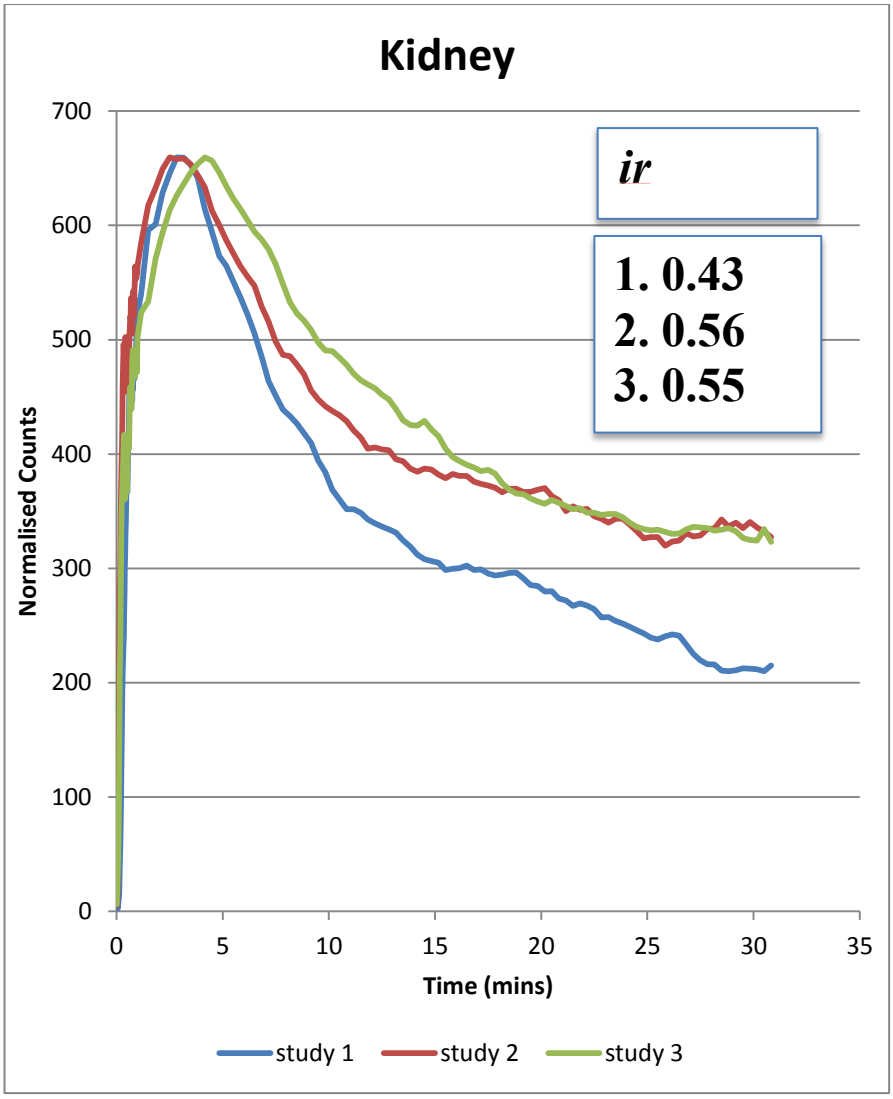

Figure 6.2 Early renal T-99m-MIBI kinetics before and after CsA treatment in the patient 1 (*ABCB1* genotypes: 3435TC,2677TG, 1236TT) with the highest blood CsA level of 810 µg/ml (target 100-300).

For patient 1, renogram curves demonstrated reduced renal Tc-99m-MIBI elimination following pharmacological inhibition with CsA between the 1st and 2nd study and increase in renal index ratio (ir) from 0.43 to 0.56. There was a possible further inhibition in the 3rd study, as shown by the renogram curve, but no change in ir between the 2nd and 3rd studies. Index ratios were calculated at 0.43, 0.55, 0.56 in the studies 1, 2, 3, respectively (Figure 6.2). Baseline GFR (108 ml/min/1.73m^2) for this patient did not significantly change at the 3rd study (104 ml/min/1.73m^2).

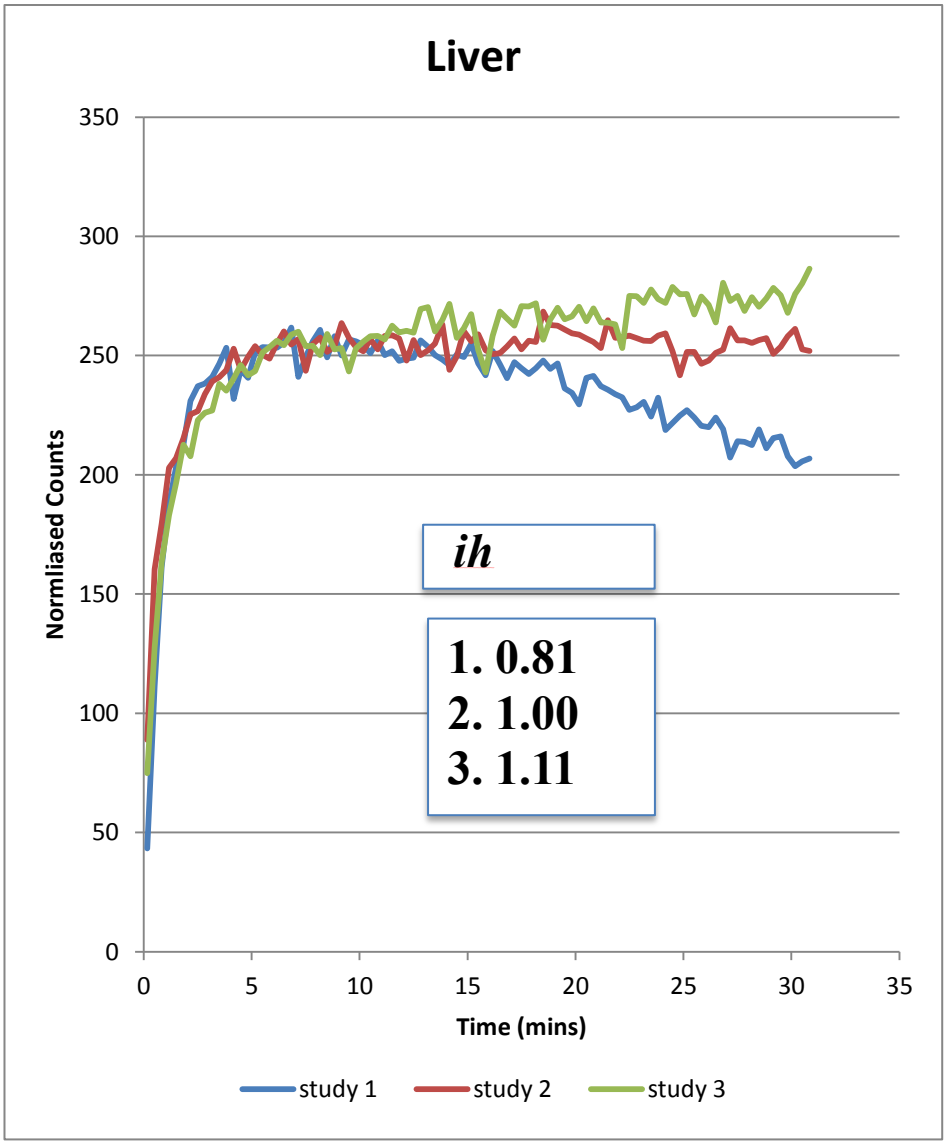

Figure 6.3 Early hepatic T-99m-MIBI kinetics before and after CsA treatment in the patient 1(*ABCB1* genotype: 3435TC, 2677TG, 1236TT) with the highest blood ciclopsorin level of 810 µg/ml (target 100-300).

For patient 1, a slower hepatic Tc-99m-MIBI elimination following pharmacological inhibition with CsA between the 1st and 2nd study and possible further inhibition at 3rd study is noted. 30 min/10 min hepatic index

ratios (*ih*) were calculated at 0.81, 1.00 and 1.11 in the study 1, 2, 3, respectively (Figure 6.3).

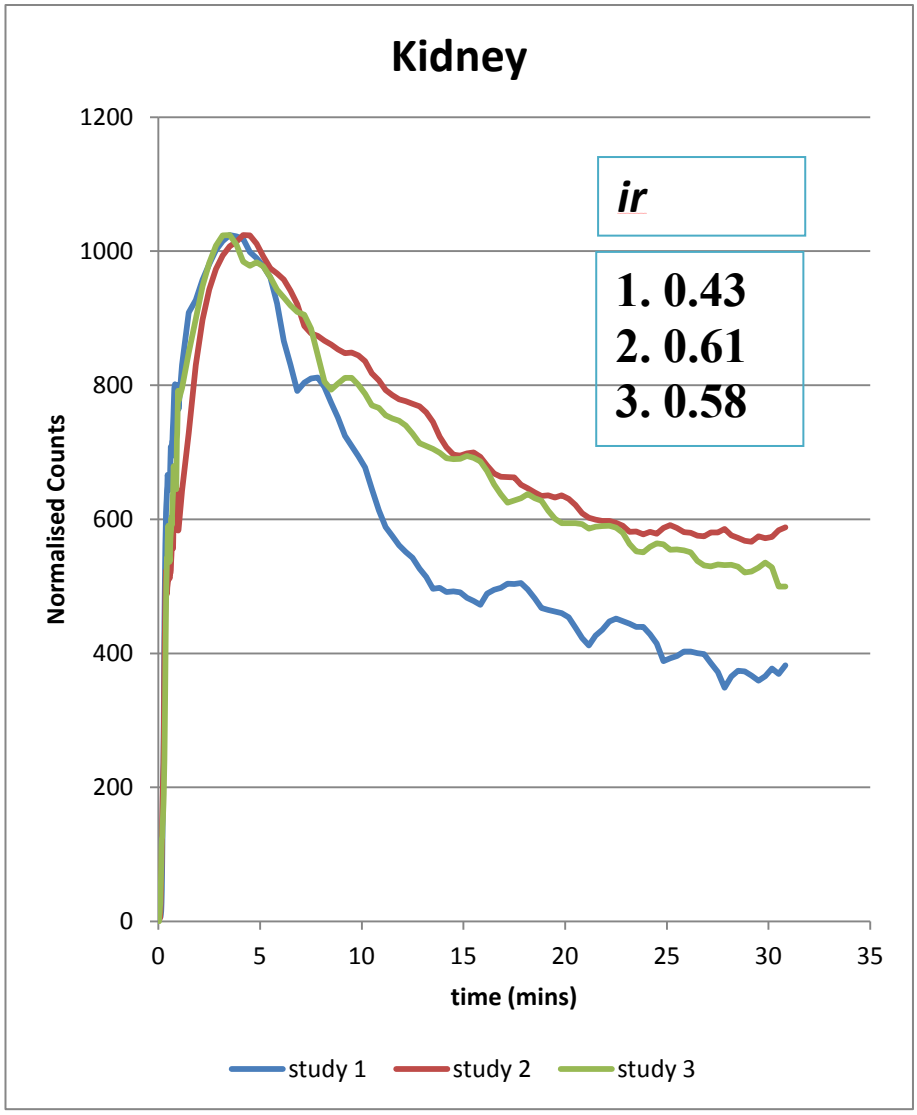

Figure 6.4 Early renal T-99m-MIBI kinetics before and after CsA treatment in patient 2 (*ABCB1* Genotype 3435TC, 2677TG, 1236TC) with high blood CsA level of 473 µg/l (target 100-300).

For patient 2, renogram curves demonstrated slower renal Tc-99m-MIBI elimination following pharmacological inhibition with CsA between the 1st and 2nd study and probably no significant change at the 3rd study. 20-min/ peak renal index ratios (*ir*) were calculated at 0.43, 0.61, 0.58 in studies 1, 2, 3,

respectively (Figure 6.4).This patient's baseline GFR was 91 ml/min/1.73m^2), while GFR at the 3rd study was 81 ml/min/1.73m^2. .

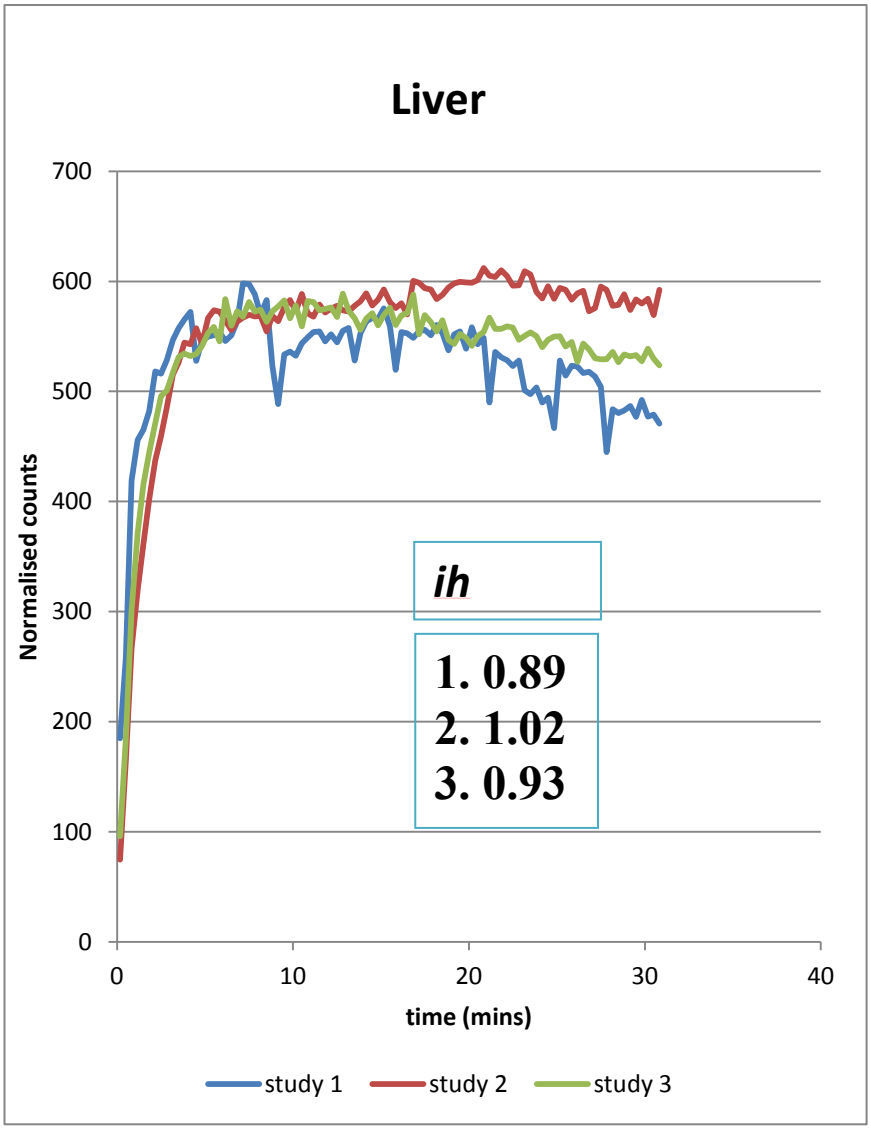

Figure 6.5 Early hepatic T-99m-MIBI kinetics before and after CsA treatment in patient 2 (*ABCB1* Genotype: 3435TC, 2677TG, 1236TC) with high blood CsA level of 473 µg/l (target 100-300).

For patient 2, hepatogram curves demonstrated slower hepatic Tc-99m-MIBI elimination following pharmacological inhibition with CsA between the 1st and 2nd study, and a possible slight compensatory quicker elimination between

2nd and 3rd studies. 30 min/10 min hepatic index ratios (*ih*) were calculated at 0.89, 1.02 and 0.93 in the studies 1, 2, 3, respectively (Figure 6.5).

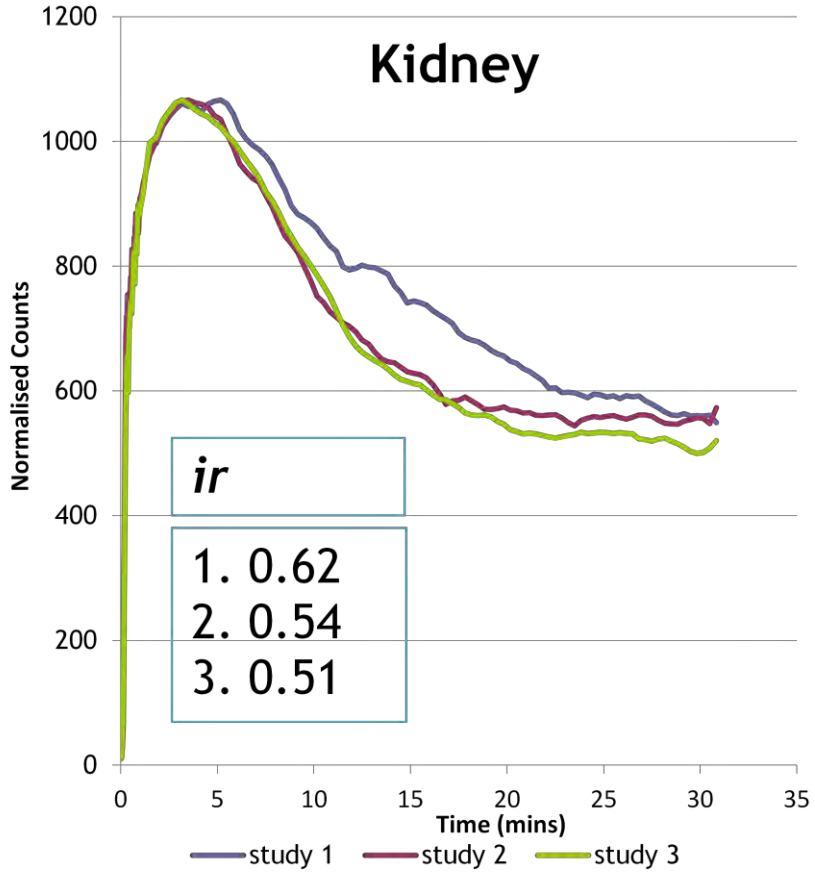

Figure 6.6 Early renal T-99m-MIBI kinetics before and after CsA treatment in patient 3 *(ABCB1* Genotype 3435CC, 2677GG,1236CC) with CsA blood level within the target range of 175 µg/l (target range 100-300).

For patient 3, renogram curves demonstrated no reduction in Tc-99m-MIBI renal elimination following oral administration of CsA between the 1st and 2nd studies. A slight compensatory quicker elimination between 1st, 2nd and 1st and 3rd studies is observed and no change between 2nd and 3rd studies. 20 min /peak renal index ratios (*ir*) were calculated at 0.62, 0.54, 0.51 in the studies 1, 2, 3, respectively (Figure 6.6). This patient's baseline GFR (92 ml/min/1.73 m^2) has slightly increased to 104 ml/min/1.73m^2 at the 3rd study.

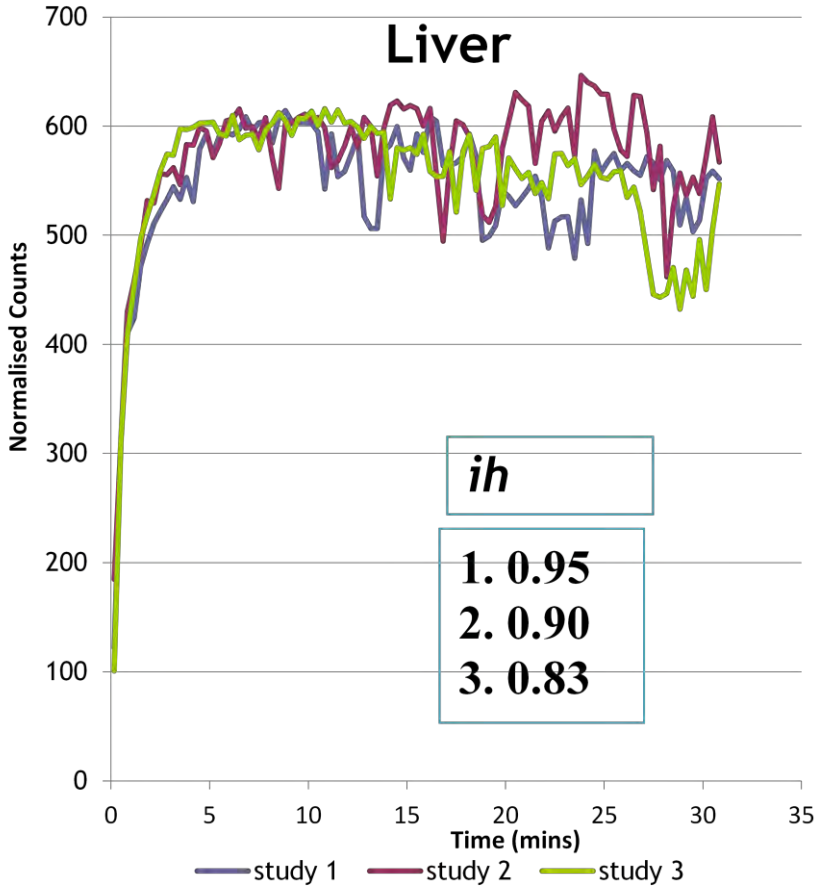

Figure 6.7 Early hepatic T-99m-MIBI kinetics before and after CsA treatment in patient 3 (*ABCB1* Genotype: 3435CC, 2677GG,1236CC) with blood CsA level within the target range of 175 µg/l (target 100-300).

For the patient 3, hepatogram curves demonstrated no reduction in Tc-99m-MIBI hepatic elimination following oral administration of ciclopsorin between 1st and 2nd study, and no significant change between 2nd and 3rd studies. A possible slight compensatory quicker elimination between 1st / 2nd and 3rd studies is observed. 30min/10 min hepatic index ratios (*ih*) were calculated at

0.95, 0.90 and 0.83 in the study 1, 2, 3, respectively (

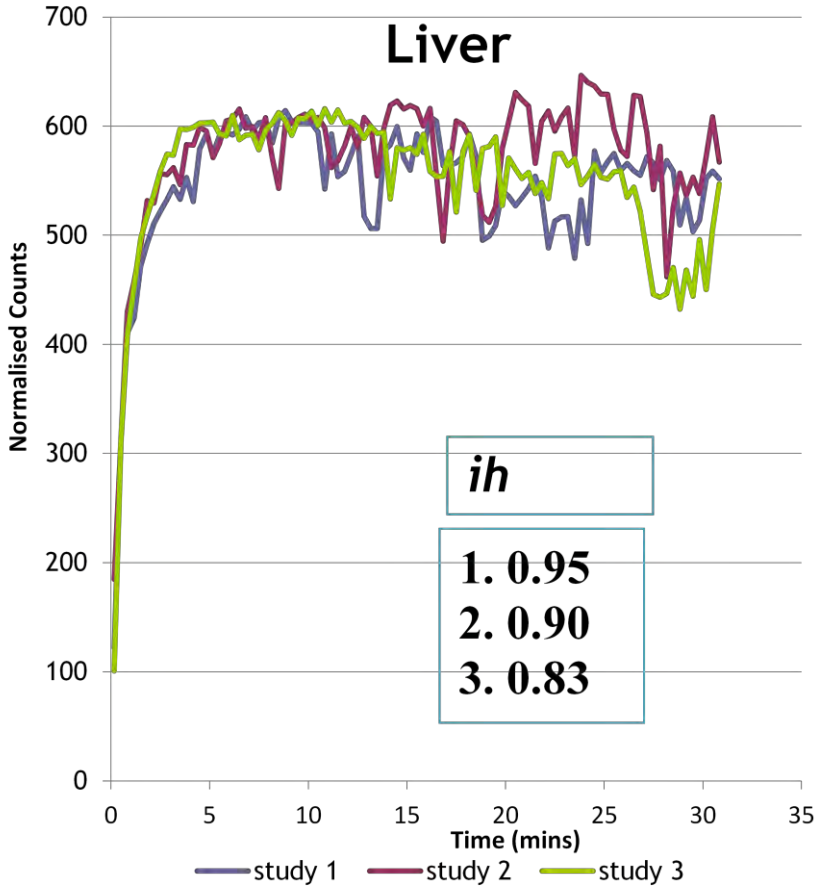

Figure **6.7**).

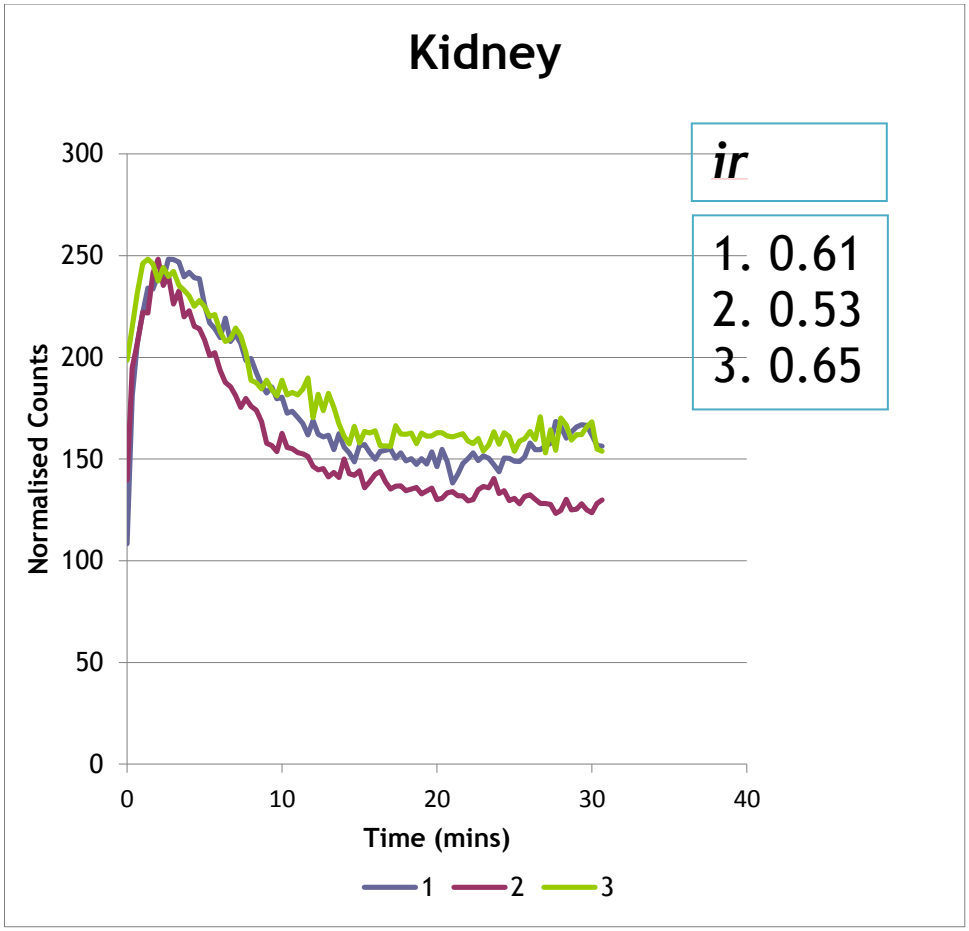

Figure 6.8 Early renal T-99m-MIBI kinetics before and after CsA treatment in the patient 4 (*ABCB1* genotypes: 3435TC,2677GG,1236CC) with low, below the target blood CsA level of 58 µg/l (target 100-300).

For the patient 4, renogram curves and renal indices (*ir*) demonstrate no reduction in Tc-99m-MIBI renal elimination following oral administration of CsA between 1st and 2nd study. A possible slight compensatory quicker elimination between 1stand 2nd studies is observed with return to above baseline at the 3rd study. 20-min/ peak renal index ratio (*ir*) were calculated at 0.61, 0.53, 0.65 in the study 1, 2, 3, respectively (Figure 6.8). This patient's baseline GFR was 88 ml/min/1.73m^2, while GFR at the 3rd study was 78 ml/min/1.73m^2.

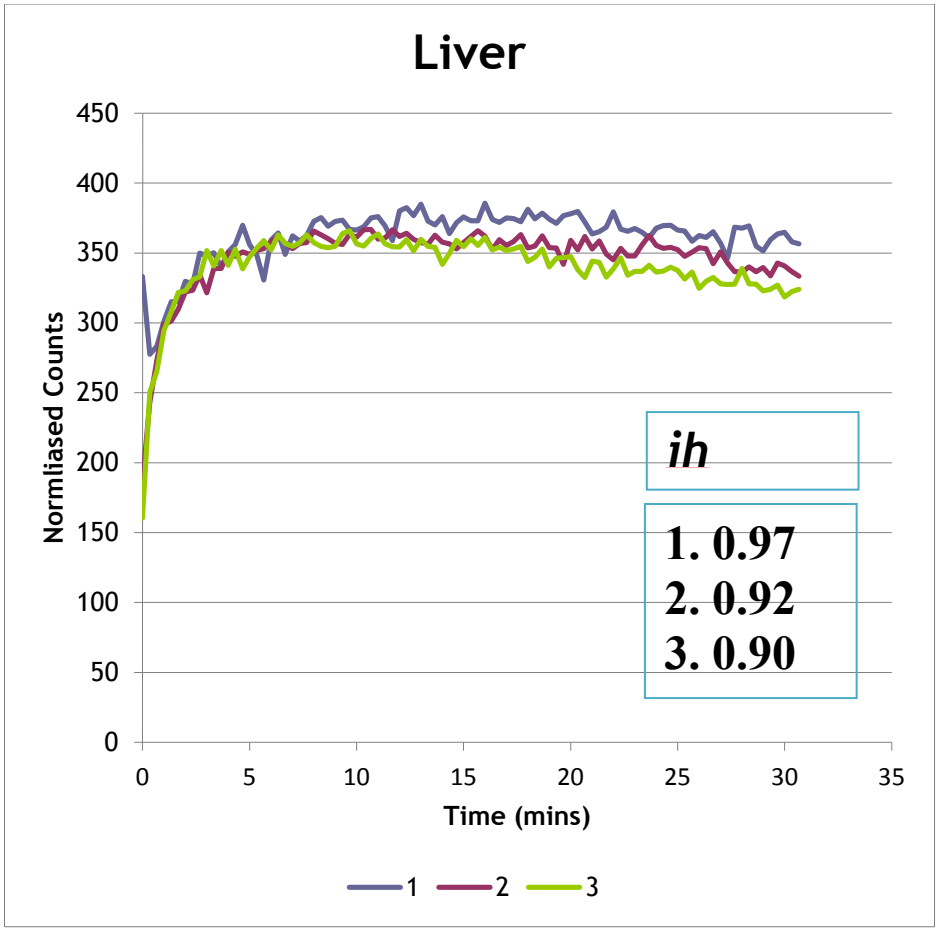

Figure 6.9 Early hepatic Tc-99m-MIBI kinetics before and after CsA treatment in the patient 4 (*ABCB1* genotypes 3435TC,2677GG,1236CC) with low, below the target blood CsA level of 58 µg/l (target 100-300).

For patient 4, hepatogram curves demonstrated no reduction in Tc-99m-MIBI renal elimination following pharmacological inhibition with CsA between the 1st and 2nd study. A possible slight compensatory quicker up-regulated elimination between 1st, 2nd and 3rd studies is observed as shown by hepatic indices and curves. 30-min/peak hepatic index ratios were calculated at 0.97, 0.92, 0.90 in studies 1, 2 and 3, respectively (Figure 6.9).

6.4.4 Effect of CsA on delayed (phase 2) Tc-99m-MIBI elimination

6.4.4.1 Planar and SPECT rates (k) vs. genotype

CsA treatment delayed elimination between 30 and 120 min in all patients (Table 6.3 and Table 6.4). Planar *k* values were calculated from 5 minute static planar views at 30 min and 2 h post intravenous injection of Tc-99m-MIBI (Table 6.3). Due to overlying adjacent extra-renal activity and to improve analysis, *k* values were also measured from SPECT data (Table 6.4).

Patient (study_no)	Kidney *k* (h^{-1})	Liver *k* (h^{-1})	CsA (ug/l)	Genotype 1236C>T	GFR ml/min/1.73m^2
1-1	0.211	0.711	810	T:T	108
1-2	0.206	0.411			
1-3	0.183	0.427			104
2-1	0.503	0.585	473	T:T	91
2-2	0.166	0.289			
2-3	0.214	0.306			81
3-1	0.277	0.331	175	C:C	92
3-2	0.202	0.124			
3-3	0.212	0.459			104
4-1	0.340	0.735	58	C:C	88
4-2	0.141	0.295			
4-3	0.110	0.324			78

Table 6.3 Elimination rates of Tc-99m-MIBI (*k*) from kidney and liver between 30 and 120 min (phase 2) on planar imaging in relation to 1236C>T genotype and GFR.

Sagittal composite volume slices at 30 min and 2 h post intravenous injection of Tc-99m-MIBI, including all kidneys and liver slices whilst excluding the overlying and underlying activity, were created (Figure 6.11) and *k* values

were measured for 3 Tc-99m-MIBI studies for 3 patients (Table 6.4). Patient number 1 had only 2 SPECT studies (studies 2 and 3) as a result of technical problems with the gamma camera during the first SPECT study (Table 6.4). SPECT values for this patient's study 1 were extrapolated from the planar study, as planar *k* values for the other 2 studies for this patient were consistent with values for planar imaging (Table 6.3, Table 6.4).

6.4.4.1.1 Visual analysis

Comparing the 2nd and 3rd studies by visual analysis it was clearly noticeable that hepatic Tc-99m-MIBI washout is much faster in the 3rd study than in the 1st and 2nd studies (Figure 6.10, 1st row = study 1, 2nd row =study 2, 3rd row =study 3). This is suggestive of up-regulation of ABC/P-gp transporters. Kidneys are more difficult for direct visual assessment, but their *k* values indicated the same. A slight retention in the liver, between the 1st and 2nd studies is explained by initial inhibition of ABC/P-gp (Figure 6.10).

However, comparing the 2nd and 3rd studies for the patient with 1236TT genotype (Figure 6.11, 1st row = 2nd study, 2nd row =3rd study) by visual analysis, there was no obvious change in liver appearances between the 2nd and 3rd studies. This was consistent with hepatic *k values* (Table 6.4; 1.2 and 1.3.), which showed slightly lower values possibly due to further ABC/Pgp down-regulation. The scan appearances clearly differ from those for the patient with 1236CC genotype (Figure 6.10).

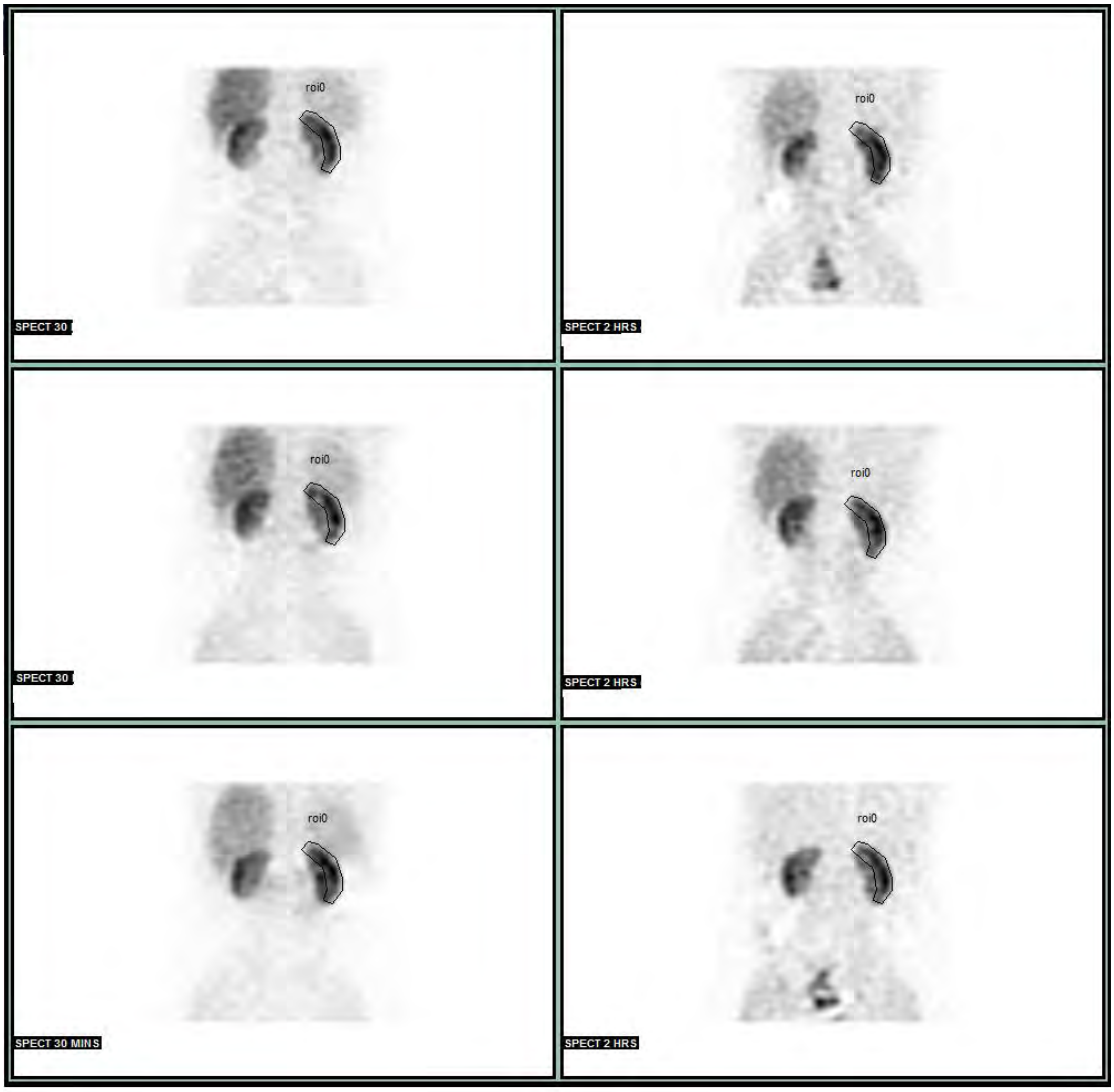

Figure 6.10 Coronal composite renal and hepatic volume slices at 30 min and 2 h post intravenous injection of Tc-99m-MIBI for all 3 studies, for patient 3 (Table 6.4) with 1236CC genotype.

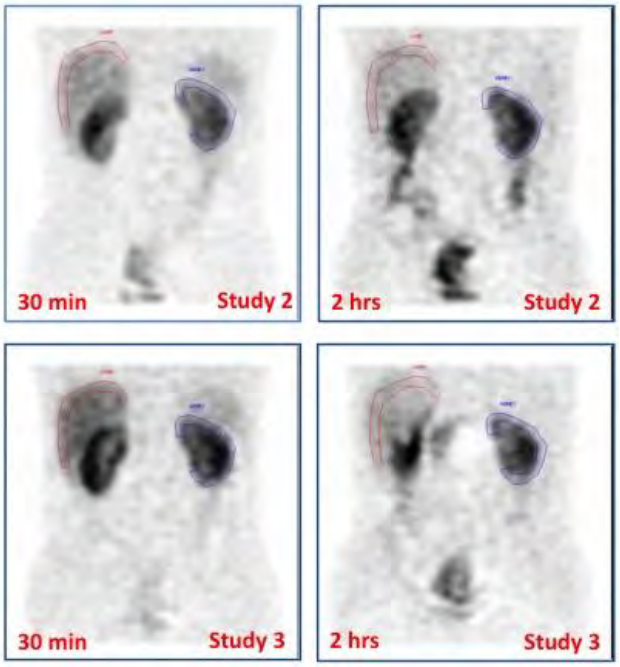

Figure 6.11 Coronal composite renal and hepatic volume slices at 30 min and 2 h post intravenous injection of Tc-99m-MIBI for 2nd (1st row) and 3rd (2nd row) studies, for patient 1 (Table 6.4) homozygous for 1236TT genotype.

6.4.4.1.2 SPECT renal and hepatic k

SPECT renal *k* was slower between the baseline and 2nd studies in 2 patients with 1236CC and 2677GG (levels of 175 and 58 µg/l), and one patient with 1236TC (473 µg/l). There was also a slight reduction in *k* in the patient with 1236TT and the highest CsA blood level of 810 µg/l, as extrapolated from planar imaging.

Hepatic *k* was slower in all patients between the baseline and 2nd studies.

The 3rd Tc-99m-MIBI study showed subsequent compensatory up-regulation in both the kidney and liver in 2 patients homozygous for 1236CC and 2677GG with *k* values exceeding the baseline value, but further inhibition in both renal and hepatic *k* in a patient homozygote 1236TT.

A 1236TG heterozygote showed increased hepatic *k* in the 3rd study, but this had not returned to the baseline level, without change in renal *k*.

There was little correlation with 3435C>T at exon 26, namely one patient had 3435CC genotype (CsA within the target), while the other 3 had CT genotypes.

No correlation was seen with 1199G>A at exon 11. All patients had the same GG genotype.

Patient (study_no)	Kidney SPECT *k* (h^{-1})	Liver SPECT *k*(h^{-1})	CsA (µg/l)	Genotype 1236C>T	GFR ml/min/1.73m2
1-1	0.219	0.88	810	T:T	108
1-2	0.214	0.51			
1-3	0.110	0.46			104
2-1	0.398	1.46	473	T:C	91
2-2	0.292	0.50			
2-3	0.292	0.93			81
3-1	0.192	0.45	175	C:C	92
3-2	0.133	0.21			
3-3	0.211	0.63			104
4-1	0.180	0.32	58	C:C	88
4-2	0.161	0.24			
4-3	0.266	0.96			78

Table 6.4 SPECT renal and hepatic *k* values before (study 1) and after CsA treatment (study 2 and 3) in relation to blood CsA levels, *ABCB1* genotypes and GFR.

6.4.5 Clinical assessment and outcomes

All patients presented with severe skins lesions with DLQI – severe impairment >10 (range 12 – 24) and PASI >10 (range 10.8 – 14.8). The patient with 1236TT and highest blood CsA level had an excellent response (PASI 14.8 to 1.4), but his CsA treatment was discontinued soon after his 3rd

study due to clinical concern because of his high blood CsA level. Another patient with a high CsA level with a heterozygote 1236TC responded very well and his CsA treatment was stopped after 6 months with no change in renal function.

One patient homozygote for 1236CC had a partial response and has been controlled reasonably well with no change in renal function. Another patient homozygous for 1236CC had an initial partial response within the first two months and very good response after 4 months of treatment and no change in renal function.

6.5 Discussion

This project is clinically relevant insofar as it improves our understanding of CsA effect on Tc-99m-MIBI kinetics. In addition, it also explores CsA effects on renal and hepatic Tc-99m-MIBI pharmacokinetics in relation to *ABCB1* genotypes. This preliminary proof-of principle study is the first study to demonstrate effects of CsA on renal Tc-99m-MIBI kinetics and provides the impetus for the development of imaging methods for predicting the risk of developing nephrotoxicity or dose selection of drugs that are ABC/P-gp substrates, including CNI, pending correlation with clinical outcomes.

6.5.1 Semi-quantitative measurement of Tc-99m-MIBI elimination

In the early phase up to 20 - 30 min (phase 1), Tc-99m-MIBI elimination was semi-quantitatively assessed by renal and hepatic renal index ratios (*ir and ih*). In the delayed phase (phase 2) of Tc-99m-MIBI elimination, I have also

developed a semi-quantitative method for measurement of functional ABC/Pgp expression with Tc-99m-MIBI rate constants (*k*) using planar and SPECT data. SPECT acquisition and analysis allowed the whole parenchyma of the kidney and liver to be analysed, thereby giving better counting statistics and minimising error due to the activity adjacent to the kidneys. This has enabled a clear outline of the target organ, producing more reliable results than by planar imaging. Subsequently, I have correlated *i* and *k* results with blood CsA levels, genotyping and GFR.

6.5.2 CsA blood levels and bioavailability

The introduction of CsA in the early 1980s, together with advances in surgical procedures, has revolutionised organ transplantation. CsA has been the mainstay of most immunosuppressive regimens in organ transplantation until recently. CsA is extensively distributed in peripheral tissues. CsA distribution in the blood is approximately 41 to 58% in erythrocytes, 33 to 47% in plasma, 5 to 12% in granulocytes, and 4 to 9% in lymphocytes. In plasma, CsA binds primarily to lipoproteins and secondarily to albumin. CsA is highly lipophilic and its oral absorption is slow and incomplete (168). Food causes a clinically significant decrease in peak concentration and exposure of CsA, so all patients were asked to fast for 4 hours prior to blood test, but to be well hydrated.

The original brand name of CsA is Sandimmune®, which is available as soft gelatin capsules, oral solution, and intravenous formulation (169). Subsequently, the microemulsion formulation Neoral®, which exhibits a more rapid and consistent absorption than Sandimmune®, has become available

as soft gelatin capsules and oral solution (170). The absolute oral bioavailability of CsA administered as Sandimmune® is dependent on the patient population, estimated to be less than 10% in liver transplant patients and as great as 89% in some renal transplant patients. Neoral® has increased bioavailability compared to Sandimmune® and it has therefore been used in this study. In previous studies of renal transplant, rheumatoid arthritis and psoriasis patients, the mean CsA AUC was approximately 20% to 50% greater and the peak blood CsA concentration (Cmax) was approximately 40% to 106% greater following administration of Neoral® compared to Sandimmune®. Following oral administration of Neoral®, the time to peak blood CsA concentrations (Tmax) ranged from 1.5-2.0 hours (170).

In this study, CsA was administered orally for 2 weeks (3mg/kg/daily divided in two doses i.e. 1.5mg/kg bd). The blood CsA level was determined 30 min after oral administration of the morning dose. This timing was chosen as *in vitro* Tc-99m-MIBI studies have shown that P-gp inhibitors can reverse P-gp expression in adenocarcinoma cells if given shortly before the administration of cytotoxic drug (171). This *in vitro* study indicated that a P-gp inhibitor should be administered close to incubation with Tc-99m-MIBI i.e. 30-60 min prior to incubation (171) and therefore all 4 patients had their second Tc-99m-MIBI study close to administration of CsA in order to try to 'challenge' Tc-99m- MIBI kinetics with 'acute' CsA exposure. As this oral dose was small when compared to transplant doses, all patients were also already on the same treatment regimen (3mg/kg/day) in a duration of 2 weeks.

Therapy with CsA is characterised by considerable inter and intra-individual variability (172) (173) in its pharmacokinetics (PK) and it is difficult to remain within the therapeutic window. All 4 patients in this study had different blood CsA levels in spite of a standardised treatment regimen, confirming inter-individual variability of CsA.

It is difficult to predict the exposure of CsA in a patient on a particular dose due to the large variability in its pharmacokinetics. Therefore, to optimise therapy in clinical practice, therapeutic drug monitoring (TDM), aimed at individualised CsA dosing, is common practice (172) (174) (175) (176); however an imaging assay, which can help in dose selection, would be very useful in clinical practice.

In the post-transplant setting, TDM is performed on the basis of a limited sampling strategy (blood concentration at t=0, 2, and 3 h). It has been previously indicated that individualising CsA treatment in adult kidney transplant recipients can be achieved by a body weight-based dosage followed by a TDM strategy (172). However, in clinical practice in transplant recipients this is proven to be difficult and not readily optimised. Also, in my study, in spite of the body-weight adjusted treatment all patients had different blood CsA levels. However, their blood CsA levels were consistent with Tc-99m-MIBI kinetics, particularly in the first phase of elimination, and hence Tc-99m-MIBI may potentially provide a way for imaging variability in CsA pharmacokinetics.

6.5.3 Effects of CsA on Tc-99m-MIBI kinetics

Previous studies have demonstrated the effect of CsA on Tc-99m-MIBI kinetics in liver (49) and more recently with the development of PET, new P-gp-specific radiopharmaceticals were used for investigating inhibition of P-gp in the brain at the blood-brain–barrier (Figure 6.12). However, my study is the first study to image a CsA effect in the kidney *in vivo* by a radiopharmaceutical. Some PET tracers could potentially be applicable in assessment of renal P-gp. However, in spite of their advantage of higher energy and subsequent higher PET resolution as well as a possibility for true quantification, PET agents have major limitations for use in clinical practice as most are cyclotron produced and labelled with C-11, which has a half-life of only 20 min.

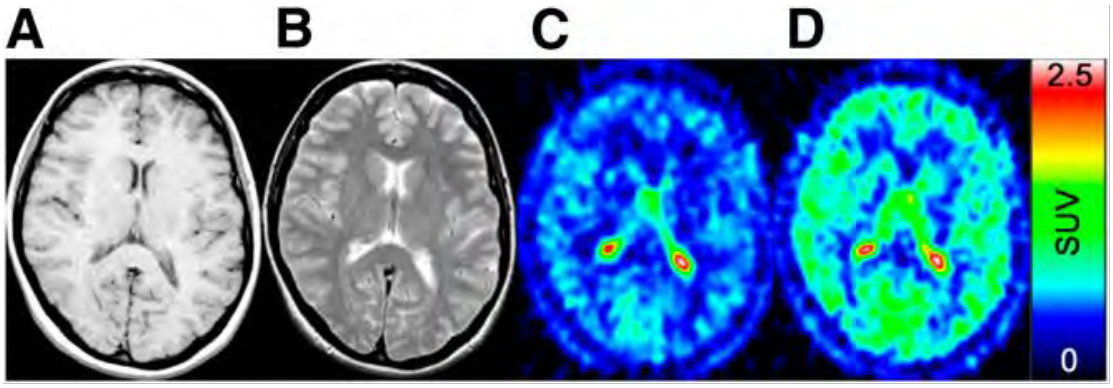

Figure 6.12 C-11-verapamil images demonstrating inhibition of P-gp in the brain after 1 hour of CsA infusion.

Figure 6.12 demonstrates the T1-weighted MR image (A) from a representative subject and corresponding T2-weighted MR image (B) provide anatomic reference. C: C-11-verapamil uptake image (SUV) before CsA treatment was acquired between 5 and 25 min after injection. D: C-11-verapamil uptake image after 1 h of CsA infusion shows a general increase

in verapamil uptake in all areas of brain after inhibition of P-gp by CsA. The colour scale reflects SUV as shown by thermometer. (Reprinted with permission from the Society of Nuclear Medicine from Muzi M, Mankoff D, Link J, et al. Imaging of CsA inhibition of P-glycoprotein activity using C-11-Verapamil in the brain: Studies of healthy humans. J Nucl Med. 2009;50: 1267–1275. Figure 5. (39))

It is important to image the kidney in CNI nephrotoxicity, as there is evidence that local renal CNI concentrations are important for development of CNI nephrotoxicity in association with P-gp expression (147).

Only 6% of the CsA dose, including parent drug and metabolites with just 0.1% unchanged CsA dose, is excreted in the urine. However, in spite of this small proportion of urinary excretion, it has been demonstrated that local renal accumulation has a significant effect on development of adverse side effects. The high exposure to CsA is associated with serious adverse effects such as hypertension, post-transplant diabetes mellitus, dyslipidemia, intermittent renal hypoperfusion, and both reversible acute toxicity and irreversible tubule-interstitial fibrosis (168) (176) (177). The low exposure to CsA has been shown to be associated with acute and/or chronic rejection (168) (178) (179).

CsA is extensively metabolised in the liver via the CYP3A pathway, and the metabolites are extensively excreted in the bile. The blood clearance of CsA is 0.3-0.4 L/kg and the half-life ranges from 5 to 27 h (169) (170). Elimination of CsA is primarily biliary and hepatotoxicity is also known, but a less frequently documented adverse effect than CNI nephrotoxicity. Therefore,

hepatic Tc-99m-MIBI kinetics was also investigated at the same time as the renal kinetics. In the liver, transportation of Tc-99m-MIBI from heptobiliary canalicular cells to bile is driven by ABC/P-gp and can be blocked by CsA (49) or tarquidar (88). Tc-99m-MIBI elimination from renal cells is also mediated by P-gp (88) (54). It has been observed that treatment with another P-gp modulator, PSC 833, increased renal retention of Tc-99m-MIBI in 3 patients with refractory cancer (54). However, mine is the first study to investigate Tc-99m-MIBI handling by the kidneys in patients receiving CNI (chapter 6) and in the pre-transplantation setting in healthy potential kidney donors (Chapters 3,4,5,) (96) (121).

In phase 1, 2 patients with high blood CsA levels showed slower Tc-99m-MIBI early elimination following exposure to CsA treatment as a result of pharmacological *in vivo* inhibition of ABC/P-gp transporters. This can be explained by initial down-regulation of ABC/P-gp transporters. Contrary, pharmacological inhibition of ABC/P-gp measured by Tc-99m-MIBI elimination rate was not demonstrated in the 2 patients with low blood CsA level and a level within the target.

In the delayed phase of Tc-99m-MIBI elimination, an inverse relation between blood CsA level and Tc-99m-MIBI kinetics has been observed. In phase 2, contrary to the above, between 1st and 2nd MIBI studies some inhibition was demonstrated in all 4 patients with minimal pharmacological inhibition in the patient with the highest blood CsA level and apparent inhibition in the other 3 patients. These findings indicate that different mechanisms and/or ABC transporters govern phase 1 and 2. Certainly, in phase 1, glomerular filtration has an important role in very early Tc-99m-MIBI

elimination, while ABC/P-gp transporters mostly regulate phase 2. Furthermore, there was an inverse relation observed between CsA levels and pharmacokinetic changes between the 2nd and 3rd Tc-99m-MIBI studies in 3 patients and an inconsistent response in one patient heterozygote for 1236TC genotype. Between the 2nd and 3rd studies, there was no inhibition of Tc-99m-MIBI elimination in the patient with the highest CsA level, while much faster Tc-99m-MIBI elimination was noted with *k* values exceeding the baseline values in 2 patients with low and on-target blood CsA levels. This finding may be due to compensatory up-regulation of ABC/P-gp transporter related elimination after prolonged CsA treatment. The remaining patient showed an increase in *k* hepatic values, but this did not return to baseline *k* and there was no change in renal *k* values. Kabasakal et al. described inhibition of Tc-99m-MIBI elimination from the liver following 2 weeks of CsA treatment (49), but did not investigate a prolonged CsA effect on liver kinetics. Mine is the first study to monitor a prolonged effect of CsA (Tc-99m-MIBI study 3; 6-12 weeks after CsA treatment) on Tc-99m-MIBI elimination from both kidney and liver in the context of possible up-regulation or down-regulation of P-gp/ABC protein transporters.

The findings from this study imply that Tc-99m-MIBI may provide a way for imaging variability in CsA pharmacokinetics. The current trend toward minimising exposure to CNI requires insight into the variability in CNI (CsA and tacrolimus) pharmacokinetics, because of an increased risk of acute rejection episodes. However, tacrolimus influence on Tc-99m-MIBI pharmacokinetics is to yet be investigated in future research studies due to a potential role of Tc-99m-MIBI imaging to guide the target exposure early after

transplantation and subsequently to adjust CNI treatment regimen. It has previously been demonstrated that one month after tacrolimus introduction, exon 21 SNP correlated significantly with the daily tacrolimus dose ($P < 0.05$) and the concentration/dose ratio ($P < 0.02$). Tacrolimus dose requirements were 40% higher in homozygous than wild-type patients for this SNP. The concentration/dose ratio was 36% lower in the wild-type patients, suggesting that for a given dose, their tacrolimus blood concentration is lower. In addition, haplotype analysis substantiated these results and suggested that exons 26 and 21 SNP may be associated with tacrolimus dose requirements (180). Furthermore, a meta-analysis of 13 papers (1327 individuals) showed that SNP C3435T could influence the pharmacokinetic parameters. The subjects with CC genotype had lower concentration dose ratio and need a higher tacrolimus dose than the CT and TT genotype. Those results confirmed a correlation between the SNP C3435T in MDR1 gene and pharmacokinetics of tacrolimus (181).

6.5.4 Tc-99m-MIBI pharmacokinetic changes due to exposure to CsA in relation to ABCB1 genotypes

This is also the first study to investigate Tc-99m-MIBI renal and hepatic pharmacokinetic changes due to CsA exposure in relation to *ABCB1* genotypes. There is very limited data in the literature on correlation of Tc-99m-MIBI kinetics with genotypes (29) (121), including my recently published data (121).

P-gp expression is genetically determined (17). Whilst genotyping could provide pre-treatment information, the functional expression of ABC/Pgp may

only become apparent after treatment is started. In addition, different SNPs may be associated with response to treatment when compared to those associated with constitutional baseline P-gp expression.

Further to administration of P-gp inhibitor and following initial down-regulation, P-gp is expected to be typically up-regulated in response to prolonged exposure to a P-gp substrate, however this response seems to be variable and individualised. This individualised response may lead to either nephrotoxicity (if sustained down-regulation) or failure to respond to treatment or drug resistance (in case of sustained excessive up-regulation). Tc-99m-MIBI kinetics may help to differentiate those two extreme situations and be useful for dose selection.

It has been demonstrated that the observed variability in CsA pharmacokinetics originates from biological and lifestyle-related factors, including age, body size, gender, food intake, serum albumin concentration, haematocrit, lipoproteins (HDL, LDL), and co-administration of interacting drugs (173) (172) (173). Yet, even when these factors are taken into account, a considerable part of the variability remains unexplained, which could potentially be attributed to genetic differences between patients. Insight into the relationship between CsA variability and genetic differences could potentially help in optimising CsA exposure early after transplantation (172). However, genotypes do not necessarily associate with phenotypic characteristics and functional ABC/P-gp expression, and there is controversial literature on the influence of *ABCB1* polymorphism on both

drug pharmacokinetics and P-gp expression. Therefore, a functional imaging assay may have an advantage correlating imaging findings with functional ABC/P-gp expression *in vivo* and epigenetics rather than with the underlying genome.

6.5.5 Effects of CsA on Tc-99m-MIBI renal and hepatic elimination and correlation with 3435C>T genotypes and blood CsA levels

The published data revealed conflicting results of the polymorphism of ABCB1 (MDR1) exon 26 SNP C3435T on the pharmacokinetics of CsA.

A meta-analysis of 14 papers concerning 1036 individuals using the PubMed electronic source demonstrated no major influence of SNP C3435T on the pharmacokinetic parameters, including area under the concentration - time curve from 0- 4 h (AUC0–4), area under the concentration - time curve 0-infinite (AUC0-inf), oral clearance (CL/F), maximum concentration (Cmax) and trough concentration (C0), although 0-12 h (AUC0–12) was lower in subjects with CC genotype.

A sub-analysis by ethnic population showed that C0 was lower in Caucasian individuals harbouring CC genotype. This meta-analysis of available studies has thus far failed to demonstrate a definitive correlation between the SNP C3435T in *ABCB1* gene and alterations in P-gp function that can result in altered pharmacokinetics of CsA, although it does indicate that the carrier of CC genotype of the SNP C3435T of *ABCB1* had lower CsA exposure presented as AUC0–12 than those with at least one T allele. There seemed

to be ethnic differences in the relationship between the SNP C3435T and CsA pharmacokinetics (182).

In this study, there was one patient with 3435CC genotype, who had a blood CsA level within the target range and lower than 2 other patients who had at least on T allele, but higher level than in one patient who was heterozygous for TC.

In this study, there was no apparent relation of Tc-99m-MIBI pharmacokinetic changes due to CsA exposure and C3C4C>T, but the study is limited due to a small sample size. However, the findings with respect to baseline Tc-99m-MIBI kinetics in 19 potential kidney donors showed that C3C4C>T may influence baseline Tc-99m-MIBI renal and liver kinetics (Chapter 5) (121).

It has been previously demonstrated that genetically determined responses to some anticancer drugs may influence anticancer treatment. It has been shown that imaging the liver with Tc-99m-MIBI may provide pre-treatment indicators of *ABCB1*-mediated hepatic drug clearance in cancer patients. Tc-99m-MIBI hepatic elimination (*kh*) was significantly reduced in patients with SNPs in exons 21 (2677G>TA) and 26 (C3C4C>T). The mean MIBI *kh* was respectively 1.90 times and 2.21 times higher in subjects homozygous for the wild-type alleles (CC) compared to those homozygous TT for these SNPs (29). However, mine is the first study to investigate Tc-99m-MIBI pharmacokinetics in response to CsA treatment and in context of genotypes.

6.5.6 Effects of CsA on Tc-99m-MIBI renal and hepatic elimination and correlation with 1236C>T genotypes and blood CsA levels

In this study, 1236C>T appears to influence response to CsA as measured by Tc-99m-MIBI pharmacokinetics in the 4 patients studied. Two of the 4 patients were homozygous for 1236CC and one was homozygous for 1236TT. Patients with 1236CC genotype clearly handled Tc-99m-MIBI differently in both the early (phase 1) and delayed phases (phase 2) when compared with patients with at least one T allele (one patient homozygous for TT and one patient heterozygous for TC). Two homozygotes for 1236CC also had lower blood CsA values (i.e. low and on the target) when compared to those harbouring at least one T alleles. The patient homozygote for 1236TT genotype had the highest blood CsA level.

Potential phenotypic associations for this silent SNP are also controversial (183) (184). Similarly to findings from this study, under the same CsA regimen, it was found that the trough CsA concentrations of variant genotype (*ABCB1* 1236TT or *ABCB1* 2677TT) were significant greater than those of wild-type (ABCB1 1236CC or ABCB1 2677GG, respectively) (P = 0.0222 and 0.0081) in myasthenia gravis patients. In addition, the trough concentrations of wild-type haplotype pair group were significantly lower than those of the mutant type pair group (TT-TT-TT) (P = 0.007) (185). Consistent with the above findings, the homozygous T allele of the ABCB1 1236C>T polymorphism was also associated with significantly increased exposure to irinotecan (P = 0.038) and its active metabolite SN-38 (P = 0.031) in cancer

patients (186). It was concluded that genotyping for ABCB1 1236C>T may be one of the factors assisting with dose optimisation of irinotecan chemotherapy in cancer patients (186).

However, with respect to treatment with temozolamide, the genotype of the *ABCB1* exon12 C1236T SNP was shown to be a novel independent predictive factor for outcome in glioblastoma patients. Controversially, CC variant of the exon12 C1236T SNP was predictive for survival of patients treated with temozolomide. Patients with the CC genotype had a 2-year overall survival of 37% compared with 8% and 10% for patients with CT and TT genotypes, respectively (P=0.02) (187). However, this seems to be in disequilibrium with respects to AML. Patients with AML FLT3 wild-type 1236CC patients had significantly shorter overall survival compared to patients carrying the variant allele; medians 20 vs. 49 months, respectively (p = 0.017). This was consistent with previously described findings for 3435CC genotype, which was also linked with poor prognosis in AML (6). There was also an inferior outcome in FLT3 wild-type 2677GG patients compared to patients carrying the variant allele, median OS 20 vs. 35 months, respectively (p = 0.039) (188).

Further controversial findings were related to HAART treatment where ABCB1 1236C>T, 2667G>T/A and 3435C>T genotypes and haplotypes were found not to predict lopinavir and ritonavir concentrations in blood plasma, semen or saliva of HIV-infected men under stable treatment (189).

6.5.7 Effects of CsA on Tc-99m-MIBI renal and hepatic elimination and correlation with 2677G>T/A genotypes and blood CsA levels

With respect to *ABCB1* 2677G>T/A, 2 patients were homozygous for CC and two heterozygous for TG. This SNP was shown to be in functional disequilibrium with C3C4 site (167). Hebert et al. demonstrated that the frequency of renal dysfunction was reduced among patients with liver transplant with an *ABCB1* 2677TT genotype (which is opposite to previously described 3435CC), as compared to those with a *2677GG* genotype. Subjects with a heterozygote genotype behaved phenotypically like the 2677GG group. Comparing those subjects with a 2677TT genotype to the combined group of subjects with a 2677GG, TG, AT, or AG genotype resulted in an odds ratio of 0.26 (0.09 - 0.77). When subjects were stratified by gender, the frequency of renal dysfunction was reduced among men with an *ABCB1* 2677TT genotype, relative to men with different genotypes. A similar odds ratio was obtained for women, but it did not achieve significance. Based on these results, Hebert et al. conclude that homozygosity for the *ABCB1* 2677T allele is associated with reduced risk of chronic renal dysfunction among liver transplantation patients receiving an immunosuppressive regimen containing CNIs (167).

In my study, there was no single patient homozygote for 2677TT genotype. There are also no data available for this genotype in renal transplant patients and further studies are required to establish a role of this genotype in potential CNI nephrotoxicity in renal transplant setting.

6.5.8 Correlation with GFR and treatment outcomes up to 12 weeks

The ability to induce nephrotoxicity *in vivo* correlates with the immunosuppression activity of CNIs (190). Previous research strongly suggested that the mechanisms of immunosuppression are the same as those of toxicity, that is, calcineurin inhibition (190).

There appears to be an inverse relation in the kidney transplant setting between likelihood of rejection, which is associated with strong P-gp expression in infiltrating leucocytes of the recipient, and nephrotoxicity, which is associated with weak P-gp expression in the donor (24) (26). This implies that in other diseases treated by CsA, such as psoriasis, there may be an inverse relation between nephrotoxicity (low P-gp expression) and resistance to treatment (high P-gp expression). On the other hand, in a study on heart transplant recipients receiving CsA, there was no relation between *MDR-1* genotype and nephrotoxicity (191).

The patient with homozygote 1236TT genotype and the highest blood CsA level had an excellent response to treatment, but his CsA treatment was ceased due to clinical concerns regarding his blood CsA level. It therefore remains unknown if this patient would develop nephrotoxicity if his CsA treatment had not been discontinued.

One patient homozygous for 1236CC genotype and blood CsA level within the target had reasonable partial response and remained on the same dose for 6 months without development of nephrotoxicity. Another patient with CC also had a good response to treatment without reduction of CsA dose. The

heterozygote patient with a high blood CsA level responded very well with no change in renal function within 3 months. The relationship between neprotoxicity and treatment response in relation to *ABCB1* genotype remains unclear as this sample size is small and may require a longer clinical follow up, but this is an area for further research.

It is likely that functional imaging with Tc-99m-MIBI can be a helpful tool to optimise CsA therapy in clinical practice, but correlation of Tc-99m-MIBI pharmacokinetic changes following exposure to CsA with later treatment response outcomes requires further prospective studies. It is suspected that the patients with functional inhibition of P-gp between the 1st and 2nd study in phase 2, which does not compensate at the third study are likely to require lower doses of CsA, or *vice versa,* i.e. patients that are up-regulating at the 3rd study may require higher doses of CsA. This should be prospectively investigated further as it is highly relevant for CNI treatment in general and in transplant medicine.

6.5.9 Limitations of the study

Four Caucasian patients were investigated in this 'proof of principle' study, so the sample size is small, but showed potentially relevant results.

With respect to Tc-99m-MIBI kinetics, the data so far indicate that Tc-99m-MIBI elimination is affected by CsA oral administration and in phase 1 is consistent with measured blood CsA levels. This should be further investigated in larger studies. The C allele of the synonymous (Gly412Gly) SNP, rs1128503 (1236T>C), ranges in allele frequency from 30 to 93%

depending upon the ethnic population, with C being the minor allele in Asians, and T being the minor allele in Africans (183). According to dbSNP genotype details, 66/254 subjects had 1236CC genotype (25.98%), 140/254 subjects had CT genotype (55.1%) and 48/254 subjects had TT genotype (18.8%) (192). Another study of NK-AML showed TT frequency of 18.9% CC 32.3% and CT 48.8% (188).

Two of four patients in this study were homozygous for 1236CC genotype and one was homozygous for 1236TT genotype. Patients with CC genotype clearly handled Tc-99m-MIBI differently in both the early (phase 1) and delayed phases (phase 2) when compared to patients with at least one T allele (one patient homozygous for TT and one patient heterozygous for TC genotype).

Although these data are encouraging for a potential relation of 1236C>T genotype with pharmacokinetics of Tc-99m-MIBI when challenged with CsA, there is a chance that the findings from this study were purely random, taking into an account that the frequency of 1236TT is 18.8 % and frequency of 1236CC 26%-32.3% in the total population.

Furthermore, a role for 2677G>T or combination of different *ABCB1* genotypes may also be important and should be further investigated.

6.6 Conclusion

Pharmacological *in vivo* blockade of ABC/MDR proteins alters Tc-99m-MIBI kinetics in patients receiving CsA. However, CsA inter-individual variable bioavailability may influence early (phase 1) and delayed (phase 2) Tc-99m-MIBI kinetics in different ways. High blood CsA levels result in pharmacological inhibition of ABC/P-gp as visualised by Tc-99m-MIBI imaging and slower Tc-99m-MIBI elimination in phase 1. In phase 2, blood CsA levels seem to be inversely related to pharmacological change caused by exposure to CsA.

Tc-99m-MIBI pharmacokinetics are influenced by CsA possibly through *ABCB1* SNPs 1236C>T and to a lesser extent 2677G>T rather than 3435C>T alone, unlike the baseline Tc-99m-MIBI kinetics which appeared mostly influenced by 3435C>T and not through other studied *ABCB1* SNPs (see chapter 5).

Functional influence of *ABCB1* SNPs 1236C>T (at exon 12) on pharmacological Tc-99m-MIBI handling rather than 3435C>T alone is more apparent in this preliminary study and therefore should be further investigated. With respect to 1236 site, patients homozygous for 1236CC genotype demonstrated different and opposite pharmacological effects of CsA on Tc-99m-MIBI kinetics when compared to those patients with at least one T allele, in both early and delayed phases of Tc-99m-MIBI elimination. These observed effects of CsA on Tc-99m-MIBI kinetics should be correlated with treatment outcomes and adverse or side effects of CNI treatment in larger prospective studies.

Since the 3435C>T site does not alter the protein sequence, it would appear most likely that the effects on gene expression associated with this single nucleotide polymorphism may well be due to other SNPs (1236C>T and 2677G>T) which may be physically linked to it. Correlation of Tc-99m-MIBI kinetics with different haplotypes may also need to be investigated.

It is likely that functional imaging with Tc-99m-MIBI can be a helpful tool to optimise CNI, including CsA therapy in clinical practice. It seems that Tc-99m-MIBI may provide a way for imaging bioavailability of CsA and variability in CsA pharmacokinetics. The current trend toward minimising exposure to CNI requires insight into the variability in CNI pharmacokinetics because of an increased risk of acute rejection episodes. This functional molecular imaging modality may potentially be used to reach target exposure early after transplantation and subsequently be used to adjust CNI treatment regimen to avoid chronic rejection or prevent nephrotoxicity.

This approach may lead to delivering personalised treatment with CNI tailored to the individual patient and guided by imaging and/or combination with genotyping. Functional imaging may have a role in assessing epigenetic and phenotypic characteristic of CNI nephrotoxicity rather than underlying genetic association for which the up-to-date literature is controversial and complex.

Chapter 7 Conclusions and General discussion, including suggestions for further work

7.1 Conclusions

Tc-99m-MIBI and Tc-99m-MAG3 show different patterns of renal elimination, but good agreement with respect to perfusion phase imaging and differential renal function, which can therefore be accurately measured with Tc-99m-MIBI. Tc-99m-MIBI can therefore replace Tc-99m-MAG3 for pre-transplant workup.

Neither renal nor hepatic Tc-99m-MIBI kinetics appear to be gender-dependant. The 4 organs studied (kidney, liver, spleen and myocardium) showed variable tissue elimination rates from 30 min, with the myocardium the lowest, consistent with minimal myocardial P-gp expression as shown in previously published immunohistochemical studies. However, one tissue cannot be used as a surrogate for another.

The liver rapidly excretes a more variable and lower proportion of Tc-99m-MIBI than the kidney. P-gp located at the urine/tubule and bile/hepatocyte boundaries prevents Tc-99m-MIBI re-entering cells and thereby influences elimination and retention in both early (up to 30 min) and delayed phases (up to 2 h), although other ABC transporters are probably also involved.

With respect to the liver, a variable amount of Tc-99m-MIBI is rapidly transported from blood to bile, possibly by passive diffusion, and then prevented from returning to the hepatocytes by ABC transporter proteins.

This is followed by slow excretion into bile of mitochondrial-bound tracer. Passive diffusion of some tracer back into blood is likely, as happens with bilirubin and HIDA analogues. On the basis of the amount of urinary activity and the fact that it follows the time course of renal handling, early renal Tc-99m-MIBI elimination is predominantly consistent with either glomerular filtration and urinary excretion or rapid tubular secretion. In this first phase, P-gp located at the urine/tubule barrier prevents reabsorption of Tc-99m-MIBI and therefore indirectly influences Tc-99m-MIBI elimination from, and retention within, the kidney. Later elimination (second phase), as from the liver, is likely governed by mitochondrial tracer release and subsequent elimination of Tc-99m-MIBI from cells by ABC transporters.

The baseline tissue elimination rate of Tc-99m-MIBI may represent an *in vivo* assay of constitutional ABC, effectively P-gp, transporter expression. Pharmacological *in vivo* blockade of ABC/MDR proteins alters Tc-99m-MIBI kinetics in patients receiving CsA. However, CsA bioavailability is variable and individual-specific, which influences early and delayed Tc-99m-MIBI kinetics in different ways. Tc-99m-MIBI pharmacokinetics are influenced by CsA possibly through *ABCB1* SNPs 1236C>T and to a lesser extent 2677G>T rather than 3435C>T alone, unlike the baseline Tc-99m-MIBI kinetics which appeared mostly influenced by 3435C>T and not through other studied *ABCB1* SNPs.

A role for P-gp in Tc-99m-MIBI renal handling needs to be confirmed with further experiments, including studies based on immunohistochemical staining and challenge studies with other P-gp inhibitors, such as tacrolimus. Having established such a role, the way would be opened to use Tc-99m-MIBI as a tool of predicting either nephrotoxicity due to CNI/anti-rejection therapy or allograft failure in the setting of renal transplantation, thereby providing useful information regarding dose selection of immunosuppressants, but also other nephrotoxic drugs that are P-gp substrates. Further prospective trials are required to establish the full potential of Tc-99m-MIBI in renal transplant management.

Although limited, my preliminary data suggest that baseline renal and hepatic Tc-99m-MIBI handling may be influenced by *ABCB1* C3435T polymorphism, while *ABCB1* 1236C>T polymorphism may have a more prominent role in drugs pharmacokinetics of Tc-99m-MIBI when exposed to P-gp/MRP1,2 inhibitor, such as CsA. However, larger studies are required to investigate the impact of genotype, but also haplotype variation on ABC transporter-associated Tc-99m-MIBI elimination.

In the era of personalised medicine, further prospective trials are required to investigate the impact of genotype variation on Tc-99m-MIBI imaging findings in routine clinical practice and research.

ABC/P-gp transporters play a major role in the distribution and excretion of drugs and are involved in intrinsic and acquired drug resistance and toxicity. However, the regulation of *ABCB1* expression is complex and actually has

not been well validated in a clinical setting. Various molecular signalling, genetic network and epigenetic interactions govern *ABCB1* expression (193) and the functional imaging may help to portray the phenotypic characteristics of two opposite phenomena such as drug toxicity and resistance.

7.2 General discussion and suggestions for future work

There is an unexplored potential for use of Tc-99m-MIBI imaging in a variety of diseases where ABC protein transporters, including P-gp have a probable important pathophysiological role. More research is needed to identify patients, through imaging, who are susceptible to multidrug resistance, but also drug toxicity side effects, to provide information concerning dose adjustment and to allow better decision making when considering therapy with anti-cancer or HIV drugs that are also ABC-protein transporter substrates. In the post-genomic era of individualised medicine, ABC imaging may be helpful to adjust the treatment dose of drugs that are known P-gp substrates in individual patients. For example, Tc-99m-MIBI imaging has not been used in renal transplant assessment and autoimmune disease up to now, but also not sufficiently explored in investigating underlying mechanisms or treatment adjustment in neurodegenerative disease, MRP1/2 lung expression and parathyroid imaging.

7.2.1 Evolving P-gp role in renal transplantation - potential for Tc-99m-MIBI techniques

Tc-99m-MIBI has been used to image P-gp expression in several clinical settings, especially cancer in which it has been shown that tracer accumulation correlates inversely with P-gp expression and predicts response to drug treatment (124) (125). Although Tc-99-MIBI has also been used to study MDR function in a physiological setting in several organs, the kidney has received less attention despite an important potential role for P-gp in renal transplantation (26). Structurally, the kidney is relatively complex in the setting of MDR because xenobiotics could access renal tissue either via glomerular filtration and tubular reabsorption or peritubular capillary blood. Likewise elimination could be via filtration or by tubular secretion or into blood. The only known mechanism of Tc-99m-MIBI elimination from renal tubular cells involves ABC transporter proteins, so Tc-99m-MIBI kinetics may allow inference of renal P-gp status (88). Patients who constitutionally express low levels of P-gp may require lower doses of immuno-suppressants, including CsA, and tacrolimus and other drugs that are MDR substrates and potentially nephrotoxic (26). Tc-99m-MIBI renography may therefore provide relevant information in transplant recipients regarding dose selection of such drugs and could also potentially be used in predicting graft outcome (121). Importantly, tacrolimus is more commonly used after renal transplant than CsA and hence the influence of tacrolimus on Tc-99m-MIBI pharmacokinetics should be investigated in future research studies due to a potential role of Tc-99m-MIBI imaging to guide the target exposure early after transplantation and subsequently to

adjust the treatment regimen. It has previously been demonstrated that SNP *C3435T* could influence the tacrolimus pharmacokinetic parameters. The subjects with CC genotype had lower concentration dose ratio and needed a higher tacrolimus dose than the CT and TT genotype (180). Following my 'proof of principle study' demonstrating pharmacological effects of CsA on Tc-99m-MIBI kinetics in subjects with normal renal function, the way is now open to investigate the pharmacokinetics of Tc-99m-MIBI in renal transplant recipients receiving tacrolimus.

This potential role for Tc-99m-MIBI imaging in renal transplant management with respect to dose titration of CNI and prediction of nephrotoxicity versus rejection or glomerulopathy should be further investigated. Individual P-gp response to CNI may be linked to nephrotoxicity or rejection. High kidney P-gp levels may be associated with rejection and low levels with nephrotoxicity. Likewise, P-gp up-regulation in lymphocytes increases resistance to anti-rejection therapy (26). P-gp expression in kidney and lymphocytes may therefore predict graft outcome.

It is possible that low versus high levels of P-gp expression in the kidney predict risk of nephrotoxicity and low versus high levels of expression in recipient lymphocytes predict risk of immunological rejection, leading to glomerulopathy. Leucocytes accumulate Tc-99m-MIBI *in vitro* and eliminate it over a few hours (194). Therefore, measuring lymphocyte *k* and correlating it with P-gp expression may help to predict risk of immunological rejection.

In addition, rapid Tc-99m-MIBI washout from the graft is expected during rejection due to increased local renal expression of P-gp resulting in low

retention of Tc-99m-MIBI. The uptake would therefore appear reduced in the perfusion phase. This has already been demonstrated after ischemia and reperfusion in the porcine kidney (105). After intermittent hypoxia P-gp was also shown to be up regulated in liver and myocardium in rodent model (195).

There are no non-invasive methods that might guide nephrologists in the individual tailoring of immuno-suppressive therapy in kidney transplant recipients so as to reduce the chances of rejection while at the same time preventing nephrotoxicity. The only currently available technique is renal biopsy, which is invasive and potentially harmful to the graft. The risk of biopsy-induced damage persuades a significant minority of patients to refuse biopsy, either protocol biopsy at 3 months post-transplant or follow-up biopsies. Moreover, histological interpretation of biopsy specimens is not straightforward and histopathologists disagree concerning the diagnosis of CNI nephrotoxicity.

A simple, widely available non-invasive diagnostic imaging test that would inform clinicians of the relative risks of nephrotoxicity and rejection and help tailor individual drug regimens could transform the outcome of renal transplantation in many patients.

Tc-99m-MIBI renal and lymphocyte kinetics could be attractive functional surrogate markers for P-gp expression in the transplant setting as indicators of short and long term transplant outcome potentially replacing biopsy. Tc-99m-MIBI may therefore provide relevant information regarding CNI treatment response and dose selection to identify patients who are likely to

benefit most from a CNI minimisation regimen. So, in line with above, there is a need to develop novel non-invasive methods for assessing functional P-gp activity in the setting of renal transplantation to achieve a balance between efficacy and toxicity through optimal individualised therapy in a potentially cost-effective way, preventing side effects and complications of CNI treatment that are also causing significant health service costs.

Renal function would be better maintained and patient survival risk could be minimised through prediction and prevention of drug toxicity or rejection. Quality of life could be subsequently improved in a cost-effective manner. In addition to the direct side effects of CNI, i.e. nephrotoxicity, immunosuppressive drugs also have chronic indirect side effects, such as diabetes mellitus, hyperlipidaemia and hypertension, which also contribute adversely to renal allograph function and quality of life and thereby increase the overall health cost burden.

The prevalence of kidney failure is increasing at 5% per year, 3,000 people are dying on dialysis per year and 7,000 are waiting for a kidney transplant in the UK. In 2010, approximately 2600 renal transplants were performed in the UK (196). Loss of function of renal transplants over time remains a significant problem in spite of advances in transplant immuno-suppressive therapy. By offering an alternative approach to biopsy, Tc-99m-MIBI kinetic studies may offer cost saving possibilities by providing information that will facilitate transplant management. Thus, treatment would be adjusted, tailored and personalised, thereby reducing CNI toxicity, but also preventing rejection.

7.2.2 Other potential applications

It would be also interesting to investigate a role of Tc-99m-MIBI imaging in other P-gp mediated and linked diseases, such as neurodegenerative disease, including Alzheimer's disease (AD), Parkinson's disease (PD) and autoimmune disease.

7.2.2.1 Investigating ABC transporters expression and their role in choroid plexus

Tc-99m-MIBI SPECT images of brain give strongly positive image of the choroid plexus. This area seems to have received relatively little attention in the transport of ABC agents between blood and CSF.

The choroid plexus could be imaged with Tc-99m-MIBI in neurodegenerative conditions. Tc-99m-MIBI uptake may be reduced as a result of leakage of tracer into the CSF. The choroid plexus appears to be different from other tissues in that the functions of P-gp and MRP1 are distinctly segregated, as opposed to being effectively integrated and overlapping. P-gp seems to be the main transporter in cerebral microvessels, but is absent from the endothelial cells of the choroid plexus. P-gp is located on the apical side of the epithelial cells of the choroid plexus, functioning as a barrier to the transport of ABC agents out of CSF.

MRP1, in contrast, is located on the basal side, functioning as a barrier to the transport of ABC agents from blood into CSF. As it is a substrate for MRP1 as well as P-gp, Tc-99m-MIBI, which gives a strongly positive image of the choroid plexus, must therefore be accumulating in the endothelial cells of the

choroid plexus, not the epithelial cells. Once inside the CSF, ABC agents are locked in by the action of P-gp. Blockade of MRP1 would let them in, while blockade of P-gp would let them out. This pre-supposes that P-gp is present in arachnoid villi, through which CSF is re-absorbed, and functions to maintain ABC substrates within the CSF.

The differential effects of MRP1 blockade and P-gp blockade on the accumulation of an ABC agent such as Tc-99m-MIBI in both the choroid plexus (by SPECT) and the CSF (by sampling) can be imaged with Tc-99m-MIBI.

I suspect that the blockade of either protein would have no effect on uptake of Tc-99m-MIBI by choroid plexus, that blockade of P-gp would have little effect on accumulation of Tc-99m-MIBI in CSF and that blockade of MRP1 would increase accumulation of Tc-99m-MIBI in CSF. Having confirmed the hypothesis in neurologically intact subjects, the patients with neurodegenerative disease can be imaged with Tc-99m-MIIBI, possibly revealing functional differences between MRP1 and P-gp. There are contradictory data so far from Piwnica-Worms' group (10) and Kaddoumi et al., who respectively showed an increase in CSF Tc-99m-MIBI and no change in CSF nelfinavir (in spite of huge increase in brain concentration) after P-gp blockade (11).

7.2.2.2 Investigating P-gp role in neurodegenerative disorders

A potential role of drug transporters (mostly P-gp and MRP1) in mechanisms of neurodegeneration and drug refractory brain disorders, that may involve the elimination of CNS derived amyloid-beta which is P-gp mediated, may be investigated from uptake and clearance of Tc-99m-MIBI within and out of the brain.

A potential role of multidrug resistance in neurodegenerative conditions, using Tc-99m-MIBI as a probe, and its potential influence, for example, on the effectiveness of agents for imaging and therapy that are substrates for the multi-drug resistance proteins (ABC agents) may also be investigated (197).

Cirrito et al. demonstrated a direct link between P-gp and amyloid–beta (Aβ) metabolism in Alzheimer's disease mouse model. Their data indicated that P-gp activity at the blood -brain barrier (BBB) could influence the risk of developing Alzheimer's disease (AD) and that ablation of P-gp at the BBB enhances Aβ deposition (90).

Patients with neurodegenerative disorders may express low levels of P-gp in the BBB (198), leading to a higher retention of Tc-99m-MIBI with delayed washout, along with lower initial uptake as a result of probable underlying mitochondrial dysfunction in AD (199). It should be emphasised that unlike Tc-99m-MIBI washout, which is ABC-transporter function, Tc-99m-MIBI uptake is proportionally related to mitochondrial number cells, so that the role

of Tc-99m-MIBI role in imaging AD may be 2-fold in investigating both P-gp related mechanism and mitochondrial hypothesis of AD.

Another interesting area for imaging ABC-transporters, such as P-gp and MRPs, in the BBB and BCB is epilepsy. There is increasing evidence that over-expression of such ABC-transporters may be involved in the generation of pharmaco-resistance in epileptic patients. If so, inhibitors of these drug transporters may prove useful in pharmaco-resistant refractory epilepsy, although the adverse effects of ABC-transporter inhibition need careful consideration and it is also likely that different factors underlie multidrug resistance in epilepsy (200).

At the blood-brain barrier, ABC-transporters limit CNS uptake of foreign chemicals. Thus, they are neuroprotective, but also major obstacles to CNS pharmacotherapy, as they cannot distinguish between neurotoxicants and therapeutic drugs. New findings in animal models *in vitro* and *in vivo* show that basal transport activity of P-gp and BCRP can be rapidly and transiently reduced through targeting of specific signalling pathways within the brain capillary endothelium. Three pathways have been identified: oestrogen signalling to BCRP, vascular endothelial growth factor signalling to P-gp and TNFα/PKC/ sphingolipid signalling to P-gp. Translation of these results to the clinic could provide improved pharmacotherapy for a number of CNS diseases, including brain tumours, neuro-AIDS and epilepsy (201).

In vivo imaging of ABC-transporters may help facilitating those drug discoveries.

7.2.2.3 In vivo imaging of lung ABC- protein transporters

The effects of cigarette smoke and environmental pollution on ABC/P-gp expression has also already been studied using the lung clearance rate of Tc-99m-MIBI administered by inhalation with or without co-inhalation of aerosolised P-gp blockers (91) (92). More recently it has been indicated that Tc-99m-MIBI lung clearance is MRP1 rather than P-gp mediated (202). It has also been demonstrated that various demographic and environmental factors affect the clearance of inhaled Tc-99m-MIBI from human lungs. Male gender and older age significantly delayed the clearance rate, but the environmental pollution seemed to have no effect (203). In contrast to my study, where no gender difference in hepatic and renal Tc-99m-MIBI clearance was demonstrated, Mohan et al. showed a significant difference in gender lung clearance. This implies that MRP1, but not P-gp (or mixed P-gp/MRp1,2) related Tc-99m-MIBI clearance may be gender dependant. Smoking also significantly delays Tc-99m-MIBI clearance rate (203), while diminished MRP1 was shown in bronchial epithelium of COPD patients (204). In addition, it would be interesting to investigate whether smoking up-regulates ABC-protein transporters at other sites, including circulating leucocytes (from uptake of Tc-99m-MIBI *ex vivo*).

7.2.2.4 In vivo imaging of intestinal P-gp/ABC expression

P-gp can play a crucial role in limiting the absorption and distribution of harmful xenobiotics, including drugs that are also P-gp substrates by decreasing their intracellular accumulation. Such a defence mechanism can be of particular relevance at the intestinal level, by significantly affecting the

intestinal absorption of the xenobiotic and consequently their bioavailability in targeted organs. If up-regulated efflux proteins may limit drug absorption and vice versa. Therefore, another interesting route of Tc-99m-MIBI administration, which has not been previously attempted, would be oral.

7.2.2.5 In vivo imaging of P-gp expression in parathyroid glands

Tc-99m-MIBI scintigraphy is widely used in for imaging parathyroid adenomas. Two-phase Tc-99m-MIBI scintigraphy is routinely performed at 20 min and 2-4 hr post injection. Focal increased uptake of Tc-99m-MIBI in the 20 min images, due to parathyroid adenomas being rich in mitochondria, combined with delayed Tc-99m-MIBI washout on the images at 2 h, are features consistent with parathyroid adenoma. However, the parathyroid tissue retention of Tc-99m-MIBI is variable and correlates with tissue expression of P-gp. Imaging of parathyroid tumours for example has a false negative rate of about 10% as a result of variable P-gp expression (205). *In vitro* Tc-99m-MIBI studies have shown that P-gp inhibitors, such as verapamil, can reverse P-gp expression in adenocarcinoma cells if given shortly before the administration of cytotoxic drug (171).

Administration of P-gp inhibitor (e.g. verapamil) may decrease the false negative rate of parathyroid scans as a result of reversal or down-regulation of P-gp expression in parathyroid adenomas expressing high levels of P-gp.

7.2.2.6 In vivo imaging of P-gp expression in autoimmunity

Maillefert et al. first described a role of P-gp in autoimmunity. They reported an overexpression of P-gp on the surface of peripheral lymphocytes of rheumatoid arthritis (RA) patients treated with corticosteroids (CCS) (206). P-gp expression/function also has a role in the development of drug resistance in patients affected by systemic autoimmune diseases e.g. systemic lupus erythematosus (SLA), RA and psoriatic arthritis (PsA), and hence P-gp may be a therapeutic target in the control of abnormal immune response and inflammation (207).

P-gp has a role in modulating inflammation by direct or indirect tuning the secretion of cytokines, chemokines and other small peptides. Several studies on patients with systemic autoimmune diseases in particular SLE, RA and PsA have demonstrated a significant correlation between P-gp expression/function, disease activity and the development of resistance to immunosuppressive therapy. Furthermore, P-gp inhibition/reduction by CsA or anti-TNF-α agents can control, reduce or overcome drug resistance. The existing data already suggest that the measurement of P-gp expression could be a useful biomarker to evaluate drug resistance in these autoimmune conditions (207). Tc-99m-MIBI kinetics studies may be utilised to measure P-gp function in above autoimmune disease.

7.2.2.7 Multidrug resistance imaging in cancer

Functional up-regulation of ABC transporter proteins often results from exposure to inhibitors (26). As many inhibitors are also modulators, initial down-regulation may be followed by up-regulation, resulting in acquired drug resistance. Thus, treatment of patients with malignant tumours using a variety of structurally unrelated classes of drugs that include anthracyclines, taxanes and epipodophyllotoxines, to which the tumour had previously been sensitive, is sometimes rendered inadequate because of the activation of cellular biochemical mechanisms that result in multidrug resistance (MDR). The development of drug resistance and acquired expression of ABCB1 may be associated with genomic instability of cancer cells, including mutational events that alter chromatin structures, gene rearrangements, and mutations in tumour suppressor proteins (e.g., mutant p53), which guard the integrity of genome (193). In tumour cell lines, MDR is associated with an ATP-dependent decrease in cellular drug accumulation attributable to over-expression of ABC transporter proteins.

Tc-99m-MIBI, a substrate for ABC transporter proteins, has therefore been used for imaging MDR in breast cancer (56) (208), lung cancer (57), brain tumours (209) (210), gastric cancer (211), head and neck cancer (59), hepatobilliary cancer (212), haematological malignancies (213) (62) (214) (215) and thyroid follicular neoplasm (61) (31).

7.2.2.7.1 Imaging MDR in Drug Trials

Clinical trials optimally tailored to tumour types, genetic polymorphism and adequate dosing regimens need to be conducted. Imaging in such trials may be useful for selecting patients whose cancers express MDR primarily though ABC-mediated mechanisms. For accurate assessment of tumour P-gp levels, patients should be scanned twice with a P-gp radiolabelled substrate: firstly at baseline and again after P-gp inhibition. Patients whose tumours show enhanced uptake of the radiotracer following P-gp blockade would be suitable candidates for P-gp inhibitor trials (13) (88) (see Chapter 6, Figure 6.1). Two studies using Tc-99m-MIBI have shown the potential value of this approach with respect to the administration of tariquidar or valspodar. Another study was using Tc-99m-MIBI to monitor progress throughout the trial (13) (31).

Functional imaging of MDR in cancer may be helpful not only in the detection of drug-resistant tumours, but also in the identification of patients who are susceptible to the development of certain malignancies or drug toxicities.

7.2.2.8 Tc-99m-MIBI imaging for predicting treatment response and preventing drug toxicity

Understanding physiological renal and hepatic Tc-99m-MIBI handling may be useful for the development of imaging assays for investigating drug toxicity.

This study may further impact on the development of novel imaging modalities in investigating, monitoring effects and predicting toxicity versus

drug resistance of important drugs that are transported by ABC-transporters and known P-gp substrates or inhibitors such as not only immunosuppressive drugs (CsA and tacrolimus), but also Ca^{2+} channel blockers (verapamil, diltiazem), cardiac drugs (digoxin), dipyridamole, HIV protease inhibitors, anti-rheumatics (methotrexate), some antibiotics (rifampicin, erythromicin), and many antineoplastic drugs .

More research is needed to identify patients, through imaging, who are susceptible to drug toxicity side effects or drug resistance, to provide information concerning dose adjustment and to allow better decision making when considering therapy with drugs that are ABC transporter substrates. In the post-genomic era of individualised medicine, ABC imaging may be helpful to adjust the treatment dose in individual patients (31).

Chapter 8 Appendices

8.1 Publications

8.1.1 Peer reviewed journal publications

1) Dizdarevic S, Aplin M, Newport MJ, N Ryan, Holt SG, Goubet S, Goldberg L, Miles KA, Peters AM. Old tracer for a new purpose: potential role for 99mTc-2-Methoxyisobutylisonitrile (99mTc-MIBI) in renal transplant care. Nucl Med Commun. 2014;35:1058-66.

2) Dizdarevic S, Aplin M, Ryan N, Holt SG, Goldberg L, Miles KA, Peters AM. Renal and hepatic kinetics of Tc-99m-labelled hexakis-methoxy-isobutyl isonitrile. Drug Metab Lett. 2012;6:242-6.

3) Dizdarevic S, Peters A.M. Imaging MDR in Cancer. Cancer Imaging 2011;11:1-8.

8.1.2 Published Book Chapters

1) Dizdarevic S, Peters AM. Radiopharmaceuticals for the imaging of ABC-transporter mediated multidrug resistant in cancer in T. Efferth ed. Resistance to targeted ABC transporters in Cancer. 2015, 1st ed. Springer 133-151.

2) Dizdarevic S, Peters AM. Radionuclide imaging of multidrug resistance in Chapter 34 Investigative methods for studying tumour biology and microenvironment in C Aktolun, S J Goldsmith eds. Nuclear oncology. 2015 2nd ed. Wolters Kluwer Health 530-5.

8.1.3 Manuscript pending submission for publication

1) Dizdarevic S, Aplin M, Newport MJ, Lee M, Ballinger J, Atkinson L, Derrick E, Peters AM. Tc-99m-MIBI pharmacokinetics are influenced by cyclosporine A possibly through *ABCB1* SNPs 1236C>T.

8.1.4 Abstract publications

1) Dizdarevic S, Aplin M, Holt SG, Goldberg L, Miles KA, Peters AM. Renal Scintigraphy using Tc-99m-2-Methoxyisobutylisonitrile: Validation of Differential Renal Function and Development of a Functional Assay of P-Glycoprotein Expression in Renal Transplant Donors. Eur J Nucl Med Mol Imaging 2010;37:S254

2) Dizdarevic A, Aplin M, Holt SG, Miles KA, Goldberg L, Peters AM. A novel approach to transplant renography using 99mTc-2-Methoxyisobutylisonitril (MIBI): An in vitro Assay of Constitutional P-glycoprotein (P-gp) Expression in Renal Transplant Donors. Nucl Med Commun 2011;32:432.

3) S. Dizdarevic, M. Aplin, S. G. Holt, L. Goldberg, K. A. Miles, A. M. Peters. Tc-99m-2-Methoxyisobutylisonitril (MIBI) renography: A potential role in renal transplant setting. Eur J Nucl Med Mol Imaging 2011;38:S142.

4) Dizdarevic A, Aplin M, Holt SG, Goldberg L, Miles KA, A M Peters. Old tracer for new purpose: Tc-99m-2-methoxyisobutylisonitril (Tc-99m-MIBI) for imaging nephrotoxicity. Journal of Nuclear Medicine Supplement 2012;53:596.

5) Dizdarevic S, Aplin M, Newport MJ, Ryan N, Holt SG, Goubert S, Goldberg L, Miles KA, Peters AM. Is Tc-99m-2-methoxyisobutylisonitril (Tc-99m-MIBI) tissue elimination influenced by variation in the MDR1 gene? Nucl Med Commun 2013;34:362 (inclusion in the Highlights lecture, BNMS Annual Meeting 2013).

6) Dizdarevic S, M Aplin, MJ Newport, N Ryan, SG Holt, S Goubet, L Goldberg, KA Miles, A M Peters. *ABCB1* gene, but not gender may influence Tc-99m-2-methoxyisobutylisonitril (Tc-99m-MIBI) imaging findings. Eur J Nucl Med Mol Imaging 2013; 40:

http://eanm13.eanm.org/abstracts/session_detail.php?sessionNumber=409

7) Dizdarevic S, Aplin M, Ryan N, Holt SG, Goldberg SG, Miles KA, Peters AM. Establishing renal and hepatic kinetics of Tc-99m-hexakis-methoxy-isobutyl isonitrile (MIBI): way towards imaging drug toxicity. Eur J Nucl Med Mol Imaging 2013; 40: http://eanm13.eanm.org/abstracts/session_detail.php?sessionNumber=P65-1

8) Dizdarevic S, Aplin M, Atkinson L, Felton J, Degiovanni J, Derrick E, Topham E, Peters AM. MIBI renal and hepatic handling is altered by ABC/MDR (multi drug resistance) transporter proteins blockade in patients receiving ciclosporin treatment. Nucl Med Commun 2014, 35:565.

9) Dizdarevic S, Newport MJ, Lee M, Aplin M, Ballinger J, Derrick E, Atkinson L, Peters AM. MIBI renal and hepatic SPECT rate constants and correlation with *ABCB1* genotypes in patients receiving ciclosporin treatment. The abstract accepted for publication in Nucl Med Commun 2015.

8.1.5 Oral presentations

1) Development of novel imaging technique targeting P-glycoprotein (P-gp) expression in kidneys

   Renal Research Day, Clinical Investigation Research Unit, Brighton, UK February 2010.

2) Renal Scintigraphy using Tc-99m-2-Methoxyisobutylisonitrile: Validation of Differential Renal Function and Development of a Functional Assay of P-Glycoprotein Expression in Renal Transplant Donors.

   European Association of Nuclear Medicine, Annual Congress, Vienna, Austria, October 2010.

   Inclusion in the Highlight Lecture.

3) A novel approach to transplant renography using 99mTc-2-Methoxyisobutylisonitril (MIBI): An in vitro Assay of Constitutional P-glycoprotein (P-gp) Expression in Renal Transplant Donors.

   British Nuclear Medicine Society National Annual Meeting, Brighton, UK, April 2011.

4) Tc-99m-2-Methoxyisobutylisonitril (MIBI) renography: A potential role in renal transplant setting. Eur J Nucl Med Mol Imaging 2011; 38:S142.

   European Association of Nuclear Medicine, Annual Congress, Birmingham, UK, October 2011

   Selected for inclusion in the Highlights Lecture

5) A novel approach to transplant renography using 99mTc-2-Methoxyisobutylisonitril (MIBI): An in vitro Assay of Constitutional P-glycoprotein (P-gp) Expression in Renal Transplant Donors.

   Postgraduate Research Symposium, Brighton and Sussex Medical School, Brighton, UK, May 2011.

6) Tc99m2methoxyisobutylisonitrile (MIBI) scintigraphy and MDR1 genotyping: indirect assays of Pglycoprotein for predicting nephrotoxicity in patients with psoriasis receiving ciclosporin A.

   Academic Dermatology Meeting, Brighton,UK, April 2012

7) Old tracer for new purpose: Tc-99m-2-methoxyisobutylisonitril (Tc-99m-MIBI) for imaging nephrotoxicity.

   Society of Nuclear Medicine Annual Meeting, Miami Beach, FL, USA, June 2012.

8) Is Tc-99m-2-methoxyisobutylisonitril (Tc-99m-MIBI) tissue elimination influenced by variation in the MDR1 gene?

   British Nuclear Medicine Society National Annual Meeting, Brighton, UK, May 2013.

   Inclusion in the Highlights lecture.

9) Potential novel radionuclide methods for predicting response of immunosuppressive therapy in renal transplant setting by using Tc-99m-2-methoxyisobutylisonitril (Tc-99m-MIBI),

   Renal Research Day, Network Meeting, Audrey Emerton, Brighton, UK, June 2013.

10) *ABCB1* gene, but not gender may influence Tc-99m-2-methoxyisobutylisonitril (Tc-99m-MIBI) imaging findings.

    European Association of Nuclear Medicine, Annual Congress, Lyon, France, October 2013.

11) MIBI renal and hepatic handling is altered by ABC/MDR (multi drug resistance) transporter proteins blockade in patients receiving ciclosporin treatment.

    British Nuclear Medicine Society National Annual Meeting, Harrogate, UK, May 2014.

8.1.6 Poster presentations

1) Establishing renal and hepatic kinetics of Tc-99m-hexakis-methoxy-isobutyl isonitrile (MIBI): way towards imaging drug toxicity.

   European Association of Nuclear Medicine, Annual Congress, Lyon, France, October 2013.

2) MIBI renal and hepatic SPECT rate constants and correlation with ABCB1 genotypes in patients receiving ciclosporin treatment.

   To be presented at the British Nuclear Medicine Society National Annual Meeting, Brighton, UK, April 2015.

Chapter 9 References

1. Lockhart A, Tirona L, Kim R. Pharmacogenetics of ATP-binding cassette transporters in cancer and chemotherapy. Mol Cancer Ther. 2003; 2: p. 685-698.

2. Piwnica-Worms D, Chiu M, Budding M, Kronauge J, Kramer R, Croop J. Functional Imaging Of Multidrug-Resistant P-glycoprotein With An Organotechnetium Complex. Cancer Res. 1993;(53): p. 977-984.

3. Leslie E, Deeley R, Cole S. Multidrug resistance proteins: role of P-glycoprotein, MRP1, MRP2, and BCRP (ABCG2) in tissue defense. Toxicol Appl Pharmacol. 2005; 1: p. 216-37.

4. Sharom F. ABC multidrug transporters: structure, function and role in chemoresistance. Pharmacogenomics. 2008; 9: p. 105-27.

5. Aller S, Yu J, Ward A, Weng Y, Chittaboina S, Zhuo R, et al. Structure of P-glycoprotein Reveals a Molecular Basis for Poly-Specific Drug Binding. Science. 2009; 323: p. 1718–1722.

6. Sailaja K, Surekha D, Nageswara Rao D, Raghunadha Rao D, Vishnupriya S. ABCB1 (MDR1, P-Glycoprotein) C3435T Gene Polymorphism and its Possible Association with Chronic Myeloid Leukemia Prognosis. Current Trends in Biotechnology and Pharmacy. 2008; 2: p. 514-522.

7. Thiebaut F, Tsuruo T, Hamada H, Gottesman M, Pastan I, Willingham M. Cellular localization of the multidrug-resistance gene product P-glycoprotein in normal human tissues. Proc. Nati. Acad. Sci. USA. 1987; 84: p. 7735-7738.

8. Lechapt-Zalcman E, Hurbain I, Lacave R, Commo F, Urban T, Antoine M, et al. MDR1-Pgp 170 expression in human bronchus. Eur Respir J. 1997;(10): p. 1837-43.

9. Bauer B, Hartz A, Fricker G, Miller D. Modulation of p-Glycoprotein Transport Function at the Blood-Brain Barrier. Exp Biol Med. 2005; 230: p. 118–127.

10. Rao V, Dahlheimer J, Bardgett M, Snyder A, Finch R, Sartorelli A, et al. Choroid plexus epithelial expression of MDR1 P glycoprotein and multidrug resistance-associated protein contribute to the blood–cerebrospinal-fluid drug-permeability barrier. Proc. Natl. Acad.

Sci. USA. 1999; 96(7): p. 3900–3905.

11. Kaddoumi A, Choi S, Kinman L, Whittington D, Tsai C, Ho R, et al. Inhibition of P-glycoprotein activity at the primate blood-brain barrier increases the distribution of nelfinavir into the brain but not into the cerebrospinal fluid. Drug Metab Dispos. 2007; 35: p. 1459-1462.

12. Mizutani T, Masuda M, Nakai E, Furumya K, Togawa H, Nakamura Y, et al. Genuine Functions of P-Glycoprotein (ABCB1). Current Drug Metabolism. 2008; 9: p. 167-174.

13. Kannan P, John C, Zoghbi S, Halldin C, Gottesman M, Innis R, et al. Imaging the Function of P-Glycoprotein With Radiotracers: Pharmacokinetics and In Vivo Applications. Clin Pharmacol Ther. 2009; 86(4): p. 368–377.

14. Szakács G, Paterson J, Ludwig J, Booth-Genthe C, Gottesman M. Targeting multidrug resistance in cancer. Nat Rev Drug Discov. 2006; 5(3): p. 219-34.

15. Chaudhary P, Mechetner E, Roninson I. Expression and activity of the multidrug resistance P-glycoprotein in human peripheral blood lymphocytes. Blood. 1992; 11: p. 2735–2739.

16. Cascorbi I, Gerloff T, Johne A, Meisel C, Hoffmeyer S, Schwab M, et al. Frequency of single nucleotide polymorphisms in the P-glycoprotein drug transporter MDR1 gene in white subjects. Clin Pharmacol Ther. 2001; 69: p. 169-174.

17. Fromm M. Genetically determined differences in P-glycoprotein function: implications for disease risk. Toxicology. 2002; 27: p. 299-303.

18. Schaeffeler E, Eichelbaum M, Brinkmann U, Penger A, Asante-Poku S, Zanger U, et al. Frequency of C3435T polymorphism of MDR1 gene in African people. Lancet. 2001; 358: p. 383-384.

19. Miller K, Kelsey K, Wiencke J, Moghadassi M, Miike R, Liu M, et al. The C3435T polymorphism of MDR1 and susceptibility to adult glioma. Neuroepidemiology. 2005; 25(2): p. 85-90.

20. Jamroziak K, Mlynarski W, Balcerczak E, Mistygacz M, Trelinska J, Mirowski M, et al. Functional C3435T polymorphism of MDR1 gene: an impact on genetic susceptibility and clinical outcome of childhood acute lymphoblastic leukemia. Eur J Haematol. 2004; 72: p. 314-21.

21. Sigesmund M, Brinkmann U, Schaffeler E, Weirich G, Schwab M, Eichelbaum M, et al. Association of the P-Glycoprotein Transporter MDR1C3435T Polymorphism with the Susceptibility to Renal Epithelial Tumours. J Am Soc Nephrol. 2002; 13: p. 1847–1854.

22. Potocink U, Ravnik-Glavac M, Glavac D. Functional MDR1 polymorphisms (G2677T and C3435T) and TCF4 mutations in colorectal tumors with high microsatellite instability. Cell Mol Biol Lett. 2002; 7(1): p. 92-95.

23. Turgut S, Yaren A, Kursunluoglu R, Turgut G. MDR1 C3435T polymorphism in patients with breast cancer. Archives of Medical Research. 2007; 38(5): p. 539-544.

24. Hauser I, Schaeffeler E, Gauer S, Scheuermann E, Wegner B, Gossmann J, et al. ABCB1 Genotype of the Donor but Not of the Recipient Is a Major Risk Factor for Cyclosporine-Related Nephrotoxicity after Renal Transplantation. J Am Soc Nephrol. 2005; 16: p. 1501–1511.

25. Von Ahsen N, Richter M, Grupp C, Ringe B, Oellerich M, Armstrong V. No influence of the MDR-1 C3435T polymor-phism or a CYP3A4 promoter polymorphism (CYP3A4-V allele) on dose-adjusted cyclosporin A trough concentrations or rejection incidence in stable renal transplant recipients. Clin Chem. 2001; 47: p. 1048-1052.

26. Koziolek M, Riess R, Geiger H, Thevenod F, Hauser I. Expression of multidrug resistance P-glycoprotein in kidney allografts from cyclosporine A-treated patients. Kidney Int. 2003; 60: p. 156-166.

27. Moore J, McKnight A, Döhler B, Simmonds M, Courtney A, Brand O, et al. Donor ABCB1 variant associates with increased risk for kidney allograft failure. J Am Soc Nephrol. 2012; 23(11): p. 1891-9.

28. Naesens M, Lerut E, de Jonge H, Van Damme B, Vanrenterghem Y, Kuypers D. Donor age and renal P-glycoprotein expression associate with chronic histological damage in renal allografts. Am Soc Nephrol. 2009; 20(11): p. 2468-80.

29. Wong M, Evans S, Rivory L, Hoskins J, Mann G, Farlow D, et al. Hepatic technetium Tc 99m-labeled sestamibi elimination rate and ABCB1 (MDR1) genotype as indicators of ABCB1 (P-glycoprotein) activity in patients with cancer. Clin Pharmacol Ther. 2005; 77: p. 33-42.

30. Brambila-Tapia A. MDR1 (ABCB1) polymorphisms: functional effects

and clinical implications. Rev Invest Clin. 2013; 4: p. 445-54.

31. Dizdarevic S, Peters A. Radiopharmaceuticals for the imaging of ABC-transporter mediated multidrug resistant in cancer. In Efferth T, editor. Resistance to targeted ABC transporters in Cancer. 1st ed.: Springer; 2015. p. 133-151.

32. Ghibellini G, Vasist L, Heizer W, Kowalsky R, Brouwer K. Quantitation of Tc-99m-Sestamibi bibliary exretion in Humans. Clinical Pharmacology & Therapeutics. 2005; 79: p. 19.

33. Ballinger J. 99mTc-tetrofosmin for functional imaging of P-glycoprotein modulation in vivo. J Clin Pharmacol. 2001; Suppl: p. 39-47.

34. Ballinger J, Sheldon K, Boxen I, Erlichman C, Ling V. Differences between accumulation of 99mTc-MIBI and 201Tl-thallous chloride in tumour cells: role of P-glycoprotein. J Nucl Med. 1995;(39): p. 122-8.

35. Yapar Z, Kibar M, Ozbarlas S, Yapar A, Uguz A, Zorludemir S, et al. 99mTc-tetrofosmin scintigraphy in musculoskeletal tumours: the relationship between P-glycoprotein expression and tetrofosmin uptake in malignant lesions. Nucl Med Commun. 2002;(23): p. 991-1000.

36. Yapar Z, Kibar M, Yapar A, Uguz A, Ozbarlas S, Gonlusen G. The value of Tc-99m-tetrofosmin scintigraphy in the assessment of P-glycoprotein in patients with malignant bone and soft-tissue tumors. Ann Nucl Med. 2003 17; 6: p. 443-9.

37. Nagengast W, Oude Munnink T, Dijkers E, Hospers G, Brouwers A, Schröder C, et al. Multidrug resistance in oncology and beyond: from imaging of drug efflux pumps to cellular drug targets. Methods Mol Biol. 2010; 596: p. 15-31.

38. Bigott H, Prior J, Piwnica-Worms D, Welch M. Imaging multidrug resistance P-glycoprotein transport function using microPET with technetium-94m-sestamibi. Mol Imaging. 2005; 4(1): p. 30-9.

39. Muzi M, Mankoff D, Link J, Shoner S, Collier A, Sasongko L, et al. Imaging of Cyclosporine Inhibition of P-Glycoprotein Activity Using 11C-Verapamil in the Brain: Studies of Healthy Humans. J Nucl Med. 2009; 50: p. 1267–1275.

40. Sharma V, Prior J, Belinsky M, Kruh G, Piwnica-Worms D. Characterization of a 67Ga/68Ga radiopharmaceutical for SPECT and PET of MDR1 P-glycoprotein transport activity in vivo: validation in multidrug-resistant tumors and at the blood-brain

barrier. J Nucl Med. 2005; 46(2): p. 354-64.

41. Kurdziel K, Kalen J, Hirsch J, Wilson J, Bear H, Logan J, et al. Human dosimetry and preliminary tumor distribution of 18F-fluoropaclitaxel in healthy volunteers and newly diagnosed breast cancer patients using PET/CT. J Nucl Med. 2011; 52(9): p. 1339-45.

42. Bauer F, Mairinger S, Dorner B, Kuntner C, Stundner G, Bankhstahl J, et al. Synthesis and µPET of the radiolabelled P-glycoprotein inhibitor 11-C-Tariquidar. Eur J Nucl Med Mol Imaging. 2009; 36: p. S222.

43. Hendrikse N, Kuipers F, Meijer C, Havinga R, Bijleveld C, Van der Graaf W, et al. In vivo imaging of hepatobiliary transport function mediated by multidrug resistance associated protein and P-glycoprotein. Cancer Chemother Pharmacol. 2004; 54: p. 131-138.

44. Lewis J, Dearling J, Sosabowski J, Zweit J, Carnochan P, Kelland L, et al. Copper bis(diphosphine) complexes: radiopharmaceuticals for the detection of multi-drug resistance in tumours by PET. European Journal of Nuclear Medicine. 2000; 27(6): p. 638-646.

45. Dizdarevic S, Peters A. Imaging of multidrug resistance in cancer. Cancer Imaging. 2011; 1(11): p. 1-8.

46. Dizdarevic S, Peters A. Radionuclide imaging of multidrug resistance. In Aktolun C, Goldsmith C, editors. Nuclear Oncology. 2nd ed.: Wolters Kluwer Health; 2015. p. 530-5.

47. Piwnica-Worms D, Kronauge J, Chiu M. Uptake and retention of hexakis (2-methoxyisobutyl isonitrile) technetium(I) in cultured chick myocardial cells: mitochondrial and plasma membrane potential dependence. Circulation. 1190; 82: p. 1826-1838.

48. Piwnica-Worms D, Kronauge J, LeFurgey A, Backus M, Hockett D, Ingram P, et al. Mitochondrial localization and characterization of 99Tc-SESTAMIBI in heart cells by electron probe X-ray microanalysis and 99Tc-NMR spectroscopy. Magn Reson Imaging. 1994;(12): p. 641-52.

49. Kabasakal L, Halaĉ M, Nisli C, Oguz O, Onsel C, Civi G, et al. The effect of P-glycoprotein function inhibition with cyclosporine A on the biodistribution of Tc-99m-sestamibi. Clin Nucl Med. 2000;(25): p. 20-23.

50. Márián T, Balkay L, Szabó G, Krasznai Z, Hernádi Z, Galuska L, et al. Biphasic accumulation kinetics of [99mTc]-hexakis-2-

methoxyisobutyl isonitrile in tumour cells and its modulation by lipophilic P-glycoprotein ligands. Eur J Pharm Sci. 2005;(25): p. 201-9.

51. Joseph B, Bhargava K, Malhi H, Schilsky M, Jain D, Palestro C, et al. Sestamibi is a substrate for MDR1 and MDR2 P-glycoprotein genes. Eur J Nucl Med Mol Imaging. 2003;(30): p. 1024-31.

52. Koomaji R, Stammler G, Manegold C, Mattern J, Volm M. Expression of resistance-related proteins in tumoral and peritumoral tissues of patients with lung cancer. Cancer Lett. 1996;(110): p. 129-36.

53. Chen C, Meadows B, Regis J, Kalafsky G, Fojo T, Carrasquillo J, et al. Detection of in Vivo P-Glycoprotein Inhibition by PSC 833 Using Tc-99m Sestamibi. Clinical Cancer Res. 1997; 3: p. 545-552.

54. Luker G, Fracasso P, Dobkin J, Piwnica-Worms D. Modulation of the Multidrug Resistance P-Glycoprotein: Detection with Technetium-99m-Sestamibi In Vivo. J Nuc Med. 1997; 38: p. 369-372.

55. Ciarmiello A, Del Vecchio S, Silvestro P, Potena M, Carriero M, Thomas R, et al. Tumor clearance of technetium 99m-sestamibi as a predictor of response to neoadjuvant chemotherapy for locally advanced breast cancer. J Clin Oncol. 1998; 16: p. 1677-83.

56. Mubashar M, Harrington K, Chaudhary K, Lalani eN, Stamp G, Sinnett D, et al. 99mTc-sestamibi imaging in the assessment of toremifene as a modulator of multidrug resistance in patients with breast cancer. J Nucl Med. 2002; 43: p. 519-25.

57. Mohan H, Miles K. Cost-effectiveness of 99mTc-sestamibi in predicting response to chemotherapy in patients with lung cancer: systematic review and meta-analysis. J Nucl Med. 2009; 50: p. 376-81.

58. Chen Y, Wang W, Chan T, Sun S, Kao A. A review of the cost-effectiveness of Tc-99m sestamibi scintimammography in diagnosis of breast cancer in Taiwanese women with indeterminate mammographically dense breast. Surg Oncol. 2002; 11: p. 151-5.

59. Mubashar M, Harrington K, Chaudhary K, Lalani eN, Stamp G, Peters A. Differential effects of toremifene on doxorubicin, vinblastine and Tc-99m-sestamibi in P-glycoprotein-expressing breast and head and neck cancer cell lines. Acta Oncol. 2004; 43: p. 443-52.

60. Giovanella L, Suriano S, Maffioli M, Ceriani L, Spriano G. (99m)Tc-sestamibi scanning in thyroid nodules with nondiagnostic

cytology. Head Neck. 2010; 32(5): p. 607-11.

61. Saggiorato E, Angusti T, Rosas R, Martinese M, Finessi M, Arecco F, et al. 99mTc-MIBI Imaging in the presurgical characterization of thyroid follicular neoplasms: relationship to multidrug resistance protein expression. J Nucl Med. 2009; 50(11): p. 1785-93.

62. Pace L, Catalano L, Del Vecchio S, De Renzo A, Fonti R, Salvatore B, et al. Washout of [99mTc] sestamibi in predicting response to chemotherapy in patients with multiple myeloma. Q J Nucl Med Mol Imaging. 2005; 49(3): p. 281-5.

63. Vazquez S, D'Giano C, Carpintiero S, Coronel K, Ugarnes G, Lazarowski A. Increase 99m-Tc-sestamibi (MIBI) liver clearence could identified epileptic pharmacoresistant patients.A preliminary study. In American Epilepsy Society Abstract; 2004. p. 120.

64. Erba P, Pizzanelli C, Di Paolo A, Galli R, Ludice A, Murri L, et al. Pharmacokinetics of 99m-Tc-sestamibi uptake in the brain for exploring the role of multidrug resistance in patients with drug-resistant epilepsy. In 4th International Meeting of the Hellenic Society of Nuclear Medicine in cooperation with ten medical societies Proceedings; 2008; Thessaloniki. p. 76-7.

65. Seo T, Ishitsu T, Ueda N, Nakada N, Yurube K, Ueda K, et al. ABCB1 polymorphisms influence the response to antiepileptic drugs in Japanese epilepsy patients. Pharmacogenomics. 2006; 7: p. 551-61.

66. Administration of Radioactive Substances Advisory Committee. Notes for guidance on the clinical administration of radiopharmaceuticals and use of sealed radioactive sources. [Online].; 2006 [cited 2015. Available from: https://www.gov.uk/government/uploads/system/uploads/attachment_data/file/304835/ARSAC_Notes_for_Guidance.pdf.

67. Public Health England. Government – UK. Guidance - Ionising radiation: Ionising dose comparison. [Online].; 2011 [cited 2015. Available from: https://www.gov.uk/government/publications/ionising-radiation-dose-comparisons/ionising-radiation-dose-comparisons.

68. Smokvina A, Grbac-Ivankovic S, Girotto N, Subat Dezulovic M, Saina G, Miletic Barkovic M. The Renal Parenchyma Evaluation: MAG3 vs. DMSA. Coll. Antropol. 2005; 29(2): p. 649–654.

69. ACR–SPR–SNM. ACR–SPR–SNM practice guideline for the performance of adult and pediatric radionuclide cystography. [Online]. [cited 2015. Available from:

http://www.guideline.gov/content.aspx?id=32526.

70. Maisey M. Radionuclide renography: a review. Curr Opin Nephrol Hypertens. 2003; 12: p. 649-652.

71. British Nuclear Medicine Society. Dynamic Renal Radionuclide Studies (Renography) Clinical Guidelines. [Online]. [cited 2015. Available from: http://www.bnms.org.uk/~bnms/images/stories/downloads/documents/microsoft_word_-_dynamic_renal_radionuclide_studies_.pdf.

72. Gordon I, Piepsz A, Sixt R. Guidelines for standard and diuretic renogram in children. Eur J Nucl Med Mol Imaging. 2011; 38(6): p. 1175-88.

73. European Association of Nuclear Medicine. Guidelines for standard and diuretic renogram in children. [Online]. [cited 2014. Available from: http://www.eanm.org/scientific_info/guidelines/guidelines_intro.php.

74. Nimmo B, Merrick M, Allan P. Measurement of relative renal function - A comparison of methods and assessment of reproducibility. Br J Radiol. 1987; 60: p. 861-864.

75. Piepsz A, Kinthaert J, Tondeur M, Ham H. The robustness of the Patlak-Rutland slope for the determination of split renal function. Nucl Med Commun. 1996; 17(9): p. 817-21.

76. Piepsz A, Tondeur M, Ham H. Relative Tc-99m MAG3 renal uptake : reproducibility and accuracy. J Nucl Med. 1999; 40: p. 972-976.

77. Moonen M, Jacobsson L, Granerus G, Friberg P, Volkmann R. Determination of split renal function from gamma camera renography: a study of three methods. Nucl Med Commun. 1994; 15(9): p. 704-11.

78. Groothedde R. The individual kidney function. A comparison between frame summation and deconvolution. Nucl Med Commun. 1985; 6: p. 513-518.

79. Rutland M. A comprehensive analysis of renal DTPA studies. I. Theory and normal values. Nucl Med Commun. 1985; 6: p. 11-20.

80. Taylor A. Radionuclide renography: a personal approach. Semin Nucl Med. 1999; 29(2): p. 102-27.

81. Taylor A, Blaufox M, De Palma D, Dubovsky E, Erbas B, Eskild-Jensen A, et al. Guidance Document for Structured Reporting of Diuresis Renography. Semin Nucl Med. 2012; 42(1): p. 41–48.

82. Lezaic L, Hodolic M, Fettich J, Grmek M, Milcinski M. Reproducibility of 99mTc-mercaptoacetyltriglycine renography: population comparison. Nucl Med Commun. 2008; 29(8): p. 695-704.

83. Dubovsky E, Russell C, Erbas B. Radionuclide evaluation of renal transplants. Semin Nucl Med. 1995; 25(1): p. 49-59.

84. Dubovsky E, Russell C, Bischof-Delaloye A, Bubeck B, Chaiwatanarat T, Hilson A, et al. Report of the Radionuclides in Nephrourology Committee for evaluation of transplanted kidney (review of techniques). Semin Nucl Med. 1999; 29(2): p. 175-88.

85. Porn U, Rossmüller B, Alalp S, Fischer S, Dresel S, Hahn K. Calculation of the partial function of the kidney with DMSA in pediatrics: is the evaluation of the geometric mean necessary? Nuklearmedizin. 2001; 40(4): p. 107-10.

86. British Nuclear Medicine Society. Renal Cortical Scintigraphy (DMSA scan) Clinical Guidelines. [Online]. [cited 2015. Available from: http://www.bnms.org.uk/images/stories/Procedures_and_Guidelines/Renal_Cortical_Scintigraphy_Guidelines_2011a.pdf.

87. O'Reilly P. Standardization of the renogram technique for investigating the dilated upper urinary tract and assessing the results of surgery. BJU Int. 2003; 91: p. 239–243.

88. Agrawal M, Abraham J, Balis F, Edgerly M, Stein W, Bates S, et al. Increased 99mTc-sestamibi accumulation in normal liver and drug-resistant tumors after the administration of the glycoprotein inhibitor, XR9576. Clin Cancer Res. 2003;(9): p. 650-6.

89. Chan L, Lowes S, Hirst B. The ABCs of drug transport in intestine and liver: efflux proteins limiting drug absorption and bioavailability. Eur J Pharm Sci. 2004;(21): p. 25-51.

90. Cirrito J, Deane R, Fagan A, Spinner M, Parsadanian M, Finn M, et al. P-glycoprotein deficiency at the blood-brain barrier increases amyloid-beta deposition in an Alzheimer disease mouse model. J Clin Invest. 2005; 115: p. 3285-90.

91. Ruparelia P, Cheow H, Evans J, Banney L, Shankar S, Szczepura K, et al. Pulmonary elimination of inhaled 99mTc-sestamibi radioaerosol is delayed in healthy cigarette smokers. Br J Clin Pharmacol. 2008; 65: p. 611-614.

92. Cheow H, Ruparelia P, Shankar S, Szczepura K, Ballinger J, Hartman N, et al. Does P-glycoprotein have a role in the lung clearances of inhaled 99mTc-sestamibi and 99mTc-tetrofosmin. Nucl Med Commun. 2009;(30): p. 617-21.

93. Hesse B, Tägil K, Cuocolo A, Anagnostopoulos C, Bardiés M, Bax J, et al. EANM/ESC procedural guidelines for myocardial perfusion imaging in nuclear cardiology. Eur J Nucl Med Mol Imaging. 2005; 32: p. 855–897.

94. Yoon Y, Bom H, Lee J, Jaegal Y. Double-phase Tc-99m sestamibi scintimammography to assess angiogenesis and P-glycoprotein expression in patients with untreated breast cancer. Clin Nucl Med. 1999; 24(5): p. 314-8.

95. Wackers F, Berman D, Maddahi J, Watson D, Beller G, Strauss H, et al. Technetium-9 9m Hexakis 2-Methoxyisobutyl Isonitrile: Human Biodistribution, Dosimetry, Safety, and Preliminary Comparison to Thallium-201 for Myocardial Perfusion Imaging. J Nucl Med. 1989; 30: p. 301-311.

96. Dizdarevic S, Aplin M, Ryan N, Holt S, Goldberg L, Miles K, et al. Renal and hepatic kinetics of Tc-99m-labelled hexakis-methoxy-isobutyl Isonitrile. Drug Metab Lett. 2012; 6(4): p. 242-6.

97. Hurwitz G, Duan H, Blais M, Mattar A, Gravelle D. An atlas of renography with Tc-99m sestamibi: comparison with Tc-99m DTPA. Clin Nucl Med. 1995; 20(9): p. 821-9.

98. Heaf J, Iversen J. Uses and limitations of renal scintigraphy in renal transplantation monitoring. Eur J Nucl Med. 2000; 27(7): p. 871-879.

99. Boubaker A, Prior J, Meuwly J. Bischof-Delaloye Radionuclide investigations of the urinary tract in the era of multimodality imaging. J Nucl Med. 2006; 47: p. 1819-1836.

100. Baxter G. Imaging in renal transplantation. Ultrasound Q. 2003; 19(3): p. 123-138.

101. Brown E, Chen M, Wolfman N, Ott D, Watson N. Complications of renal transplantation: evaluation with US and radionuclide imaging. Radiographics. 2000; 20(3): p. 607-622.

102. Broome D, Girguis M, Baron P, Cottrell A, Kjellin I, Kirk G. Gadodiamide-associated nephrogenic systemic fibrosis: why radiologists should be concerned. AJR Am J Roentgenol. 2007; 188(2): p. 586-592.

103. Weller A, Barber J, Olsen O. Gadolinium and nephrogenic systemic fibrosis: an update. Pediatr Nephrol. 2014; 29(10): p. 1927-37.

104. American College of Radiology. ACR Appropriateness Criteria. [Online].; 2012 [cited 2015. Available from: https://acsearch.acr.org.

105. Pedersen S, Keller M, Jespersen B, Falborg L, Rasmussen J, Heegaard C, et al. Cell injury after ischemia and reperfusion in the porcine kidney evaluated by radiolabelled microspheres, sestamibi, and lactadherin. EJNMMI Res. 2013; 3(1): p. 62.

106. Schwarz A, Gwinner W, Hiss M, Radermacher J, Mengel M, Halle H. Safety and Adequacy of Renal Transplant Biopsy Protocols. American Journal of Transplantation. 2005; 5(8): p. 1992-1996.

107. Hurwitz G, Ghali S, Mattar A, Gravelle D, Husni M. Dynamic renal imaging with technetium-99m-sestamibi in hypertension: potential for assessment of renovascular disorders. J Nucl Med. 1994; 35(12): p. 1959-64.

108. Inoue Y, Yoshikawa D, Ishii H, Isobe S, Kumagai S, Suzuki S, et al. Post-stress perfusion abnormalities detected on myocardial perfusion single-photon emission computed tomography predict long-term mortality after elective abdominal aortic aneurysm repair. Circ J. 2013; 77(5): p. 1229-34.

109. Papaioannou G, Heller G. Risk assessment by MPI for coronary revascularisation, medical therapy and noncardiac surgery. Cardiol. Rev. 2003; 11: p. 60-72.

110. Vaquette B, Clargeus F, Kalangos A, Dorsaz P, Righetti A. Prognostic value of thallium 201 myocardial scintigraphy with dipyridamole before peripheral arterial surgery. Arch Mal Coeur Vaiss. 2003; 96: p. 281-7.

111. Pannell L, Reyes E, Underwood S. Cardiac risk assessment before non-cardiac surgery. Eur Heart J Cardiovasc Imaging. 2013; 14: p. 316-22.

112. Weinstein H, Steingart R. Myocardial perfusion imaging for preoperative risk stratification. J Nucl Med. 2011; 52: p. 750-60.

113. Hashimoto J, Suzuki T, Nakahara T, Kosuda S, Kubo A. Preoperative risk stratification using MPS with electrocardiographic gating. J Nuc Med. 2003; 44: p. 385-90.

114. Antonello M, Menegolo M, Piazza M, Bonfante L, Grego F, Frigatti P. Outcomes of endovascular aneurysm repair on renal function

compared with open repair. Journal of Vascular Surgery. 2013; 58(4): p. 886–893.

115. Nordon I, Hinchliffe R, Holt P, Thompson M, Loftus I. Should the role of EVAR be re-evaluated in light of the 10 year results of EVAR-1? J Cardiovasc Surg. 2011; 52(2): p. 179-87.

116. Allie D, Lirtzman M, Wyatt C, Keller V, Mitran E, Hebert C, et al. Targeted renal therapy and contrast-induced nephropathy during endovascular abdominal aortic aneurysm repair: results of a feasibility pilot trial. J Endovasc Ther. 2007; 14(4): p. 520-7.

117. Sennewald K, Taylor AJ. A pitfall in calculating differential renal function in patients with renal failure. Clin Nucl Med. 1993; 18: p. 377-381.

118. Gordon I. Dynamic renal scintigraphy. The Update Paediatrics. 1996; 2(3): p. 32-8.

119. Eskild-Jensen A, Gordon I, Piepsz A, Frokiaer J. Interpretation of the renogram: problems and pitfalls in hydronephrosis in children. BJU Int. 2004; 94(6): p. 887-92.

120. Gluckman G, Baskin L, Bogaert G, Mevorach R, Hattner R, Kogan B. Contradictory renal function measured with mercaptoacetyltriglycine diuretic renography in unilateral hydronephrosis. J Urol. 1995; 154(4): p. 1486-9.

121. Dizdarevic S, Aplin M, Newport M, Ryan N, Holt S, Goubet S, et al. Old tracer for a new purpose: potential role for 99mTc-2-Methoxyisobutylisonitrile (99mTc-MIBI) in renal transplant care. Nucl Med Commun. 2014; 35(10): p. 1058-66.

122. Girardin E. Membrane transporter proteins: a challenge for CNS drug development. Dialogues Clin Neurosci. 2006;(8): p. 311-21.

123. Magnarin N, Morelli M, Rosati A, Bartoli F, Candussio L, Giraldi T, et al. Induction of proteins involved in multidrug resistance (P-glycoprotein, MRP1, MRP2, LRP) and of CYP 3A4 by rifampicin in LLC-PK1 cells. Eur J Pharmacol. 2004;(483): p. 19-28.

124. Burak Z, Moretti J, Ersoy O, Sanli U, Kantar M, Tamgac F, et al. 99mTc-MIBI imaging as a predictor of therapy response in osteosarcoma compared with multidrug resistance-associated protein and P-glycoprotein expression. J Nucl Med. 2003;(44): p. 1394-1401.

125. Zhou J, Higashi K, Ueda Y, Kodama Y, Guo D, Jisaki F, et al. Expression of multidrug resistance protein and messenger RNA

correlate with 99mTc-MIBI imaging in patients with lung cancer. J Nucl Med. 2001;(42): p. 1476-83.

126. Burrell S, MacDonald A. Artifacts and Pitfalls in Myocardial Perfusion Imaging. J Nucl Med Technol. 2006; 34: p. 193–211.

127. Chaiwatanarat T, Padhy A, Bomanji J, Nimmon C, Sonmezoglu K, Britton K. Validation of renal output efficiency as an objective quantitative parameter in the evaluation of upper urinary tract obstruction. J. Nucl. Med. 1993; 34: p. 845-8.

128. Brochner-Mortensen J. A simple method for the determination of. Scand. J. Clin. Lab. Invest. 1972; 30: p. 271-4.

129. Huls M, Kramers C, Levtchenko E, Wilmer M, Dijkman H, Kluijtmans L, et al. P-glycoprotein-deficient mice have proximal tubule dysfunction but are protected against ischemic renal injury. Kidney Int. 2007; 72(10): p. 1233-41.

130. Huls M, Schoeber J, Verfaillie C, Luttun A, Ulloa-Montoya F, Menke A, et al. Deficiency of either P-glycoprotein or breast cancer resistance protein protect against acute kidney injury. Cell Transplant. 2010; 19(9): p. 1195-208.

131. Schuetz E, Furuya K, Schuetz J. Interindividual variation in expression of P-glycoprotein in normal human liver and secondary hepatic neoplasms. J Pharmacol Exp Ther. 1995; 275: p. 1011-8.

132. Wolbold R, Klein K, Burk O, Nussler A, Neuhaus P, Eichelbaum ea. Sex is a major determinant of CYP3A4 expression in human liver. Hepatology. 2003 38; 978-88.

133. Albermann N, Schmitz-Winnenthal F, Z'graggen K, Volk C, Hoffmann M, Haefeli W, et al. Expression of the drug transporters MDR1/ABCB1, MRP1/ABCC1, MRP2/ABCC2, BCRP/ABCG2, and PXR in peripheral blood mononuclear cells and their relationship with the expression in intestine and liver. Biochem Pharmacol. 2005; 70(6): p. 949-58.

134. Levey A, Inker L, Coresh J. GFR Estimation: From Physiology to Public Health. Am J Kidney Dis. 2014; 63(5): p. 820-834.

135. Garnett E, Parsons V, Veall N. Measurement of glomerular filtration-rate in man using a 51Cr-edetic-acid complex. Lancet. 1967; 15(1): p. 818-9.

136. Fleming J, Zivanovic M, Blake G, Burniston M, Cosgriff P. Guidelines for the Measurement of Glomerular Filtration Rate using Plasma

Sampling. Nucl Med Commun. 2004; 25(8): p. 759-69.

137. Cosgriff P, Fleming J, Jarritt P, Skyrpniuk J, Bailey D, Whalley D, et al. UK audit of GFR measurements. Nuclear Medicine Communications. 2002; 23: p. 286.

138. Haycock G, Schwartz G, Wisotsky D. Geometric method for measuring body surface area: a height-weight formula validated in infants, children, and adults. J Pediatr. 1978; 93(1): p. 62-6.

139. Takano A, Kusuhara H, Suhara T, Ieiri I, Morimoto T, Lee V, et al. Evaluation of in vivo P-glycoprotein function at the blood-brain barrier among MDR1 gene polymorphisms by using 11C-verapamil. J Nucl Med. 2006;(47): p. 1427-33.

140. Woillard J, Rerolle J, Picard N, Rousseau A, Guillaudeau A, Munteanu E, et al. Donor P-gp polymorphisms strongly influence renal function and graft loss in a cohort of renal transplant recipients on cyclosporine therapy in a long-term follow-up. Clin Pharmacol Ther. 2010; 88(1): p. 95-100.

141. Bebawy M, Chetty M. Gender differences in p-glycoprotein expression and function: effects on drug disposition and outcome. Curr Drug Metab. 2009; 10(4): p. 322-8.

142. Suzuki T, YL Z, M N, Naruhashi K, Shimizu A, Takagi K, et al. Gender-related differences in expression and function of hepatic P-glycoprotein and multidrug resistance-associated protein (Mrp2) in rats. Life Sci. 2006; 79(5): p. 455-61.

143. Meissner K, Sperker B, Karsten C, Meyer zu Schwabedissen H, Seeland U, Böhm M, et al. Expression and localization of P-glycoprotein in human heart: effects of cardiomyopathy. J Histochem Cytochem. 2002;(50): p. 1351–1356.

144. Dizdarevic S, Singh N, Nair S, de Belder A, Ryan N, Aplin M, et al. Early gated SPECT adenosine myocardial perfusion imaging may influence the therapeutic management of patients with coronary artery disease. Nucl Med Commun. 2015; 36(4): p. 386-91.

145. Calne R, Rolles K, White D, Thiru S, Evans D, McMaster P, et al. Cyclosporin A initially as the only immunosuppressant in 34 recipients of cadaveric organs: 32 kidneys, 2 pancreases, and 2 livers. Lancet. 1979; 2: p. 1033–1036.

146. Calne R, White D, Thiru S, Evans D, McMaster P, Dunn D, et al. Cyclosporin A in patients receiving renal allografts from cadaver donors. Lancet. 1978; 2: p. 1323-1327.

147. Naesens M, Kuypers D, Sarwal M. Calcineurin Inhibitor Nephrotoxicity. Clin J Am Soc Nephrol. 2009; 4: p. 481–508.

148. Caccavo D, Lagana B, Mitterhofer A, Ferri G, Afeltra A, Amoroso A, et al. Long-term treatment of systemic lupus erythematosus with cyclosporin. 1997; 40(1): p. 27–35.

149. Starzl T, Todo S, Fung J, Demetris A, Venkataramman R, Jain A. FK 506 for liver, kidney, and pancreas transplantation. Lancet. 1989; 2: p. 1000–1004.

150. Fung J, bu-Elmagd K, Todo S, Shapiro R, Tzakis A, Jordan M, et al. Overview of FK506 in transplantation. Clin Transpl. 1990;: p. 115–121.

151. Kung L, Batiuk T, Palomo-Pinon S, Noujaim J, Helms L, Halloran P. Tissue distribution of calcineurin and its sensitivity to inhibition by cyclosporine. Am J Transplant. 2001; 1: p. 325–333.

152. Rao A, Luo C, Hogan P. Transcription factors of the NFAT family: Regulation and function. Annu Rev Immunol. 1997; 15: p. 707–747.

153. Liu E, Siegel R, Harlan D, O'Shea J. T cell-directed therapies: Lessons learned and future prospects. Nat Immunol. 2007; 8: p. 25–30.

154. Halloran P, Helms L, Kung L, Noujaim J. The temporal profile of calcineurin inhibition by cyclosporine in vivo. Transplantation. 1999; 6: p. 1356–1361.

155. Iwasaki K, Shiraga T, Matsuda H, Teramura Y, Kawamura A, Hata T, et al. Absorption, distribution, metabolism and excretion of tacrolimus (FK506) in the rat. Drug Metab Pharmacokinet. 1998; 13: p. 259–265.

156. Anglicheau D, Pallet N, Rabant M, Marquet P, Cassinat B, Meria P, et al. Role of Pglycoprotein in cyclosporine cytotoxicity in the cyclosporine-sirolimus interaction. Kidney Int. 2006; 70: p. 1019–1025.

157. Napoli K, Wang M, Stepkowski S, Kahan B. Relative tissue distributions of cyclosporine and sirolimus after concomitant peroral administration to the rat: Evidence for pharmacokinetic interactions. Ther Drug Monit. 1998; 20: p. 123–133.

158. Podder H, Stepkowski S, Napoli K, Clark J, Verani R, Chou T, et al. Pharmacokinetic interactions augment toxicities of sirolimus/cyclosporine combinations. J Am Soc Nephrol. 2001;

12: p. 1059–1071.

159. Saeki T, Ueda K, Tanigawara Y, Hori R, Komano T. Human P-glycoprotein transports cyclosporin A and FK506. J Biol Chem. 1993; 268: p. 6077–6080.

160. Ernest S, Rajaraman S, Megyesi J, Bello-Reuss E. Expression of MDR1 (multidrug resistance) gene and its protein in normal human kidney. Nephron. 1997; 77: p. 284–289.

161. del Moral R, Andujar M, Ramirez C, Gomez-Morales M, Masseroli M, Aguilar M, et al. Chronic cyclosporin A nephrotoxicity, P-glycoprotein overexpression, and relationships with intrarenal angiotensin II deposits. Am J Pathol. 1997; 151: p. 1705–1714.

162. Jette L, Beaulieu E, Leclerc J, Beliveau R. Cyclosporin A treatment induces overexpression of P-glycoprotein in the kidney and other tissues. Am J Physiol. 1996; 270: p. 756–765.

163. Joy M, Nickeleit V, Hogan S, Thompson B, Finn W. Calcineurin inhibitor-induced nephrotoxicity and renal expression of P-glycoprotein. Pharmacotherapy. 2005; 25(6): p. 779-89.

164. Kimchi-Sarfaty C, Oh J, Kim I, Sauna Z, Calcagno A, Ambudkar S, et al. A "silent" polymorphism in the MDR1 gene changes substrate specificity. Science. 2007; 315: p. 525–528.

165. Komar A. Silent SNPs: Impact on gene function and phenotype. Pharmacogenomics. 2007; 8: p. 1075–1080.

166. Gow J, Hodges L, Chinn L, Kroetz D. Substratedependent effects of human ABCB1 coding polymorphisms. J Pharmacol Exp Ther. 2008; 325: p. 435–442.

167. Hebert M, Dowling A, Gierwatowski C, Lin Y, Edwards K, Davis C, et al. Association between ABCB1 (multidrug resistance transporter) genotype and post-liver transplantation renal dysfunction in patients receiving calcineurin inhibitors. Pharmacogenetics. 2003; 13(11): p. 661-74.

168. Han K, Pillai V, Venkataramanan R. Population Pharmacokinetics of Cyclosporine in Transplant Recipients. The AAPS Journal. 2013; 15(4): p. 901-912.

169. Novartis Pharmaceuticals. SANDIMMUNE® oral soft gelatin capsules, oral solution, injection for infusion. [Online].; 2005 [cited 2015. Available from: http://www.pharma.us.novartis.com/cs/www.pharma.us.novartis.c

om/product/pi/pdf/sandimmune.pdf.

170. Novartis Pharmaceuticals. NEORAL® soft gelatin capsules, oral solution. [Online].; 2005. Available from: http://www.pharma.us.novartis.com/cs/www.pharma.us.novartis.com/product/pi/pdf/neoral.pdf.

171. Casalta-Lopez J, Abrantes A, Rio J, Laranjo M, Oliveiros B, Goncalves C, et al. MDR and MDR reversal kinetics in humana adenocarcinoma cell lines. Eur J Nucl Med Mol Imaging. 2009; 36: p. S242.

172. Press R, Ploeger B, den Hartigh J, van der Straaten T, van Pelt H, Danhof M, et al. Explaining variability in ciclosporin exposure in adult kidney transplant recipients. Eur J Clin Pharmacol. 2010; 66: p. 579–590.

173. McMillan M. Clinical pharmacokinetics of cyclosporin. Pharmacol Ther. ; 42: p. 135–156.

174. Cremers S, Scholten E, Schoemaker R, Lentjes E, Vermeij P, Paul L, et al. A compartmental pharmacokinetic model of cyclosporin and its predictive performance after Bayesian estimation in kidney and simultaneous pancreas-kidney transplant recipients. Nephrol Dial Transplant. 2003; 18: p. 1201–1208.

175. Mahalati K, Belitsky P, Sketris I, West K, Panek R. Neoral monitoring by simplified sparse sampling area under the concentration-time curve: its relationship to acute rejection and cyclosporine nephrotoxicity early after kidney transplantation. Transplantation. 1999; 68: p. 55–62.

176. Knight S, Morris P. The clinical benefits of cyclosporine C2-level monitoring: a systematic review. Transplantation. 2007; 83: p. 1525–1535.

177. Olyaei A, de Mattos A, Bennett W. Nephrotoxicity of immunosuppressive drugs: new insight and preventive strategies. Curr Opin Crit Care. 2001; 7(6): p. 384–9.

178. Jorga A, Holt D, Johnston A. Therapeutic drug monitoring of cyclosporine. Transplant Proc. 2004; 36(2): p. 396-403.

179. Dunn C, Wagstaff A, Perry C, Plosker G, Goa K. Cyclosporin: an updated review of the pharmacokinetic properties, clinical efficacy and tolerability of a microemulsion-based formulation (neoral)1 in organ transplantation. Drugs. 2001; 61(13): p. 1957–2016.

180. Anglicheau D, Verstuyft C, Laurent-Puig P, Becquemont L, Schlageter M, Cassinat B, et al. Association of the Multidrug Resistance-1 Gene Single Nucleotide Polymorphisms with the Tacrolimus Dose Requirements in Renal Transplant Recipients. J Am Soc Nephrol. 2003; 14: p. 1889–1896.

181. Li Y, Hu X, Cai B, Chen J, Bai Y, Tang J, et al. Meta-analysis of the effect of MDR1 C3435 polymorphism on tacrolimus pharmacokinetics in renal transplant recipients. Transpl Immunol. 2012; 27(1): p. 12-8.

182. Jiang Z, Wang Y, Xu P, Liu R, Zhao X, Chen F. Meta-Analysis of the Effect of MDR1 C3435T Polymorphism on Cyclosporine Pharmacokinetics. Basic Clin Pharmacol Toxicol. 2008; 103(5): p. 433-44.

183. Hodgesa L, Markovac S, Chinnc L, Gowc J, Kroetzc D, Kleina T, et al. Very important pharmacogene summary: ABCB1 (MDR1, Pglycoprotein). Pharmacogenet Genomics. 2011; 21(3): p. 152–161.

184. Leschziner G, Andrew T, Pirmohamed M, Johnson M. ABCB1 genotype and PGP expression, function and therapeutic drug response: a critical review and recommendations for future research. Pharmacogenomics J. 2007; 7: p. 154–179.

185. Zhang Y, Yang L, Shao H, Li K, Sun C, Shi L. ABCB1 polymorphisms may have a minor effect on ciclosporin blood concentrations in myasthenia gravis patients. Br J Clin Pharmacol. ; 66: p. 240–246.

186. Mathijssen R, Marsh S, Karlsson M, Xie R, Baker S, Verweij J, et al. Irinotecan pathway genotype analysis to predict pharmacokinetics. Clin Cancer Res. 203; 9(9): p. 3246-53.

187. Schaich M, Kestel L, Pfirrmann M, Robel K, Illmer T, Kramer M, et al. A MDR1 (ABCB1) gene single nucleotide polymorphism predicts outcome of temozolomide treatment in glioblastoma patients. Ann Oncol. 2009; 20(1): p. 175-81.

188. Jakobsen Falk I, Fyrberg A, Paul E, Nahi H, Hermanson M, Rosenquist R, et al. Impact of ABCB1 single nucleotide polymorphisms 1236C>T and 2677G>T on overall survival in FLT3 wild-type de novo ML patients with normal karyotype. British Journal of Haematology. 2014;(167): p. 671–680.

189. Estrela R, Ribeiro F, Barroso P, Tuyama M, Gregório S, Dias-Neto E, et al. ABCB1 polymorphisms and the concentrations of lopinavir and ritonavir in blood, semen and saliva of HIV-infected men

under antiretroviral therapy. Pharmacogenomics. 2009; 10(2): p. 311-8.

190. Sigal N, Dumont F, Durette P, Siekierka J, Peterson L, Rich D, et al. Rich DH, Dunlap BE, Staruch MJ, Melino MR, Koprak SL: Is cyclophilin involved in the immunosuppressive and nephrotoxic mechanism of action of cyclosporin A? J Exp Med. 1991; 173: p. 619–628.

191. Taegtmeyer A, Breen J, Smith J, Burke M, Leaver N, Pantelidis P, et al. ATP-binding cassette subfamily B member 1 polymorphisms do not determine cyclosporin exposure, acute rejection or nephrotoxicity after heart transplantation. Transplantation. 2010; 89(1): p. 75-82.

192. National Center for Biotechnology Information. dbSNP - National Center for Biotechnology Information. [Online]. [cited 2015. Available from: http://www.ncbi.nlm.nih.gov/SNP/.

193. Chen K, Sikic B. Molecular pathways: regulation and therapeutic implications of multidrug resistance. Clin Cancer Res. 2012; 18(7): p. 1863–1869.

194. Segall G, Lang E, Chaovapong W. In vitro evaluation of white blood cell labelling with 99mTc radiopharmaceuticals. Nucl Med Commun. 1994; 15: p. 845-849.

195. Dopp J, Moran J, Abel N, Wiegert N. Influence of intermittent hypoxia on myocardial and hepatic P-glycoprotein expression in a rodent model. Pharmacotherapy. 2009; 29(4): p. 365-72.

196. The Renal Association. UK Renal Registry. [Online]. Available from: www.renalreg.org.

197. Sivapackiam J, Gammon S, Harpstrite S, Sharma V. Targeted chemotherapy in drug-resistant tumors, noninvasive imaging of P-glycoprotein-mediated functional transport in cancer, and emerging role of Pgp in neurodegenerative diseases. Methods Mol Biol. 2010; 596: p. 141-81.

198. Bartels A, Kortekaas R, Bart J, Willemsen A, de Klerk O, de Vries J, et al. Blood–brain barrier P-glycoprotein function decreases in specific brain regions with aging: A possible role in progressive neurodegeneration. Neurobiol Aging. 2009; 30(11): p. 1818–1824.

199. Lynn B, Wang J, Markesbery W, Lovell M. Quantitative changes in the mitochondrial proteome from subjects with mild cognitive impairment, early stage, and late stage Alzheimer's disease. J

Alzheimers Dis. 2010; 19: p. 325-39.

200. Loscher W, Potschka H. Role of multidrug transporters in pharmacoresistance to antiepileptic drugs. J Pharmacol Exp Ther. 2002; 301: p. 7-14.

201. Miller D, Cannon R. Signaling pathways that regulate basal ABC transporter activity at the blood- brain barrier. Curr Pharm Des. 2014; 20(10): p. 1463-71.

202. Mohan H, Ballinger J, Livieratos L, Karugaba R, Routledge T, Cane M, et al. Inhaled 99mTc-Sestamibi clearance from lungs - A novel technique for interrogating MRP1 expression in lungs. [Online].; 2014. Available from: http://eanm14.eanm.org/abstracts/P698.

203. Mohan H, Ballinger J, Livieratos L, Karugaba R, Routledge T, Cane M, et al. actors affecting the clearance of inhaled 99m-Tc Sestamibi from lungs in humans. [Online].; 2014. Available from: http://eanm14.eanm.org/abstracts/P699.

204. van der Deen M, Marks H, Willemse B, Postma D, Muller M, Smit E, et al. Diminished expression of multidrug resistance-associated protein 1 (MRP1) in bronchial epithelium of COPD patients. Virchows Arch. 2006;(449): p. 682-8.

205. Gupta Y, Ahmed R, Happerfield L, Pinder S, Balan K, Wishart G. P-glycoprotein expression is associated with sestamibi washout in primary hyperparathyroidism. Br J Surg. 2007; 94: p. 1491-1495.

206. Maillefert J, Maynadie M, Tebib J, Aho S, Walker P, Chatard C, et al. Expression of the multidrug resistance glycoprotein 170 in the peripheral blood lymphocytes of rheumatoid arthritis patients. The percentage of lymphocytes expressing glycoprotein 170 is increased in patients treated with prednisolone. Br. J. Rheumatol. 1996; 35(5): p. 430–435.

207. Picchianti-Diamanti A, Rosado M, Scarsella M, Laganà B, D'Amelio R. P-Glycoprotein and Drug Resistance in Systemic Autoimmune Diseases. Int. J. Mol. Sci. 2014; 15(3): p. 4965-76.

208. Vecchio S, Zannetti A, Salvatore B, Paone G, Fonti R, Salvatore M. Functional imaging of multidrug resistance in breast cancer. Phys Med. 2006; 21: p. 24-7.

209. Bleichner-Perez S, Le Jeune F, Dubois F, Steinling M. 99mTc-MIBI brain SPECT as an indicator of the chemotherapy response of recurrent, primary brain tumors. Nucl Med Commun. 2007; 28(12): p. 888-94.

210. Sasajima T, Shimada N, Naitoh Y, Takahashi M, Hu Y, Satoh T, et al. (99m)Tc-MIBI imaging for prediction of therapeutic effects of second-generation MDR1 inhibitors in malignant brain tumors. Int J Cancer. 2007; 121(12): p. 2637-45.

211. Kawata K, Kanai M, Sasada T, Iwata S, Yamamoto N, Takabayashi A. Usefulness of 99mTc-sestamibi scintigraphy in suggesting the therapeutic effect of chemotherapy against gastric cancer. Clin Cancer Res. 2004; 10(11): p. 3788-93.

212. Wang H, Chen X, Qiu F. Correlation of expression of multidrug resistance protein and messenger RNA with 99mTc-methoxyisobutyl isonitrile (MIBI) imaging in patients with hepatocellular carcinoma. World J Gastroenterol. 2004; 10(9): p. 1281-5.

213. Kostakoglu L. Noninvasive detection of multidrug resistance in patients with hematological malignancies: are we there yet? Clin Lymphoma. 2002; 2(4): p. 242-8.

214. Fonti R, Salvatore B, Quarantelli M, Sirignano C, Segreto S, Petruzziello F, et al. 18F-FDG PET/CT, 99mTc-MIBI, and MRI in evaluation of patients with multiple myeloma. J Nucl Med. 2008; 49(2): p. 195-200.

215. D'Sa S, Abildgaard N, Tighe J, Shaw P, Hall-Craggs M. Guidelines for the use of imaging in the management of myeloma. Br J Haematol. 2007 137; 1: p. 49-63.